Chapter 4

Studies on Physico-chemical Characteristics of Progressively Alkylated Thiazine Dyes in Micellar and Microemulsion Media

4.1 Introduction and Review of the Previous Work

In aqueous solution, micelle formation is usually detected by some change in the physical properties of the solution, such as surface tension, conductivity, viscosity and e.m.f. or some optical or spectroscopic property of the solution [1-3]. Hartley [4] first noticed that the colour of sulphonaphthalein indicators changed on the addition of detergents, and this effect occurred only when the charge on the detergent aggregate was opposite in sign to that of the dissociated indicator molecule. This behaviour proved to be quite general, as azo [5] triphenyl methane [6] and merocyanine dyes [7] all exhibited the same effect.

At concentrations below the cmc addition of a surfactant to a dye solution may bring about the formation of colloidal dye surfactant submicellar aggregates (mixed micelles) or insoluble dye surfactant salts, ion pair, molecular complex, dye-rich induced micelles, induced self-aggregates of dye, aggregation of dye-surfactant complex and change in chromophore microenvironment [8-14]. The actual species formed depends mainly on the nature of the dye and their own tendency to form the aggregate [15,16].

Formation of an insoluble salt between ionic dyes and oppositely charged detergents is most common, but is not a completely general phenomenon. In fact, some dyes, such as phenol red [17] or 8-hydroxy quinoline-5-sulphonic acid produce neither turbidity nor precipitation [18] along with the spectral change induced by addition of the cationic surfactant.

Dyes are also amphiphiles, in the sense that bulky non-ionic moieties are attached to the ionic or analytical groups, but as they lack long-chain alkyl groups they have weak surface activity and do not form micelles in water. Depending on the balance between the hydrophobic and hydrophilic tendencies of any particular dye, increase in dye concentration can lead to stepwise aggregation i.e. the formation of dimers, trimers, polymers and finally colloids [19].

If a surfactant is added to such a dye solution at submicellar concentrations, both the surfactant monomer and the dye aggregates can interact to form a special kind of micelle (mixed micelle) [20] at concentrations far below the normal cmc, characteristic of the surfactant. This dye-surfactant interaction accounts for the often observed fact that the so-called 'spectroscopic probe method' [21] does not provide a true cmc value. In fact in such cases, the change in absorbance or fluorescence

intensity of a dye probe in the presence of increasing surfactant concentrations may not reflect the formation of micelles of the surfactant (homomicelles) but that of mixed micelles or dye-surfactant salts. But there are also many reports in the literature where these spectroscopic methods [22-24] have been used to determine the cmc of both ionic and non-ionic surfactants. García-Río et al. [2] recently discard the possibility in a cmc change due to the presence of dye. They however, got the same result by measuring the cmc of SDS conductometrically with and without the presence of crystal violet (CV)

Once the surfactant concentration has reached a value close to or above the cmc neither turbidity nor precipitation is observed. Solubilization of the dye-surfactant 'salt like' ion pairs in the micellar phase and/or the final incorporation of the dye into the micelles (homomicelles) takes place. Many of the features observed in the spectral behaviour of dye-surfactant systems having opposite charge can often be extended to general sensitized reactions in micellar media [25,26].

In past, Mukherjee and Mysels [27] using spectrophotometric and electrical conductivity measurements of the pynacyanolsodium dodecyl sulphate system identified the presence of two types of dye-surfactant aggregates : (i) below the cmc a dye-surfactant salt which formed a coarse (visible suspension) stable slurry in the presence of more than a stoichiometric amount of surfactant and (ii) dye-rich micelles, at below and around the cmc which solubilized the water-insoluble dye-detergent salt. Malik et al. [28,29] reported that spectral changes for several dyes are due to electrostatic forces involving interactions between the anionic (or cationic) surfactant and the basic (or acidic) dye. They claimed that chemical interaction giving a stoichiometric dye-surfactant complex was very improbable.

Guha et al. [30] attributed the changes in the absorption spectra and the decrease in fluorescence intensity of thionine to the formation of a dye-surfactant complex at SDS concentration below the cmc. At concentration above the cmc the appearance of the dye absorption spectrum with a small red shift and increased extinction co-efficient, was interpreted as due to the incorporation of the dye into the micelles.

The existence of true ion-association complexes formed below the cmc between ionic surfactants and dyes with opposite charge is supported by most of the

published data [6,31,32]. These complexes are electrically neutral and often poorly soluble in water but readily extractable by low-polarity solvents. They have stoichiometric surfactant ratios. At surfactant concentrations equal to the cmc value and above, the solubilizing effect of the micelles begins to be important and the ion-association complexes are incorporated into the micelles.

Electrostatic interaction of anionic dyes with the surface of cationic surfactant micelles takes place through the negatively charged groups of the dye (e.g. - SO_3^-, - COO^-). However, this kind of electrostatic interaction could not explain by itself the spectral changes observed during the interaction. In fact, bulky non-micelle forming species such as the diphenylguanidinium or tetra ethyl ammonium ion have no effect *per se*. Moreover, simple ion-pairing between a negative group such as -SO_3^-, or - COO^-, of the dye and a quaternary ammonium ion does not perturb the chromophore [32]. In the presence of cationic surfactants, aromatic compounds with sulphonic [33] or carboxylic acid groups [34] do not act simply as counterions, but are incorporated into the water-rich stern layer of the micelle in a sandwich arrangement. This permits not only the hydration of the hydrophilic -SO_3^- (or - COO^-) group, but also the solvation of the aromatic ring of the dye by the -$N(CH_3)_2$ group and the participation of vander Waals interaction between adjacent surfactant chains and the dye organic moiety (hydrophobic forces). In this situation, the micro-environment of the chromophore has clearly changed, from that existing in the bulk aqueous phase, and this change is the cause of the spectral shifts observed. Since dyes based on aromatic rings are widely used in spectrophotometry and fluorimetry, this picture can be considered general and is probably operative in most analytical dye-surfactant systems at concentration above the cmc.

The proton release occurring during the reaction between an anionic dye and a cationic surfactant produces a change in the spectrum which is similar to that observed on increasing the pH of the dye solution. Such pKa shifts for solubilized indicators have been attributed to the influence of the surface potential of micelles [35,36]. The pKa changes also appear to be related to the reduction of the difference in free energy between the acidic form of the dye and its anion in the micelle [34,37]. Extensive incorporation of an anionic dye into a cationic micelle implies that the free

energy of the anionic form decreases more than that of the un-ionized form, as the anion is more polarizable and firmly attached to the positive end groups of neighboring surfactant molecules [38].

There is multiple binding in these associated miceller species; evidence has been produced indicating that hydrophobic interaction, not charge compensation, plays the main role in binding between dyes and surfactants. The exact nature of this interaction, however, has not yet been satisfactorily explained. Chiang et al. [39] reported that their result on the interaction between 2-p-toluidinylnaphthalene-6-sulphonate and SDS micelles suggest that the binding force is hydrophobic. Analogously, Birdi et al. [37] claimed that the interaction of SDS micelles with 1-anilinonaphthalene-8-sulphonate is hydrophobic in nature. The interaction between some mono-azo dyes with a series of non ionic surfactants has been shown [40] to be hydrophobic in nature and occurs between dyes and the ethylene oxide chains of the non-ionic surfactant. Minch [7] showed, from spectral changes of merocyanine dyes in cationic and anionic micelle, that in all cases the spectra were red-shifted when the dye was incorporated into micelles and that the magnitude of the shift increased with more hydrophobic dyes. Biedermann and Datyner [41] also suggested that the interactions of some azo dyestuffs with SDS micelles increased with increasing lipophilicity of the dyes.

According to Dill et al. [42] the inclusion of a dye molecule within a micelle is not strictly akin to placing it in a hydrophobic region in the micellar core, but is more likely placing it in a hydrophobic environment where it is exposed to water. A consideration of hydrocarbon chains in micelles as disordered structures could explain why the nature of the dye may determine its binding site within the micelle assembly [41]. In other instances, the factors responsible for the spectral changes have been ascribed to the deaggregation of the dye molecules by association with micelles [43] to the joint effect of deaggregation and the change in the molecular environment [44,45] or to the localization of the chromaphore within the hydrophobic micellar interior [46]. Micelles are sensitive to small changes in the ionic strength of the aqueous solution. The change in the cmc of cetyl pyridinium bromide (CPB) in aqueous solution with electrolyte concentration [46] reveal two

trends, one occurring at low and the other at high concentrations of the added salt. Addition of salts to ionic micelle solutions reduces the mutual electrostatic repulsions of charged head groups [47].

Owing to electrostatic repulsion, the interaction between anionic dye ions and the head-groups of anionic surfactants should produce neither new spectral bands nor changes in absorbance or fluorescence intensity. Similar results are also observed in case of interaction between cationic dye ions and head groups of cationic surfactants. However, as mentioned earlier, lipophilicity may often be the driving force for interaction, rather than the electrostatic interaction [7,37,39,41] and some spectral changes can be explained in this way. A similar explanation can also be given for the effect of non-ionic surfactants on the spectral behaviour of dyes. Coomassie brilliant blue G-250 does not show any spectral shift with anionic detergents such as sodium dodecyl sulphate or sodium deoxycholate, but does with non-ionic surfactants, probably owing to transfer of the dye from a hydrophilic to a hydrophobic micellar environment [48]

If a charge-type effect can combine with the classical hydrophobic interactions then both kinds of interactions, electrostatic and hydrophobic, seem to act concurrently, bringing about the largest spectral changes, as shown for anionic dye-cationic surfactant complexes by Savvin et al. [32] or for metal chelate – cationic surfactant species by Sanz-Medel et al. [18,49]. In any case, it seems clear that the surfactant character has the decisive role in determining the observed spectral changes, since bulky ions, which are non-micelle-forming (e.g., tetraethylammonium) do not give rise to effects similar to those observed in the presence of micelle-forming agents [32,50]. The implications of a model for the interactions in micelles are significant not only for micelles in water but also for related assemblies, since the principles of organization are thought to be quite general [51]

The surfactant interactions in non-aqueous media have been investigated [52] less than those in aqueous surfactant systems. The surfactant aggregates in organic solvents are described as having a 'reverse micellar structure', in which the

hydrocarbon tails are in contact with the solvent and the polar head groups form the micellar core.

The aggregation number in such reverse micelles is relatively small, e.g. less than 10 for alkyl ammonium carboxylates, compared with up to 100 for aqueous micelles [53]. It is supposed that these systems would exhibit an experimentally determinable cmc. Although many of the common methods for cmc determination in aqueous solution are not applicable to reverse micellar systems, because of the low degree of aggregation and because ionic surfactants do not ionize in organic media, the 'spectral change method' has been proposed for determination of the cmc of Aerosol-OT (sodium bis-(2-ethyl hexyl) sulphosuccinate) [54] with the dye 7,7,8,8-tetracyano quinodimethane (TCNQ). Breaks in the plots of absorbance against surfactant concentration were interpreted as corresponding to the surfactant cmc. However, as the concept of cmc as explained for normal micelles is no longer applicable in these systems and is still subject to controversy. Reverse micelles alter the micro-environment of solubilized reactants and thus affect their stereochemistry, dissociation constants, redox potentials and reactivities [55]

4.1.1 Dye-Surfactant Interaction in Sub-Micellar Concentrations of Surfactant

There has been an increasing interest in the study of interaction of dyes with surfactants as the knowledge of dye-surfactant interaction is of great value in understanding the chemical equilibrium, mechanism and kinetics of surfactant sensitized colour and fluorescence reactions [49]. Many researchers had noticed the change in colour of the ionic dyes when they were dissolved in oppositely charged ionic micelles [44,56-62]. Most of the previous studies on dye-surfactant interaction were carried out with the concentration of the surfactants above the cmc and the colour changes have been explained on the basis of the interaction between the surfactant micelles and the dyes and the equilibrium between conjugate acid and base forms of the dye. However, there is not much information available regarding the nature and mechanism of the interaction between dyes and surfactants when the concentrations of the surfactants are much below the cmc. Dutta and Bhatt [63] carried out systematic spectroscopic and thermodynamic investigations in order to understand the nature of this interaction between ionic dyes and oppositely charged

surfactants of very low concentrations i.e., far below their cmc's. They have investigated interactions of cationic dyes viz. phenosafranin (PSF), safranine O (SFO) and safranine T (SFT) with anionic surfactants, viz. sodium dodecyl sulfate (SDS) and sodium octyl sulphate (SOS) in submicellar concentration ranges. The interaction has been shown to be an induced protonation of the dye in the dye-surfactant ion pair. Even though the opposite charges on the dye and the surfactant are the primary requirements for the ion pair formation, it is the hydrophobicity of the surfactant as well as of the dye which induces the protonation.

As the concentration of SDS is slowly increased from 1.6 x 10^{-4}M (the lowest concentration at which there was detectable decrease/increase in absorbance of PSF bands) to 3 x 10^{-3}M, λ_{max} of PSF band gradually shifted from 520 to 528 nm with a gradual decrease in intensity of the λ_{max} band, accompanied by an increase in absorbance in the longer wavelength region of ca λ 550 to ca 700 nm. The red shift of the PSF band from 520 to 528 nm was attributed partly to a change in the environment of the chromophore of PSF and partly to the overlapping of the 520 nm band with the new band in the longer wave length region. Increasing the concentration of SDS up to 4 x 10^{-4} M, for a fixed concentration of PSF (2.13 x 10^{-5} M) gives a series of spectra that go through a sharp isobestic point at 550 nm.

It was observed that the spectra of PSF in low concentration of SDS were similar to those of PSF in strong acidic media. Gopidas and Kamat [64] had reported that PSF^{+} in HCl (2M) has absorption band at 580 nm which can be attributed to $HPSF^{2+}$. They had noticed that with the increase in concentration of strong acids, e.g., H_2SO_4, $HClO_4$ etc. PSF gave rise to three bands viz. at 580, 625 and 690 nm. Similarly, with the increase of BF_3 in ether the absorption maxima of PSF were at 578, 622 and 688 nm successively. The appearance of a new band at ca. 582 nm which increases with the increase in concentration of SDS (up to ca. 3 x 10^{-3}M) and decreases with increase in temperature, and the presence of an isobestic point indicate of the presence of an equilibrium between the free PSF, SDS and complexed PSF (an interaction product of PSF and submicellar SDS). With the increase in concentration of SDS above cmc (6.0x10^{-3} M in presence of 2.2x10^{-5} M PSF), the 520 nm band shifts to higher wave length, viz., 531 nm which is attributed to the association of the dye

with the surfactant micelles. There was hardly any change in the position and intensity of this band with further addition of SDS.

The colour change observed in many dyes on the addition of very small amount of oppositely charged surfactant has been attributed to ion pair formation [60], dye-surfactant salt formation [27], the formation of dye dimer or higher aggregates [65], micelle and mixed micelle formation [44,62], etc. However, in the case of cationic dyes, like phenazinium and thiazinium dyes, the dimerizations are known to cause hypsochromic shifts in the spectra [66]

No interaction of the phenazinum dyes with N-hexadecyl pyridinium chloride (a cationic surfactant) and triton X - 100, $(CH_3)_3CCH_2C(CH_3)_2$-C_6 H_4 $(OCH_2CH_2)_{10}OH$ (a non ionic surfactant), in the submicellar concentration range was observed [63]. This indicates that the opposite charge on the dye and the surfactant is the primary requirement for this interaction. Therefore it can be suggested that as the oppositely charged ions, viz., PSF^+ and DS^- (anionic part of SDS), come closer to each other due to electrostatic attraction, the hydrophobic nature of the large organic ions and hydrogen-bonded water structure enforce them to form closely associated ion pairs, PSF^+DS^- [60,67,68].

It is clear that some more changes, in addition to the ion pair formation, occurs to the chromophore to affect the large shift of the absorption band. Gopidas and Kamat [64] reported that PSF gets protonated and gives a band at 583 nm when it is bound to H^+ -Nafion, a polymer which exhibits a strong acidic environment to the dye in aqueous solution [68]. It has been shown that the PSF absorption band remains unperturbed even on lowering of the pH of aqueous PSF solution to 1.2. Only below pH of 1.2, the 580 nm band of PSF appears. On the other hand, in the entire experimental submicellar concentration range of SDS, the pH's of the aqueous SDS solutions were 6.5. Therefore, it seems that the 582 nm band of PSF in submicellar SDS may also be due to the protonated PSF, viz., $HPSF^{2+}$ caused by a strong acidic environment exhibited by monomeric DS^- bound to PSF^+ in the hydrophobic ion pair of PSF^+DS^- [63].

The SOS has a shorter hydrocarbon chain than SDS and therefore it is expected to show weaker interactions with cationic dyes (due to lesser

hydrophobicity) [69] than that of SDS. From the equilibrium constants and other thermodynamic parameters it is evident that the interaction of cationic dyes with SOS is much weaker compared to that with SDS. The slightly lower value of ΔS for PSF - SDS may be due to more ordering of the protonated ion pair in water, as SOS is relatively less hydrophobic compared to SDS.

SFO is a 2,8-dimethyl derivative of phenosafranin and SFT is a positional isomer of SFO. Both of these dyes have absorption maxima at 520 nm in the visible range. The spectral changes in the aqueous solutions of SFO and SFT on addition of SOS were similar to those of PSF - SDS and PSF - SOS. It seems apparent that hydrophobicity of the surfactant plays an important role in the ion pair formation as well as in induced protonation of the dye in the ion pair.

4.1.2 Dye-Surfactant Interaction in Super Micellar Concentrations of Surfactant

As has already been discussed that changes in the colour of ionic dyes in the presence of oppositely charged ionic surfactants in aqueous solution have been observed by many workers [27,70,71] and these changes have been explained by proposing dimer and multimer formation of dye molecules in the surfactant micelle. Hayashi [72] studied the interaction of congo red dye with cetyltrimethylammonium bromide (CTAB) and p-t-octylphenoxypolyoxyethanol, TX-100 (Triton X-100) and interpreted the spectrophotometric data in terms of formation of a 1:2 dye surfactant complex. Matibinkov et al. [73] studied the effect of sodium lauryl sulphate (SLS) on xanthane dyes and observed shifts in their visible absorption maxima at lower surfactant concentrations. Recently the results of spectrophotometric studies on phenosafranin dye, a cationic phenazine dye, in aqueous solutions containing three different types of surfactants such as CTAB, SLS and triton X-100 were reported [61]. While the formation of 1:1 dye Triton X-100 and dye-SLS complexes were observed, there was no interaction of phenosafranin with CTAB. The thermodynamic and spectrophotometric properties of these complexes suggest that phenosafranin forms strong charge transfer (CT) complex with triton X-100 whereas the interaction with SLS is coulombic in nature. This conclusion was claimed to be confirmed by photogalvanic and photoconductivity measurements of phenosafranin in these surfactants. The interaction of triton X-100, a good electron donor [74,75] with cationic phenosafranin dye is CT in nature, it is therefore interesting to see if other

cationic dyes would also form CT complexes with triton X-100. The spectrophotometric data of the cationic dyes (rhodamin B, fuchsin and crystal violet) shown 1:1 complex. The equilibrium constant (K) and the molar extinction coefficient can be determined using Ketelaar's equation [76] or Scott equation [77]. The data presented [78] provide direct 'spectrophotometric evidence' of molecular interactions between the cationic dyes and triton X -100.

In the neutral surfactant micelle of triton X-100 a cationic dye can penetrate the micelle to form a strong molecular complex at a polar site, the interaction may occur either at phenoxy group or at the polyoxyethylene chain. The absorption spectra of phenosafranin in acetonitrile, water, dioxane, acetone, ethanol and glycol exhibit absorption maxima at 518, 520, 525, 526, 532 and 535nm respectively. The position of absorption maximum of phenosafranin - triton X-100 complex in aqueous medium occurs at 537.5 nm. These results suggest that the positive centre of the dye molecule within the micelle is associated not with the lone pair electron on ether oxygen atom but with the lone pair electron on the oxygen of the hydroxyl group.

However, there is no indication of hydrophobic interaction between the dyes and triton-X-100 in non aqueous media as the absorption spectra of the dyes do not show any characteristic change in the absorption maxima in non-aqueous media containing triton X-100. This molecular interaction between the dyes and triton X-100 in aqueous media is considered to be charge transfer (CT) interaction. This is confirmed by the fact that absorption spectra of the dye-surfactant systems in the presence of small amount of NaCl are not affected.

Progressively alkylated thiazine dyes are structurally similar to phenosafranin; the former dyes are the substituted phenothiazines, while the latter is the substituted phenazine. It is, therefore, expected that thiazine dyes behave similarly to phenosafranin towards triton X-100. The thionine shows an absorption maximum at 597 nm. A spectacular change is noticed when the triton X-100 concentration is above the cmc, where all spectra show shifted absorption band at longer wave length, 608 nm, being a function of the concentration of triton X-100. The visible absorption spectra of other thiazine dyes (such as azure A, azure B, azure C and methylene blue) in aqueous solution of triton X-100 behave similarly. Spectrophotometric data were employed to calculate the thermodynamic as well as spectrophotometric properties of dye surfactant interaction. For 1:1 complex, the

equilibrium constant (K) and molar extinction co-efficient (ε) can be determined using the Benesi Hildebrand equation [79] or Scott equation [77].

From the thermodynamic and spectrophotometric properties of these complexes, the abilities of dyes to accept an electron are in the order azure C > thionine > azure A > azure B > methylene blue, where the values of K, ΔG^0, ΔH^0 and ΔS^0 are found to vary from 21.16 to 52.63 lit mol^{-1}, 7.61 to 9.88 $kJmol^{-1}$, 19.00 to 29.25 $kJmol^{-1}$, and 38.22 to 65.00 $Jmol^{-1}$ deg^{-1} respectively for these dyes. Using Scatchard [80] and Scott [77] equations, almost identical values of K and ε were obtained. Triton X-100 in carbon tetrachloride solution can not even solubilize the dye; it is expected that the hydrophilic part of triton X-100 interacts with the dye whereas there is no hydrophobic interaction between the dyes and triton X-100. The absorption spectra of thionine in different solvents such as acetonitrile, water-dioxane, acetone, ethanol, and tert-butanol exhibit absorption maxima at 593, 597, 520, 598, 600 and 607 nm respectively. Although the absorption maximum of thionine-triton X-100 complex appears at 612 nm, the shifted band of thionine in Triton X-100 solution exhibits at 608 nm. These results suggest that the positive centre of the dye molecules within the micelle is associated not with the lone pair electron on the ether oxygen atom, but with the lone pair of electron on the oxygen of the hydroxyl group for comparatively higher electron density. This molecular interaction between the dyes and Triton X-100 in aqueous medium is again considered to be a CT interaction.

The visible absorption spectra of Thionine along with the difference spectra of mixed solutions with a fixed concentration of Thionine and varying concentrations of Tween-80 in aqueous media at 298K were studied [81]. Thionine shows an absorption maximum at 597 nm. A remarkable change was noticed when the Tween-80 concentration was above the cmc, where the difference spectra showed shifted absorption band at longer wave length, i.e. 616 nm with an isobestic point at 600 nm, the magnitude of the absorbance at 616 nm being directly proportional to the concentrations of Tween-80. The visible absorption spectra of thionine in aqueous solutions of others surfactants except CTAB, above their cmc behaved similarly. In the presence of CTAB, the Thionine spectra were not perturbed at all, indicating no interaction between thionine and CTAB, whereas the presence of sharp isobestic point and spectral shift in other cases indicated 1:1 molecular complex formation between thionine and the surfactants. The equilibrium constant (K) as well as, molar

extinction coefficient of the thionine-surfactant interaction, were evaluated using the Benesi-Hildebrand equation [79].

Mukhopadhyay et al. [81] have shown the spectra for the thionine–tween-80 complex at three different temperatures (287, 298, 313K) and calculated the equilibrium constant and other thermodynamic parameters also. They have recorded the spectra of thionine (Th)-Tw-60, Th – Tw-40, Th – Tw-20, Th – Tx-100 and have determined the thermodynamic parameters.

The cationic dye thionine is expected to form a strong complex with anionic surfactant SLS. Mukhopadhyay et al. [81] have shown that thionine forms stronger complexes with all the non-ionic surfactants compared to SLS. The nature of interaction of this dye with the non ionic surfactants is therefore different than that with SLS. The thermodynamic and spectrophotometric parameters, ΔH^0, and ΔS^0 for thionine complexes with non-ionic surfactants are also higher. Since all these surfactants can not even solubilize the dye in carbon tetrachloride solution, it is plausible that the hydrophilic part of surfactants interacts with the dye in aqueous medium. A cationic dye can penetrate the non- ionic micelles to form a strong molecular complex at a polar site on the oxygen of the hydroxyl group for having comparatively higher electron density. The molecular interaction between the thionine and non ionic surfactants in aqueous medium is considered to be CT interaction. On the other hand, with the negatively charged micelles of SLS, the cationic dye will be held in the stern region due to coulombic interaction, and the dye will be repelled by the positively charged micelles of CTAB [82].

According to Mulliken's CT theory [82] the CT complex for the present system may be represented by a resonance hybrid of a non ionic ground state structure and an ionic excited state structure. For thionine (Th) and non-ionic surfactant (S), these two states are represented as Th ..... S and $Th^-.....S^+$. The excited or CT state is formed by the transfer of an electron from the non ionic surfactant, an electron donor to the dye, an electron acceptor on light absorption of suitable energy. It is shown that upon light excitation of the dye–non ionic surfactant systems, the primary charge separation takes place, forming a negatively charged dye and a positively charged surfactant and this charge separation causes photovoltage development when the illuminated and dark compartments of the cell containing dye-surfactant are connected to the electrometer. In the case of thionine-SLS system,

the interaction is ionic in nature, so no new ionic species are generated when the system is illuminated. The prominent interaction of thionine with surfactants above their cmc in aqueous medium indicates that the charged surface formation in micelle is a necessary criterion for complex formation. The interfaces (micelle/water) catalyze the CT complex formation due to absorption of thionine from solution and thus increase the concentration of CT complex. Mukhopadhyay et al. [81] concluded that the electron donating abilities of the non ionic surfactants towards the dye are in the order: tween-80 > tween-60 > tween-40 > tween-20 > triton X-100 and this is in accordance with the increasing alkyl hydrocarbon chain length, which in turn, increases the electron density at the electron-donating centre of the molecule, due to inductive effect. The presence of an aryl group in triton X-100 results in an opposite effect. They concluded that the nature of interactions of thionine with different types of surfactants is different. Thionine undergoes CT interaction with non-ionic surfactants, ionic interaction with negatively charged SLS, and no interaction with positively charged CTAB.

The absorption spectra of methyl violet, a cationic dye, were investigated in aqueous solution containing anionic, non-ionic and cationic surfactants above their cmc. The dye forms 1:1 electron donor acceptor or charge transfer complexes with different non ionic surfactants. The dye acts as the electron acceptor and the surfactants as the electron donors. The length of the alkyl hydrocarbon chain of the non-ionic surfactants influences the stability of the complex [83]. Recently association constant for the formation of cresyl violet-surfactant complex and the binding constant for the micellization of the dye, both in absence and in the presence of electrolyte have been determined. In these experiments, the dielectric constant experienced by cresyl violet within the SDS micelles has been found to decrease due to micellization process. The environment around cresyl violet in the anionic micelle of SDS is highly polar and electrostatic attraction between cresyl violet and anionic micelle favour location of dye close to the head groups of the micelle [84].

Investigations of photo-induced electron transfer reactions in surfactant solutions are not only inherently interesting and relevant to the understanding of photobiology but they are also potentially important for efficient energy conversion and storage. Surfactant solutions help to achieve the separation of photoproducts by

means of hydrophilic-hydrophobic interaction between the products and the interface [85-88].

4.1.3 Dye-Surfactant Interaction in Microemulsion Media

Microemulsions as discussed in chapter 1, differ from micelles by the complex composition and larger sizes of the particles as they contain compartmentalized water with surfactants and alcohols having medium hydrocarbon chains (e.g. n-hexanol, n- heptanol, etc.), generally called co-surfactant along with a nonpolar solvent. They are, therefore, characterized by a higher micro heterogeneity of interfaces and a higher solubilizing capacity of organic molecules and can also be treated as analogical model of biologically functioning systems [51], which are the basis of living matter. Apart from different synthetic applications [89,90] it is also used in the removal of dyes from water [91]. Solubilization of water in microemulsion (or reverse micelle) systems has been found to be dependent on various factors involving the rigidity of the interfacial film, which in turn depends upon the size of the polar head group and the hydrocarbon moiety of surfactant, the type of oils, the presence of electrolyte, the nature and valance of counterion, the temperature, etc [92]. The structure of the interfacial water of microemulsion systems is somehow different from bulk water. In the micro-encapsulated domain, the presence of amphiphilic head groups and the counterion (in case of ionic amphiphile) may significantly affect the water mobility [93,94]. Because of the peculiar chemical and physical properties [95] of the polar interior of reverse micellar aggregates, substantial efforts have been focused on the investigation of the state of water in the pool. To explore the properties of water in the compartmentalized states as in microemulsion different absorption and fluorescence probes, viz. TCNQ [96], acridine orange [97], pyrene [98] and cyanine [99] derivatives, etc have been commonly used. In past, Oldfield et al. [100] and Fletcher [101] analyzed their spectral data on the acid-base equilibrium of both interfacially as well as bulk located dyes to illustrate their behavior in microemulsions. They examined differences in properties of interfacial and bulk water in the water-pool of microemulsions obtained by using the surfactant AOT. The interfacial water molecules can interchange H^+ ion with the Na^+ ion of AOT and thus affecting the pH of the vicinal water. Though fluorescence [102] and ^{31}P-NMR [103] techniques have been used to

estimate the pH of microemulsions, but the extent of pH change of a buffer medium in the compartmentalized condition is still debatable mostly because the exact location of the probe molecule in the water-pool remains uncertain. The dielectric constant of the compartmentalized water can also be altered by changing the dimension of microemulsion [104]. These factors can alter the dissociation equilibrium of an indicator dye along with there corresponding absorption coefficient. Observations of many researchers [99-102] on dye-surfactant interactions in reverse micellar media suggests the formation of dye-surfactant salt, ionpair, molecular complex and changes in microenvironment in dye chromophore.

It is well known that when the molecular forms of a dye are electronically neutral or have same charge with the surfactant in micellar systems, the form of the dye with less or no charge is preferentially associated to the micelles [112-114,116,117]. However, the preferential location of the dye as well as the reasons for the preference among oil-water interface, bulk oil and bulk water, which determine the spectral behavior of the dyes in microemulsions are not clearly understood. Although there are many reports on the interaction of dye molecules with non ionic [99,107,108] as well as oppositely charged ionic [99,109-111] surfactants in microemulsion, such studies of molecular interactions of dye molecules in microemulsions of surfactants with similar charge is rare. If the dye molecules with similar charges as that of surfactants are present in the aqueous pool of the microemulsion, the model offers an ideal situation for monitoring the effect of compartmentalized water on the molecular interactions because chances of finding the dye molecules in the interfacial region becomes rare, and the question of uncertainty on the actual location of the probe does not arise. The presence of cosurfactant makes the situation even more complicated. In this connection it has been reported that organic dyes including azure A changes their properties by molecular encapsulation [115].

Spectral changes on increasing concentration of an aqueous solution of many dyes which have larger planer hydrophobic skeleton with hydrophilic substituents have been known for a long time. It is now well accepted that these spectral changes are mainly due to the aggregation of such molecules. Aggregation can bring about drastic changes in physical and chemical properties of the dyes, specially their photophysics. The photophysics and photochemistry of dyes in general are of

considerable interest in the observation of various phenomena such as fluorescence, phosphorescence, long range and short range excitation energy transfer and electron transfer and other modes of quenching, as probes for liquid structures for mixed solvents and various relaxation processes in solution [118]. Certain concentration effect is also observed during the study of photophysical and photochemical properties of ionic dyes including methylene blue (one of the thiazine dyes), which leads to enquire into the molecular states of these dyes in solution [119].

The strength of dye aggregation is strongly dependant on the structure of the dye molecules, nature of solvent and temperature. A number of physical descriptions of this phenomenon have been proposed to account for the changes in the dye spectrum but none is found superior than others. In this chapter attempt have been made to understand the nature of dye-surfactant interaction in aqueous medium and dye-dye aggregation and the effect of progressive alkylation of dye molecule in the water-pool of microemulsion media. The nature of dye-dye aggregation in the compartmentalized water of microemulsion has been discussed in terms of 'molecular exciton theory'.

4.1.4 Aggregation of Organic Dyes

Interests in dye aggregates have been generated afresh recently due to its role in light energy conversion devices along with photography and xerography. Of particular interest is their ability to sensitize large band gap semiconductor material such as silver bromide nanocrystals in colour photography. Because of their practical importance, several research groups have done experiments to investigate the excited state behavior and electron transfer reactions of dye aggregates [120-130]. Moreover, discovery of lyotropic liquid crystalline phases, which are known as 'chromonics' has added considerably to the present interest on the aggregation of organic dye systems [131-133]. Spontaneous occurrence of chirality of some squarine [134], cyanine [135,136], and porphyrine [137] dye aggregates, although made up by non-chiral molecules, have also been shown recently.

Most of the basic dyes in solution show deviations from the Beer's law at higher concentrations. This behavior has been attributed to the formation of dimers and higher aggregates of the dyes [138,139]. In general, the dimerization constants are in the range of 100-10000, corresponding to free energies ~ 8 –22kJ mol^{-1}. These

are of the order of the magnitude of formation of hydrogen bonds [140], as well as, of other types of interactions such as hydrophobic [141,142], vander Waals or $\pi-\pi$ interactions, dispersion forces [142], all of which are presumed to be present when dyes undergo self aggregation in solution. Remarkable changes in the spectral characteristics with increasing concentrations, and the effect of temperature on this have been studied to unravel the nature of the forces involved in dye aggregation. Aggregates of the above type are also formed at lower concentration in the presence of some natural or synthetic polymers [143,144] or polyelectrolytes [145,146]. In these cases the equilibrium constants are, at least, a factor 10 higher, so that aggregation can be observed at concentrations which are well behaved in the absence of the additives [147]. Bergman and O'Konski [148] described a spectroscopic study of methylene blue adsorbed on Na-bentonite. Spectral changes were found to follow with the changes in the amount of methylene blue (MB) adsorbed on the clay surface. Due to the fact that these changes are similar to the spectral shifts accompanying dimerization and polymerization of MB in aqueous solution, these shift also attributed to dye-dye interaction on the surface of the montmorillonite and the corresponding dimer dissociation constant was determined as 1.7×10^{-4} mol lit^{-1} at 25^{0}C. West and Pearce [149] examined the dimeric state of cyanine dyes and showed that the stability of the dimers, as measured by the free energy of dimerization, increase steadily with chain length. Authors showed that if a solution in which 95% of the dye is present as monomer is regarded as tolerable approximation to a solution of the pure monomer, the concentration at which this conditions prevailed was found to vary from 2.8×10^{-5} M (for $K=10^{-3}$) to 2.8×10^{-8}M (for $K = 10^{-6}$).

Baranova and Levshin [150] reported that Rhodamine 6G forms aggregates upto dimerization stage at concentration below 2×10^{-3}M, but higher aggregates are formed at higher concentrations. The change in the spectrum of an aqueous solution of 3,6 -diamino acridine dye with the increase in concentration was not very large, reliable results could not be obtained by Mataga [151]. However, the degree of aggregation and log K_n were determined by means of Zanker's method [152]. Hida and Sanuki [153] opined that the maximum slope method for evaluating dimerization parameters was more reliable over some other methods viz, Zanker's method. These authors also found the dependence of dimerization constants of a

number of dyes in neutral salt concentrations. In 1972, Selwyn and Steinfeld [154] presented a very convincing and detailed account of the absorption spectra of laser active dyes rhodamine B, rhodamine 6G and acridine red in aqueous, ethanolic and EPA (2 parts ethanol : 5 parts isopentane : 5 parts ethylether by volume) solutions as a function of concentration and temperature. The observed absorbance of the aqueous solutions of rhodamine B and rhodamine 6G was analyzed in terms of monomer-dimer equilibrium. The dissociation constants, $K = C^2_{monomer}/C_{dimer}$ were 6.8×10^{-4} and 5.9×10^{-4} mol/lit at 22°C for aqueous rhodamine B and rhodamine 6G solutions respectively. The absorption spectra of pure monomer and dimer were obtained for these two systems. Acridine red in H_2O was shown to be monomeric up to 3.38×10^{-5} M. Rhodamine B in ethanol formed dimers for which the equilibrium constant for dissociation was 1.1×10^{-4} mol/lit at 62°C and 4.9×10^{-5} mol/lit at 22°C. At -78.5°C higher aggregates are formed in ethanolic rhodamine B solutions whereas rhodamine 6G solutions (2×10^{-4} M) show no evidence for the formation of aggregates in ethanol, even at -78.5°C. Small amount of dimer was noted in acridine red-ethanol solution under the same conditions. Solutions of rhodamine B in EPA are totally dimeric at -196°C. At 22°C the equilibrium constant was 6.2×10^{-5} mol/lit, at -78.5°C it was 3.1×10^{-5} mol/lit. The low value of ΔH (3.36 kJ/mol) in this solvent gives a strong support to the hypothesis that hydrogen bonding is important in dimer formation. Rhodamine 6G-EPA failed to aggregate even when cooled to -196°C. Acridine Red - EPA is predominantly monomeric at 22°C; at -78.5°C an equilibrium constant for the dissociation of dimer of 4.4×10^{-4} mol/lit was calculated. James and Robinson [155] studied the self-aggregation of N(10)-alkyl derivative of acridine orange and their interactions with cationic and anionic surfactants. The dimerization of the dyes in aqueous solution was enhanced relative to acridine orange when the alkyl substituent has more than six carbon atoms. A temperature jump study of the dimerization equilibrium of the octyl and dodecyl derivatives shows the greater stability of the dimer which is reflected in lower rate constant for dissociation. This study further shows a variation of dimerization constant of acridine orange derivatives from 1.05×10^4 to $(79 \pm 52) \times 10^4$ lit/mol for variation of the number of carbon atoms in the alkyl group from 0 to 16. Kamat and Litchin [156] examined the electron transfer in the quenching of protonated triplet methylene blue by ground state molecule of the dye. They determined the extent of dimerization of methylene

blue spectrophotometrically and found to be negligible in solvents containing 50% (vol/vol) or more organic component. Association was found to be significant in neat water and they had taken the value of dimerization constants at 25°C with μ< 0.001M, as 2.5 x 10^{-3} lit/mol from the work of Zadoroznnaya et al. [157]. From these data, monomer amount in a solution with $[MB^+]_{stoich}$ = 2 x 10^{-4} M was calculated as ~ 83%. Arbeloa found changes in the shapes of visible absorption spectra of the fluorescein dianion when the concentration was increased, due to the formation of aggregates [158]. The absorption spectra of dilute dye solutions did not change remarkably with temperature. The variations produced in the spectra of the concentrated solutions with an increase in temperature were due to the dissociation of aggregates. The author applied an iterative method in computing the formation constants of aggregation of the dyes. In the concentration range between 5 x 10^{-6} and ca. 10^{-1}M, the dimerization constant (K_d) does not change appreciably. At the higher concentration the K_d value increases due to the non-negligible existence of other aggregates. The average dimerization constant at 20°C for concentration up to 10^{-1} M was 5.0 ± 0.2 (Standard concentration 1 mol lit^{-1}). The dimer formation enthalpy (ΔH_d), entropy change (ΔS_d), and Gibbs potential (ΔG_d), were found to be -28 ±1 kJ mol^{-1}, -82 ± 5 J $mol\text{-}K^{-1}$ and -3.9± 0.1 kJ mol^{-1} respectively. At higher concentrations, possibility of trimer formation was considered and examined in considerable detail. Arbeloa and Rohatgi-Mukherjee [159] determined the formation constants and absorption spectra of the dimer and trimer of phenosafranin in aqueous solutions. Using two different iterative methods [149,158], the two average dimerization constants at room temperature (28°C) with solutions of concentration smaller than 4 x 10^{-3} M were calculated as 42 ± 2 and 44 ± 2 lit mol^{-1} respectively. Thermodynamic functions for the dimerization process have also been determined. The enthalpy of dimerization, (ΔH_0), was found to be -17 ± 1 kJ mol^{-1}. The standard free energy change and entropy variations of the dimer formation were -9.4 ± 0.1 $kJmol^{-1}$ and -25 ± 5 $J.mol^{-1}K^{-1}$ respectively, at 28°C. The calculated enthalpy change was smaller than the usual values found for hydrogen bond i.e., about -20 kJ mol^{-1}. It has been proposed that besides the possible participation of hydrogen bond, contribution of vander Waals and London forces, which are temperature dependent to some extent, were also important in the dimer formation. The formation constant and absorption spectrum of the trimer were determined assuming that the trimer hypochromism H_t

is equal to H_d^2. The average trimerization constant at 28°C, thus calculated was 65 ± 10 lit.mol^{-1}, which is greater than the dimerization constant. Values of ΔG^0, ΔH^0 and ΔS^0 were -9.4 ± 0.1, -17 ± 1 and -25 ± 5 kJ/mol respectively for the trimerization process suggest that the forces responsible for aggregation are changing from an enthalpy directed one to an entropy directed one. The contribution of hydrogen bonding in the association process is decreased and that of the vander Waals force is increased. The increased hydrophobic interactions justify the substantial increase in the entropic contribution in higher aggregates presumably due to the breaking of water structure. Neumann et al. [160] examined the formation of mixed dimers in solutions of basic dyes. Mixed dimer equilibrium constants for various dyes were estimated to be between 1.4 x 10^2 and 4.9 x 10^4 lit/mol. However, the mixed dimer formation equilibrium constants are larger than those for self dimers. These are ascribed to a charge transfer contribution to the interaction as a result of the difference in the electron densities of different dyes.

4.1.5 The Molecular Exciton Model

The molecular exciton model offers a theoretical method for treating the resonance interaction of excited states of weakly coupled composite systems [161]. The types of problems which have been dealt with on the basis of molecular exciton model among others include spectra of dimers and polymers consisting of molecules held together by weak intermolecular forces (hydrogen bond, vander Waals forces etc.) and the electronic transitions of composite molecules (polyenes, parapolyphenyles and others), considered as resulting from the interaction of excited unit chromophores. In the weakly coupled composite systems for which the molecular exciton model offers a satisfactory approximation for the treatment of excited states, intermolecular (or interchromophore) electron overlap and electron exchange are negligible. In such systems the optical electrons associated with individual component molecules (or chromophoric units) are considered localized, and the molecular units (or chromophoric units) preserve their individual characteristics in the composite (aggregate) system, with relatively slight perturbation. The mathematical formalism then takes the form of a state interaction theory, with the omission of details of atomic orbital composition usual in molecular

electronic theories. The electronic states of the aggregate are then expressed in terms of the electronic states of the component light absorbing units.

Thus, the spectral properties of a molecular aggregate are related to the spectral properties of the component molecules by theoretical expressions involving observable experimental parameters: intermolecular distance, mutual intermolecular orientation and geometry, and intensity (oscillator strength) of light absorption by component molecules. Although the spectral effects of aggregation are small enough to satisfy the use of a quantum mechanical perturbation method, nevertheless these effects are extremely characteristics and may be understood on the basis of the quantum mechanical resonance of excited states. Thus, blue shifts, red shifts, or spectral splitting may be observed, depending on the geometry of the aggregate, accompanied by characteristic changes in polarization properties. Spectral absorption intensity changes may also be observed for the aggregate, and luminescence properties may be affected profoundly compared with those for the component molecules.

The exciton concept was introduced by J. I. Frenkel in 1931 in connection with the theory of transformation of electromagnetic radiation into heat in argon crystal. In 1948, A. S. Davydov applied the molecular exciton model to the problem of electronic states of naphthalene crystals. Since then, a host of researches have appeared exploring all aspects of the model. Davydov's "Theory of Molecular Excitons" [162] summarizes his results, and contains bibliographies of the research literature in this field. Simpson [163] explored underlying elements of the model under the title "Independent Systems Approach" in his "Theories of Electrons in Molecules". McClure's review [164] on the interpretation of the spectra of molecular crystals on the basis of exciton theory is a standard reference. Kasha, on the other hand, emphasized in applications of the molecular exciton model to non crystalline molecular aggregate systems. In a first paper, the distinction between atomic excitons and molecular excitons was stressed, together with the non conductive nature of exciton bands [165]. In a second paper, diverse spectral effects for various coupling strengths were described. The quasi-classical electrostatic vector model was developed as an aid in understanding exciton band formation and various mechanisms of excitation migration were elaborated on [166].

Molecular Exciton Wave Functions:

The starting point of the molecular exciton model treatment will be singlet electronic energy states and their corresponding electronic state wave functions for a component molecule of the aggregate. It is assumed that the electronic signlet state energies E_0, E_1, E_2 ..... and wave functions ψ_0, ψ_1, ψ_2 ..... are known, satisfying the individual molecule Schrödinger equation:

$$H_n\psi_n = E_n\psi_n \tag{4.1}$$

In general, each problem will involve only a pair of states and wave functions, so these may be designated as G and E for ground and excited singlet state energy, and ψ_u and $\psi_u^\dagger$ for corresponding state wave functions for molecule u. It is a very great abstraction to represent an entire molecule in an electronic state by ψ_u or $\psi_u^\dagger$. But these are the starting states for the model.

Molecular Dimers:

The ground state wave function for a molecular dimer consisting of two identical molecules will be (Figure 4.1).

$$\Psi_G = \psi_u\psi_v \tag{4.2}$$

where, ψ_u and ψ_v are wave functions associated with molecule u and v respectively. This is the unique ground state wave function of the dimer; it is totally symmetric with respect to all symmetry operations of the dimer.

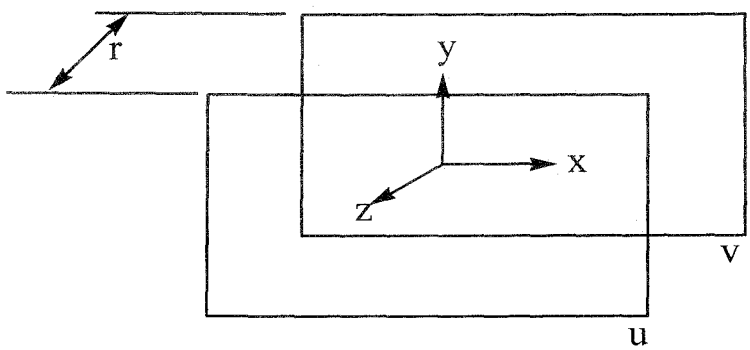

Figure 4.1 Structure and co-ordinate of parallel or card-pack dimer

The first excited state of the dimer can be described equally well by two possible wave functions,

$$\Phi_1 = \psi_u \psi_v^{\dagger} \qquad \text{and} \qquad \Phi_2 = \psi_u^{\dagger} \psi_v$$

These are degenerate and do not describe stationary states of the system. The correct zeroth order wave functions are,

$$\left.\begin{aligned} \Psi_I &= \frac{1}{\sqrt{2}}(\Phi_1 + \Phi_2) = \frac{1}{\sqrt{2}}\left(\psi_u \psi_v^{\dagger} + \psi_u^{\dagger} \psi_v\right) \\ \Psi_{II} &= \frac{1}{\sqrt{2}}(\Phi_1 - \Phi_2) = \frac{1}{\sqrt{2}}\left(\psi_u \psi_v^{\dagger} - \psi_u^{\dagger} \psi_v\right) \end{aligned}\right\} \tag{4.3}$$

Interchange of molecular levels u, v indicates that the first function is totally symmetric and the second is antisymmetric. In both of the stationary exciton states Ψ_I, Ψ_{II}, the excitation is on both molecules, u and v, i.e., the excitation is collective or delocalized. The node corresponding to minus sign in the exciton wave function is an excitation node not an electron orbital node. At an excitation node the phase relation between transition moments on the respective molecular centers changes sign.

The Intermolecular Perturbation Potential

The energy states and wave functions of molecular aggregate are determined by adding to the total Hamiltonian for the collection of unperturbed molecules a term $\sum_{l,k<l} V_{kl}$ where V_{kl} is the intermolecular interaction operator acting between molecules k and l, and the summation is carried over all pairs of molecules. This is essentially an intermolecular coulombic potential term, giving the interactions between charged particles (electron and nuclei) on the two molecules. However, the use of an exact coulombic potential, V_{coul}, would involve $1/r_{kl}$ as an operator (r_{kl} is the kl intermolecular distance), which would make simplification of the interaction integrals impossible. Accordingly, a point-multipole expansion can be used:

$$V_{coul} \cong V_{mono\text{-}mono} + V_{mono\text{-}di} + V_{di\text{-}di} + \ldots\ldots \tag{4.4}$$

For neutral total charge distribution the monopole interactions are zero. For allowed electric-dipole transitions, the dipole-dipole potential term becomes the leading one and higher multipoles are neglected. Thus, for strong absorption bands, corresponding to allowed electric dipole transitions

$$V_{coul} \cong V_{dipole-dipole} = -\frac{e^2}{r_{kl}^3}\sum_{i,j}\left(2z_k^i z_l^j - x_k^i x_l^j - y_k^i y_l^j\right) \tag{4.5}$$

where in the classical dipole-dipole potential r_{kl}, is the distance between the point dipoles in molecules k and l, and x_k^i is the x coordinate of the *i* th electron on molecule k, x_l^j is the x coordinate of the *j* th electron on molecule l, and so forth, the coordinate system being chosen with the z axis parallel to the line of molecular centers, and the summation is over all electrons in each molecule. Thus, an approximation may be introduced, which allows the physical interpretation that the excited state resonance splitting comes about from the electrostatic interaction of transition electric dipoles on neighboring or nearly neighboring molecules (the interaction falling off as the inverse cube of the intermolecular distance). Moreover, in most cases electron displacement along only one coordinate is effected by light wave causing the excitation at a particular frequency, so that in general only one term in the dipole-dipole interaction may remain, e.g., for the upper state of an x-polarized transition in a dimer consisting of two molecules u and v, whose transition moments are both parallel to the x-axis, the perturbation potential reduces to

$$V_{uv} = \frac{e^2}{r_{uv}^3}\sum_{i,j}\left(x_u^i x_v^j\right) \tag{4.6}$$

The Exciton Splitting in a Simple Dimer:

The application of the quantum mechanical molecular exciton formalism to the problem of spectral properties of vander Waals' dye aggregates was made by Simpson et al. for the case of pyridocyanine parallel or card-pack dimers [167]. The application to dimers of diverse geometries, especially for hydrogen bonded molecular pairs [168,169] was made by EL-Bayoumi and Kasha. The application to benzoic acid dimers was made by Nagakura et al. [170] considering the parallel card-pack dimer of Figure 4.1 to understand the spectral properties of such a molecular dimer, one must evaluate the excited state interaction energy to measure the exciton splitting, and the transition moment in order to determine the selection rules.

The Exciton Band Width

In evaluating the excited state interaction energy one should examine merely the exciton splitting for simplicity. The energy of interaction will be given by the

expectation value of the interaction potential with respect to the degenerate excited states of the dimer.

$$\mathscr{E} = \iint \psi_u \psi_v^{\dagger} V_{uv} \psi_u^{\dagger} \psi_v d\tau_u d\tau_v \tag{4.7}$$

where V_{uv} is the intermolecular interaction operator acting between molecules u and v. Inserting the form of V_{uv} appropriate to an x-polarized electric-dipole transition in molecules u and v (cf. Figure 4.1)

$$\mathscr{E} = \frac{e^2}{r_{uv}^3} \iint \psi_u \psi_v^{\dagger} \left(\sum_{i,j} x_u^i x_v^j \right) \psi_u^{\dagger} \psi_v d\tau_u d\tau_v \tag{4.8}$$

where x_u^i is the x co-ordinate of the i th electron on molecule u and x_v^j is the x co-ordinate of the j th electron on the molecule v. Because of the form of V_{uv}, this equation may be factored to yield.

$$\mathscr{E} = \frac{1}{r_{uv}^3} \left[\int \psi_u \left(\sum_i ex_u^i \right) \psi_u^{\dagger} d\tau_u \right] \left[\int \psi_v^{\dagger} \left(\sum_j ex_v^j \right) \psi_v d\tau_v \right] \tag{4.9}$$

where r_{uv} is the distance between the point dipoles in molecules u and v. One recognizes immediately that each of the integrals is now precisely the transition moment integral for the excitation of the individual (monomer) molecules u and v,

$$M_u = \int \psi_u \left(\sum_i ex_u^i \right) \psi_u^{\dagger} d\tau_u \tag{4.10}$$

At this point an arbitrary feature regarding the phase factor of the transition moment enters the picture. We must choose a phase relationship such that a lowering of energy or stabilization of the dimer excited state occurs for the exciton stationary state wave function Ψ_I chosen to lie lowest (cf. Figure 4.2).

Thus, in order to make the exciton stationary state wave function ψ_1 correspond to a lowering of energy $\mathscr{E}$, we can choose the phase factors so that

$$M_u = -M_v \tag{4.11}$$

This phase factor is an entirely arbitrary one. If we choose to define $M_u = +M_v$, then the stationary state exciton function Ψ_{II} of Figure 4.2 would lie lowest for the parallel dimers of Figure 4.1. The expression for the energy lowering or interaction energy for the parallel dimer of Figure 4.1 becomes

$$E = -\frac{M_u^2}{r_{uv}^3} \tag{4.12}$$

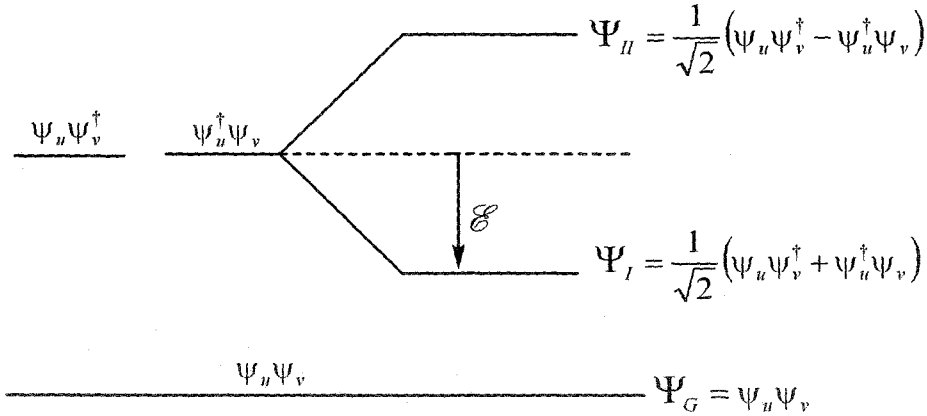

Figure 4.2 Schematic energy level diagram showing exciton splitting in molecular dimers (Displacement term omitted)

The exciton band width will be twice this value or $2\mathscr{E}$.

Thus, we see that the energy lowering for the simple dimer case at hand (Figure 4.1) is given by the monomer transition moment squared i.e., is proportional to the probability or intensity of the electric dipole allowed transition in the monomer, divided by the inter molecular distance cubed. Thus, the stronger the absorption band, the greater will be the exciton band splitting. One observes also that the r-dependence makes this a comparatively long range interaction.

For a dimer with arbitrary mutual orientations of molecular axes with respect to an x, y, z co-ordinate frame (Figure 4.1) the energy of interaction is given by

$$\mathscr{E} = -\frac{M_u^2}{r_{uv}^3}\left(2\cos\theta_u^z\cos\theta_v^z - \cos\theta_u^x\cos\theta_v^x - \cos\theta_u^y\cos\theta_v^y\right) \qquad (4.13)$$

Where again M_u represents the transition moment in a free molecule, and $\cos\theta_u^x$, $\cos\theta_u^y$, $\cos\theta_u^z$ represent the cosines of the angles which the transition moment M_u for molecule u makes with the x, y, z axes.

Selection Rules:

Although in the molecular dimer two exciton states theoretically result from the exciton splitting, both of these may not necessarily be observed as allowed spectral transitions. In fact, which exciton stationary states may be reached by electric dipole transitions from the ground state is a strictly geometry-determined problem.

Let us examine the spectral selection rules by evaluating the matrix elements of the electric dipole operator between the ground state and the stationary exciton states of the dimer. Thus, the transition moment vector of the dimer is given by

$$M^{I} = \iint \Psi_G (\mathscr{M}_u + \mathscr{M}_v) \Psi_I d\tau_u d\tau_v$$
$$M^{II} = \iint \Psi_G (\mathscr{M}_u + \mathscr{M}_v) \Psi_{II} d\tau_u d\tau_v \qquad (4.14)$$

Where $\mathscr{M}_u$, $\mathscr{M}_v$ are the electric dipole operators corresponding to the molecular electronic co-ordinates of molecules u and v. Evaluating these, and because of orthogonality and normalization properties of the intramolecular state wave functions following values of transition moments are obtained.

$$M^{I} = \frac{1}{\sqrt{2}}(M_v + M_u)$$

and (4.15)

$$M^{II} = \frac{1}{\sqrt{2}}(M_v - M_u)$$

For the card-pack dimer we had defined as required phase relations for the wave functions Ψ_I and Ψ_{II}, $M_u = -M_v$. Therefore, for the parallel or card-pack dimer of Figure 4.1, the transition moments corresponding to the stationary exciton states of Figure 4.2 are:

$$M^{I} = \frac{1}{\sqrt{2}}(M_v - M_v) = 0$$

and (4.16)

$$M^{II} = \frac{1}{\sqrt{2}}(M_v + M_v) = \frac{2M_v}{\sqrt{2}}$$

Thus, the transition moments for the dimer are given as super positions of the transition moments for the individual molecules. According to the above equation the oscillator strength (f) for electric dipole transitions between singlet states of the dimer Ψ_G and Ψ_1 is zero. For the transition to singlet state Ψ_{II} since

$f \propto (M^{II})^2 = 2 M_v^2$ or $f_{II,\,dimer} = 2f_{monomer}$

an allowed transition with no change of intensity per monomer is predicted.

4.1.6 Spectral Properties of Dimer in terms of Exciton Theory:

Three characteristics of vander Waals dye molecule parallel dimers have been recognized in the literature. These are (a) The absorption spectrum characteristically blue shifts by 2000-4000cm^{-1} in these dimers, (b) the prominent fluorescence of the monomer is invariably quenched, and (c) the relatively inefficient phosphorescence of the monomer becomes the predominant luminescence in the dimer. Simpson et al. [167] and McRae and Kasha [171] have interpreted these properties in dye molecule dimers and polymers on the basis of the molecular exciton splitting and selection rules in the dimer. In the monomer, absorption to the lowest singlet excited state is strongly allowed, and the very rapid fluorescence emission competes with excitation of the lowest molecular triplet state. In the dimer, the allowed exciton state is at significantly higher energy than the singlet excited state of the monomer: a blue shift is thus accounted for in case of the card-pack, or parallel dimer. However, collisions rapidly deactivate the excited dimer to its lower singlet exciton stationary state. But this state is a metastable signlet state with an improbable fluorescence capacity. Further deactivation of the dimer to the triplet state becomes the most probable path for the excitation. Thus the fluorescence is quenched, and a very strong triplet state to ground singlet state emission is observed. Reference [171], contains a general bibliography of the various experimental observations on spectral consequences of dye dimerization. The parallel or card-pack structure probably fits quite well to vander Waals dimers consisting of large planar dye molecules. However, numerous other dimer structures are possible, and the exciton model permits a qualitative and semi-quantitative discussion of such dimers as well. These have been described in references [166,168-170]. In particular, for head-to-tail orientation of transition moments in the dimer, a strong red shift is predicted, with the upper exciton component forbidden in the dimer; whereas, in the oblique dimer, with mutual angle between molecular transition moments between 0 and π, both exciton components are observed with a spectral splitting as the characteristic result. These general dimer results may be gleaned from the linear polymer exciton model treated by McRae and Kasha [171]. Rohatgi and Mukhopadhyay [172] studied the dimer spectra of fluorescein and some of its halogen derivatives in aqueous solution. From the splitting observed in the spectra, the inclination of the component molecules in a dimer has been obtained on application of the theory of exciton interaction. The

distance r between the two component molecules in the dimer was also calculated for various geometries. In other series of publication Arbeloa [158,173] studied molecular structures of the dimeric and trimeric states of fluorescein dianion. The absorption spectra of the dimer and trimer of the dye molecule in aqueous solution were evaluated. The geometric structures of both aggregates were determined using the exciton theory. The nature of the association forces was also studied. Evidence was presented for the formation of Eosin Y dimer as the highest aggregates of complexes between eosin Y and poly-L-lysin, poly (1-xylyl viologen) or cetyl-pyridium [174]. The absorption spectra of these complexes have been obtained free from contamination by Eosin Y monomer spectrum and were fitted with Gaussian band model, using a non-linear least square fitting computer program. Using such models, exciton theory had been employed to calculate parameters such as orientation and molecular separation of the components of the Eosin Y dimer. Where appropriate, these parameters have been compared with the dimensions of the repeating unit and the possible conformations of the polymer [174]. Basu et al. [175] studied concentration effects on the absorption and emission properties of Ni (II) and Zn(II) tetra(p-venyl phenyl) porphyrins in benzene solutions. Whereas exciton splitting of the soret band was observed for the Ni (II) complex, only a hypochromic effect is observed for the Zn(II) complex. The exciton parameters were calculated for Ni complexes. Arbeloa et al. [159] also studied the excitonic interaction and the nature of bonding in the aggregation of phenosafranin from concentration dependent spectral changes.

By applying simple exciton theory in zero order an attempt has also been made to study the geometric structure of the trimer, as has been accomplished for xanthene aggregates [158,159]. Molecular model showed that the angle θ between the chromophore groups of the monomers is due to the steric effect between the phenyl groups. Newmann et al. [160] put forward evidences of the formation of mixed dimers of basic dyes, which shows spectroscopic properties in accordance with exciton theory. The bands of these dimers can be found at wave lengths shorter and longer than those of the forming dyes, with higher and lower excited states, respectively. These bands correspond to the transitions of both the in-phase (high energy) and out-of-phase (low energy) transition moment geometries, none of which are prohibited.

In a recent publication Horng and Quitevis [176] observed that expanding the scope of analysis to include dye aggregation and exciton theory enhances the pedagogical value of studying the visible absorption spectra of conjugated dyes in the physical chemistry curriculum. As has been already mentioned, the exciton theory of dipole-dipole coupling can be used to relate the distance and relative orientation of monomeric dye molecules, cyanine and Merocyanine dyes are known to form aggregates in concentrated, aqueous solution exhibiting a strong spectral shift of absorption band toward longer wave lengths with respect to the monomer absorption. These assemblies have been named J-aggregates. In other cases the absorption band is shifted upon aggregation toward smaller wavelength and the corresponding assemblies have been termed H-aggregates [177] Practically, the J-aggregates has served as an important spectral sensitizer in silver halide photographic material as the electronically excited J-aggregates can effectively inject photo-electron into the conduction band of silver halide and its sharp absorption band allows easier control over the spectral sensitivity of the photo imaging system [178].

Progressively alkylated thiazine dyes are known to show interesting spectral characteristics in solution and have been used in photogalvanic and photochemical studies [116,179,180]. They can also be often designated as azures (Figure 1.4c-e in Chapter 1) and are also acted as useful photosensitizes [181]. Hence, they have been have selected for the present study. The absorption UV-Vis spectroscopy is one of the most suitable methods for quantitative study of the aggregation properties of the dyes as a function of concentration in both aqueous and microemulsion media.

4.2 Experimental

Five progressively alkylated thiazine dyes viz. thionine (Th), azure A (AzA), azure B (AzB), azure C (AzC) and methylene blue (MB) were supplied by Aldrich Chemical Co., USA. The structure of all thiazine dyes are shown in Figure 1.4 of Chapter 1. N-Cetylpyridiniumbromide (≥97.0 %, Fluka, Switzerland), Chloroform, n-heptane, (E-mark) used are analytical in grade. Chloroform and n- heptane were distilled for further purification by usual method [182]. CPB was used as received. Source and purification of other two surfactants, viz. SDS and AOT are mentioned in chapter 3. All the five dyes were found to contain colured impurities. They were

purified over a chromatographic column of silica gel using chloroform-methanol mixture as elutent. AzC was extracted efficiently with 8:2 chloroform-methanol mixture whereas, azure A was extracted with 7:3 solvent mixture. All other dyes were eluted by less polar solvent mixtures than that used for AzA. Finally they were recrystallised and dried at 50^0C under vacuum. Purity of the dye samples were checked by TLC using 8:2 water-acetic acid mixtures as the mobile phase and purity of all dyes except AzC were found to be excellent. The commercial AzC contained high percentage of insoluble materials in addition to other coloured impurities. Even after repeated chromatographic treatment it gave faint additional spot on the TLC plate indicating the presence of a small amount of impurity. However, although the purification of this dye was not up to the level of other dyes, various analyses (spectral and analytical) showed that final purity of the dye was satisfactory. Except thionine all dyes supplied as chloride salts and are highly soluble in aqueous medium. Thionine was also being changed to its corresponding chloride from acetate salt by passing through the ion exchange column (Amberlite IRA 400, BDH, England) containing chloride ion. Doubly distilled water having conductivity 2 μS cm^{-1} was used throughout experiment.

With in the dye solutions (of order 10^{-5} M) appropriate amount of SDS and AOT were added to investigate the influence dye on micellar aggregation at a fixed temperature of 303K.

Microemulsions were obtained by adding water in solution of CPB in 1:1 (v/v) chloroform and n-heptane and mixing them well until the mixtures become totally transparent by using a micropipette. By varying the proportion of water and CPB, the [water]/[CPB] mole ratio, ω was varied. Chloroform was used for preparing microemulsion for increasing the polarity of the oil phase to some extent so that large amount of surfactant can be dissolved in the mixture to produce larger water-pool.

Absorption spectra were recorded on a double beam Jasco V-530 UV/vis spectrophotometer (Japan). The spectra were recorded with a quartz cell having 1 cm and 1mm optical path length. The temperature of the whole experiment was maintained at 303K with a thermostatic arrangement coupled with the spectro-photometer.

4.3 Results and Discussion

4.3.1 Interaction of Thiazine Dyes with SDS and AOT in Aqueous Media

The representative visible absorption spectra of all thiazine dyes (1.17×10^{-5} – 2.10×10^{-5}M) in aqueous media with and without SDS and AOT were recorded. The spectra taken in a cell of 1 cm path length are shown in Figure 4.3 – 4.12. As the concentration of SDS is increased from 4.0×10^{-3} M to 2.82×10^{-2} M in each thiazine – SDS system, which essentially covers both pre and post micellar concentrations of SDS (cmc of SDS in aqueous solution = 8.6×10^{-5} M at 303K [183]), the intensity of spectra is increased significantly. In the visible region the dyes (10^{-5} mol.dm^{-3}) viz. Th, AzA, AzB, AzC and MB have absorption bands λ_{max} of 598, 634, 646, 620 and 661 nm with extinction coefficients of 6.16×10^4, 5.18×10^4, 6.90×10^4, 4.96×10^4 and 7.20×10^4 respectively in aqueous solution (Table 4.3). But in presence of submicellar concentration of SDS the spectral absorbance decreased markedly in case of thionine. The band shape also changed with the shifting of λ_{max} to 634 nm with a large shoulder at 520 nm. From the spectral feature it can be said that there must exist some dye-surfactant interactions.

It was reported that the degree of shifting of λ_{max} of a dye which form self-aggregation depends on the number of monomer involved in the aggregation process and on the geometry of the aggregates as has already been mentioned [184]. The planer dyes such as acridine orange and methylene blue aggregate in stacked manner and exhibit blue shifted metachromasia [184,185], where as nonplaner dyes such as pseudoisocyanine aggregate in a staggered way and depict a red shift of λ_{max} [186]. Figure 4.3 shows the effect of different concentrations of SDS on the absorption spectrum of thionine. Datta and Bhat [187,188] proposed the formation of "water-structure-enforced ion pairs in which the head groups of the surfactant molecule is attached to the sulfonate group of methyl orange (MO)" in order to explain the large blue shift in the spectrum of MO upon addition of small amount of a cationic amphiphile. Although the dye and the surfactant molecules are individually hydrated in the solution, long range electrostatic and short range hydrophobic forces may cause the formation of dye-surfactant complexes. Values of calculated monomer suggest that all the thiazine dyes in the concentration range $1\sim2 \times 10^{-5}$ M are present mostly in the monomeric form [193]. On the other hand, the dye-surfactant complex is formed involving electrostatic interaction between the negative charge of anionic

surfactant and positively charged dye molecule (particularly with the $-NH_2^+$ group), with the alkyl chain of the surfactant in close contact with the rest of the dye molecule. Some of these complexes can aggregate and precipitate in the solution which is in equilibrium with the precipitates. The loss of absorbance of dye solution in submicellar concentration region of a surfactant may be to some extent due to the precipitation of dye in the solution. However, in the present systems, hydrophobic forces do not play any significant role in the interaction of dyes with surfactants because dyes are highly water soluble and only coulombic interactions may be important. Similar premicellar aggregates were reported upon the interaction of oppositely charged 3,3'-diethylthiacarbocyuanine (DTC) and SDS at [SDS] $\geq 10^{-5}$M [189]. This kind of interaction registers a drop of fluorescence quantum yield over the premicellar concentration range of surfactant as was reported by Tatikolov and Costa [99]. These authors used cetyltrimethylammonium chloride (CTAC) as the surfactant and a synthetic cyanine as the oppositely charged dye. However, in the present investigation, further addition of SDS (>cmc) to the thionine-SDS solution leads to a small red shift of about 3nm (λ_{max} = 601nm) relative to that of aqueous solution (λ_{max} = 598nm) [representative spectra are shown in Figure 4.3]. Shape of the spectral band also appears very much similar to that of the spectra in aqueous solution. It is obvious that as the concentration of SDS micelles increased, the solubility of dye is also increased via the formation of dye-micelle aggregates in aqueous solution, resulting in a slight red shift in the spectrum with an increase in intensity of the absorption. It may also be mentioned that in post micellar concentration range, dye molecules remain in the interface of the micelles due to coulombic attractive force. Change of polarity of the associated water molecules in the vicinity of the micellar surface may be responsible for the small shift of the spectral peak. In this connection it should be noted that Tatikolov et al. [99] found only weak interaction between TX-100 and cyanine dye due to absence of any significant electrostatic attraction. Concentration of TX-100 at below and somewhat above cmc (cmc = 2.6 x 10^{-4}M) did not yield any effective change of photophysical parameters of the dye. The authors observed a slight red shift in the dye fluorescence spectrum only in presence of high surfactant concentrations ([TX-100] $\approx 10^{-3}$M), and this shifting was found to increase with surfactant concentration slowly.

All the other four thiazine dyes also behave similarly when treated separately with SDS. However, marked change of the spectral feature in submicellar concentration of surfactant was observed as a function of degree of alkylation of thiazine dyes (viz., AzA, AzB, AzC and MB). The dyes give much intense shoulder in the lower wavelength region like thionine. This observation also supports the fact that the alkylated planer thiazine dyes having comparatively larger hydrophobic moieties stacked firmly with the surfactant molecule, while the hydrophobic interactions along with the coulombic attraction play important role in the formation of the dye-surfactant complex.

Similar experiments were also carried out with another important anionic surfactant viz., AOT (Figure 4.8 – 4.12). Due to its double strand hydrophobic chain AOT has marvelous surface activity. Within a wide range of premicellar and postmicellar concentration of AOT, the λ_{max} of the spectral band does not show any significant shift. However, just like SDS, an intense shoulder appears at 564 nm in premicellar concentration of AOT. Among other dyes, Azure B gives an extra peak at 593 nm when treated with AOT in its submicellar concentration range. The characteristics of the spectral features observed due to the interaction of dye with AOT are well explanatory on the basis of intense ion-pair formation in submicellar media followed by dye-micelle interaction in the higher concentration (>cmc) ranges of the surfactant. Some of the spectral characteristics of progressively alkylated thiazine dyes in aqueous solution in presence of SDS and AOT in pre and postmicellar concentration are listed in Table 4.1.

4.3.2 Determination of cmc of Surfactants and Dye-surfactant Association Constant

Organic dyes may provide a simple and rapid method for the cmc determination of a surfactant owing to the large change in their spectrophotometric properties that accompanies micelle formation [191]. However, in many cases the apparent cmc varies with the dye's charge and concentration [191] and is in disagreement with values obtained by other physical methods, such as conductance and surface tension measurements. Samsonoff et al. [24] have successfully used UV-vis spectroscopy to determine the cmc of anionic, cationic, zwitterionic and nonionic surfactants by using

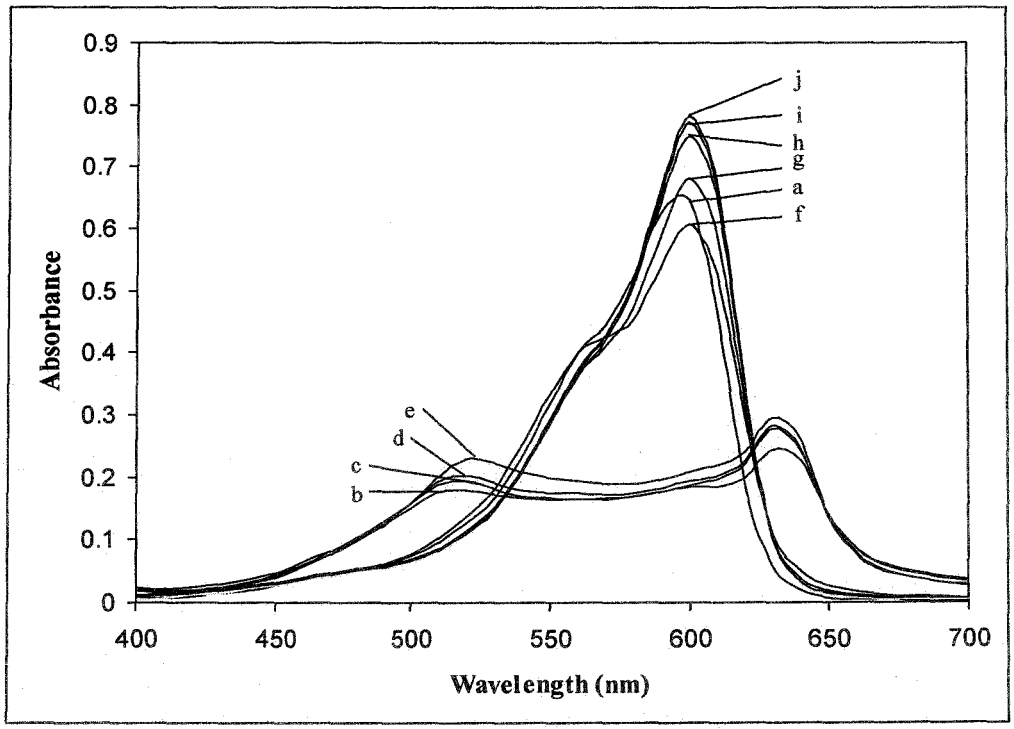

Figure 4.3 UV-Vis Spectra of Thionine (1.50 x 10^{-5}M) in aqueous solutions of various concentrations of SDS at 303K. [SDS]/10^{-3}M: (a) 0.00, (b) 4.00, (c) 4.96, (d) 5.93, (e) 7.04, (f) 8.00, (g)11.57, (h) 12.50, (i) 15.70, (j) 20.02, (k) 25.01.

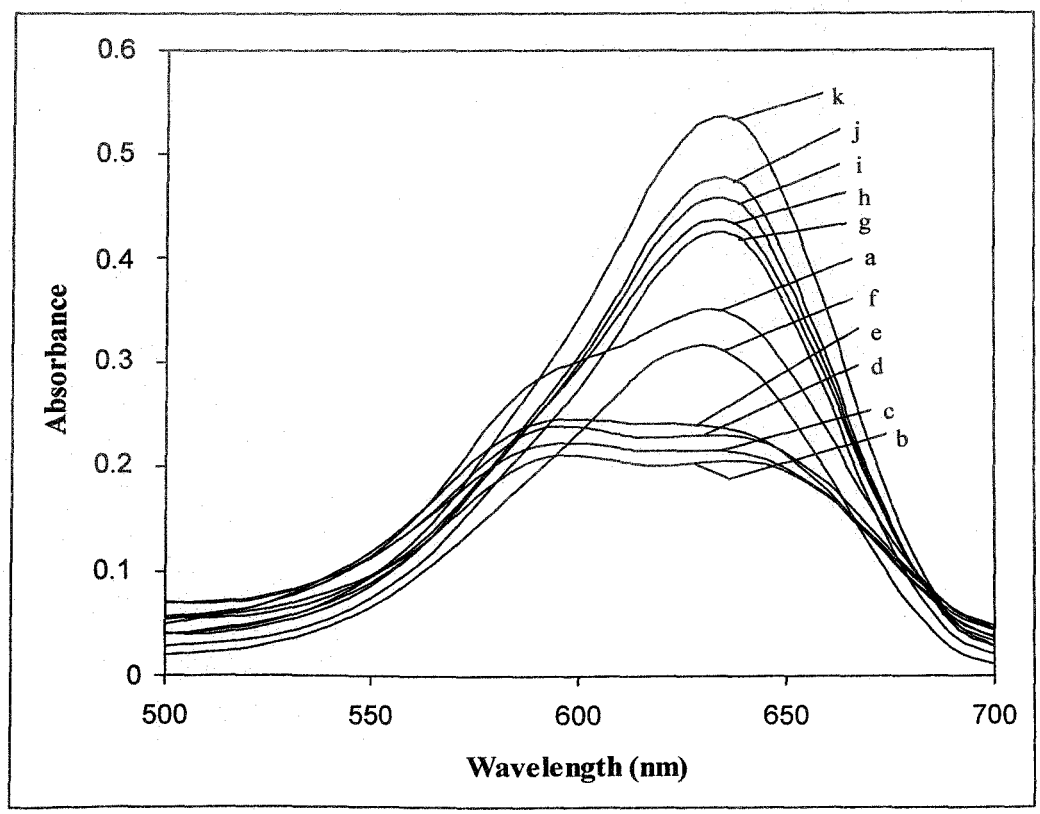

Figure 4.4 UV-Vis Spectra of Azure A (2.10 x 10^{-5}M) in aqueous solutions of various concentrations of SDS at 303K. [SDS]/10^{-3}M: (a) 0.00, (b) 4.00, (c) 4.96, (d) 5.93, (e) 7.04, (f) 10.50, (g)11.57, (h) 12.50, (i) 15.70, (j) 20.02, (k) 25.01.

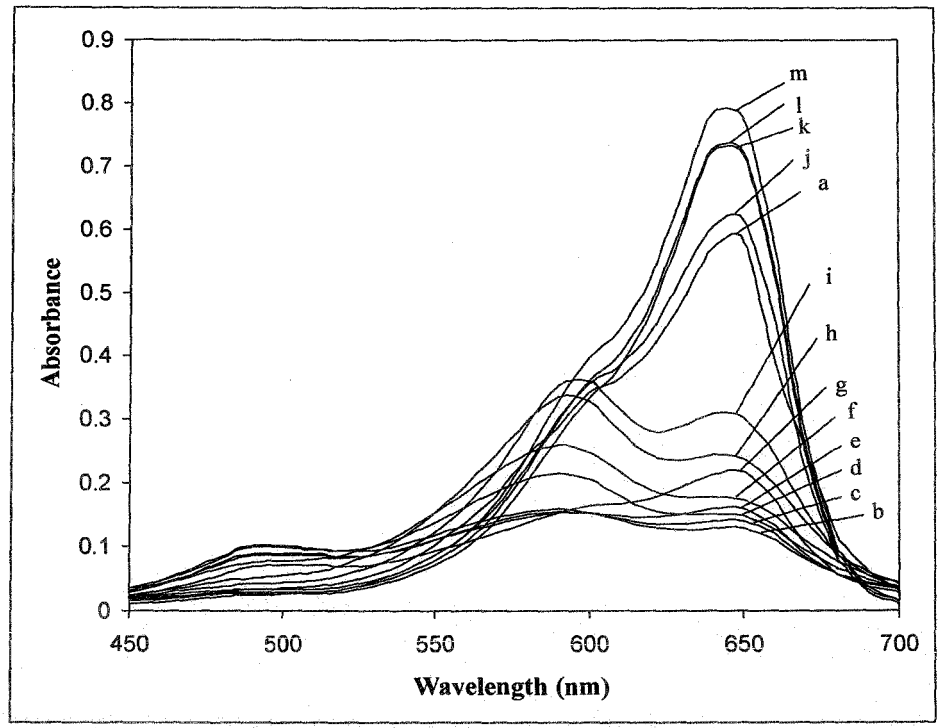

Figure 4.5 UV-Vis Spectra of Azure B (1.20×10^{-5}M) in aqueous solutions of various concentrations of SDS at 303K. [SDS]/10^{-3}M: (a) 0.00, (b) 4.00, (c) 4.96, (d) 5.93, (e) 7.04, (f) 7.55, (g) 8.02, (h) 12.50, (i) 15.70, (j) 20.02, (k) 22.03, (l) 25.01, (m) 28.2.

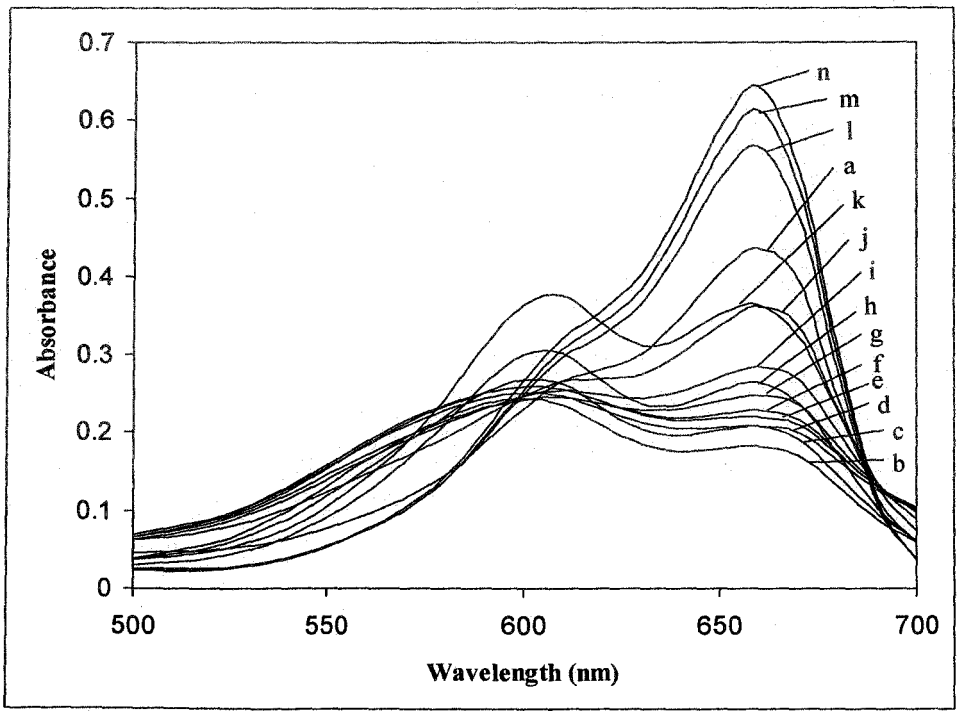

Figure 4.6 UV-Vis Spectra of Methylene Blue (1.17×10^{-5}M) in aqueous solutions of various concentrations of SDS at 303K. [SDS]/10^{-3}M: (a) 0.00, (b) 4.00, (c) 4.96, (d) 5.93, (e) 6.50, (f) 7.00, (g) 8.02, (h) 8.50, (i) 7.55, (j) 9.02, (k) 14.30, (l) 22.01, (m) 25.2, (n) 28.2

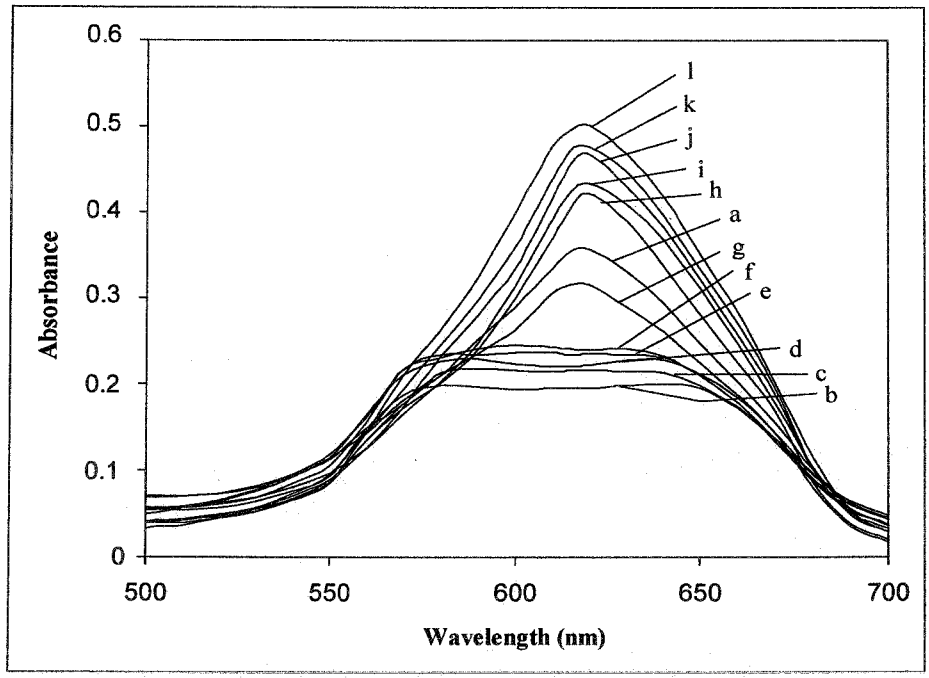

Figure 4.7 UV-Vis Spectra of Azure C (1.24×10^{-5}M) in aqueous solutions of various concentrations of SDS at 303K. [SDS]/10^{-3}M: (a) 0.00, (b) 4.00, (c) 4.96, (d) 5.93, (e) 7.04, (f) 8.00, (g) 9.23, (h) 12.50, (i) 15.70, (j) 20.02, (k) 22.3, (l) 25.01.

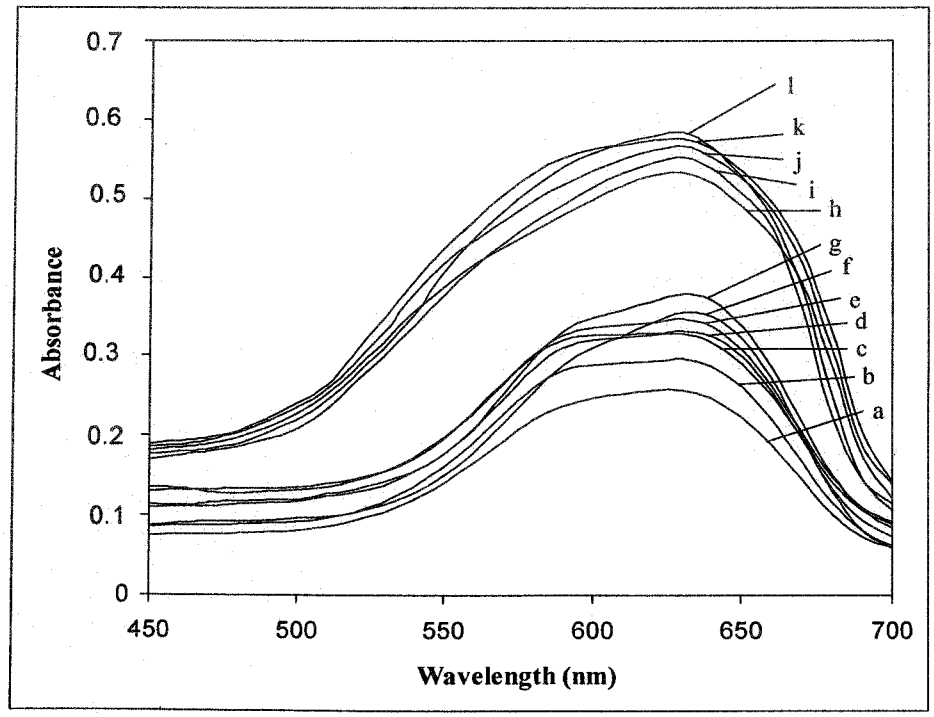

Figure 4.8 UV-Vis Spectra of Azure A (2.10×10^{-5}M) in aqueous solutions of various concentrations of AOT at 303K. [AOT]/10^{-4}M: (a) 4.00, (b) 6.02, (c) 7.28, (d) 8.80, (e) 10.01, (f) 15.06, (g) 19.80, (h) 23.96, (i) 27.00, (j) 60.23, (k) 70.30, (l) 80.51

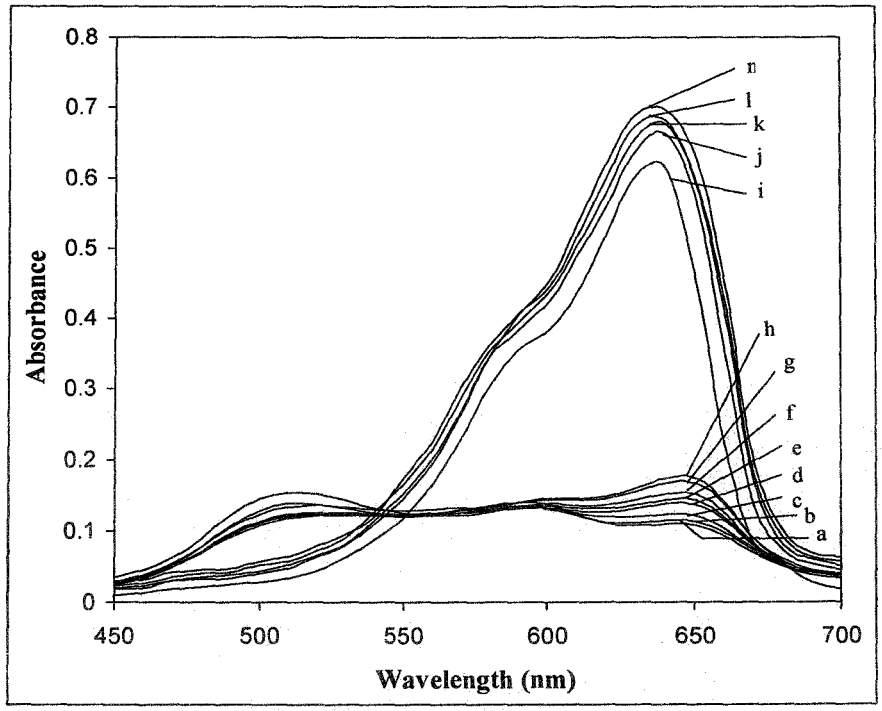

Figure 4.9 UV-Vis Spectra of Azure B (1.20 x 10^{-5}M) in aqueous solutions of various concentrations of AOT at 303K. [AOT]/10^{-4}M: (a) 4.00, (b) 6.02, (c) 7.28, (d) 8.80, (e) 10.01, (f) 15.06, (g) 19.80, (h) 23.96, (i) 27.00, (j) 60.23, (k) 70.30, (l) 80.51, (m) 92.30.

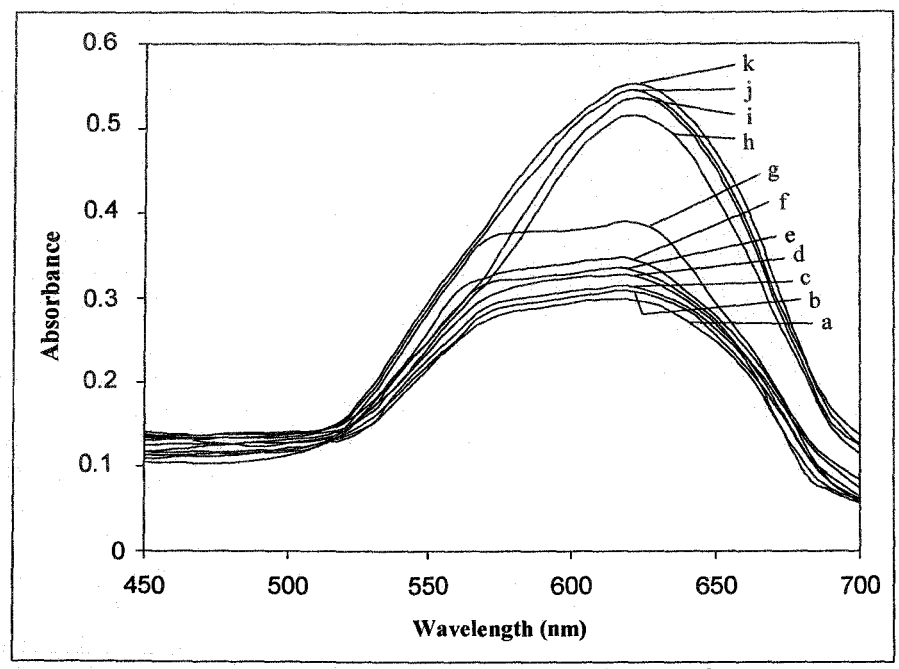

Figure 4.10 UV-Vis Spectra of Azure C (1.50 x 10^{-5}M) in aqueous solutions of various concentrations of AOT at 303K. [AOT]/10^{-4}M: (a) 4.00, (b) 6.02, (c) 7.28, (d) 8.80, (e) 15.01, (f) 20.06, (g) 25.80, (h) 40.96, (i) 50.00, (j) 60.23, (k) 70.30,

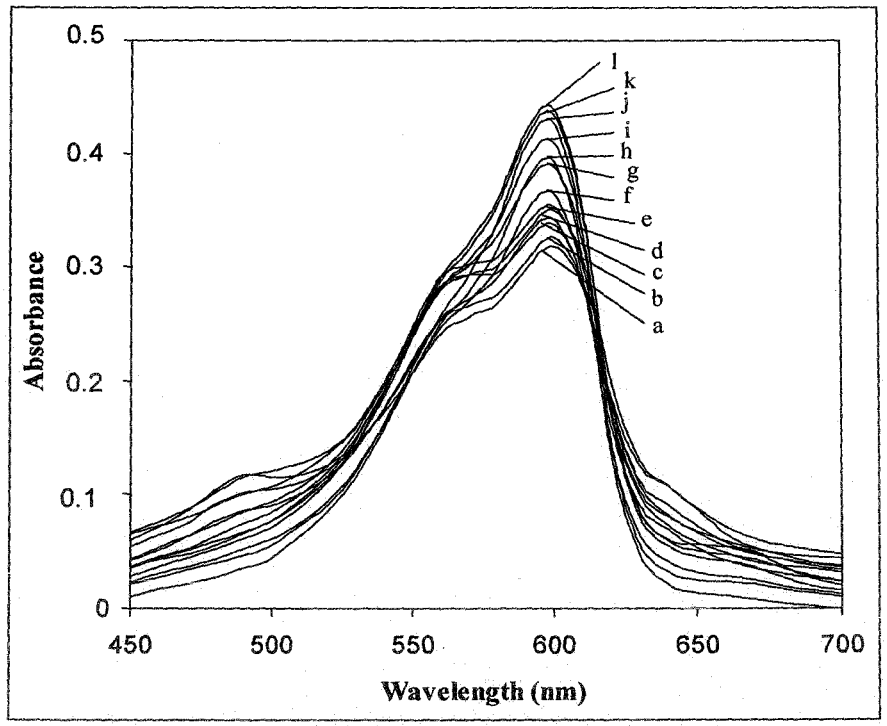

Figure 4.11 UV-Vis Spectra of Thionine (1.50×10^{-5}M) in aqueous solutions of various concentrations of AOT at 303K. [AOT]/10^{-4}M: (a) 4.00, (b) 6.02, (c) 7.28, (d) 8.80, (e) 15.01, (f) 20.06, (g) 25.80, (h) 40.96, (i) 50.00, (j) 60.23, (k) 70.30, (l) 80.51

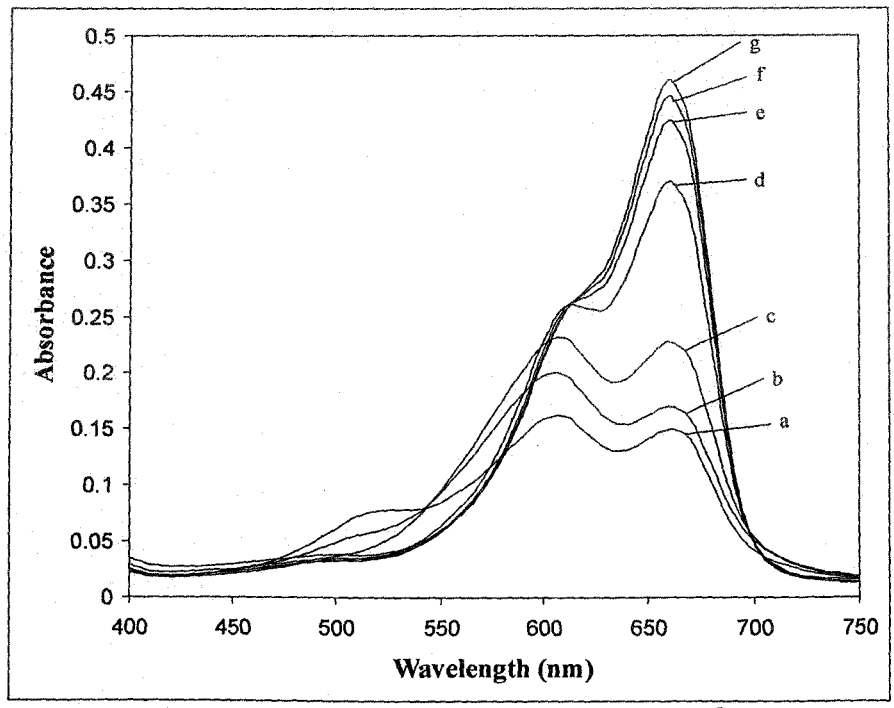

Figure 4.12 UV-Vis Spectra of Methylene Blue (1.17×10^{-5}M) in aqueous solutions of various concentrations of AOT at 303K. [AOT]/10^{-4}M: (a) 8.10, (b) 10.01, (c) 15.06, (d) 19.80, (e) 27.00, (f) 60.23, (g) 70.30.

Table 4.1

Some of the Spectroscopic Characteristics of Dyes in Aqueous Solution in pre-micellar and post-micellar concentration of SDS and AOT at 303K

Dye	Pre-micelle				Post-micelle		
	λ_{max} (nm)	λ_1(nm) (shoulder)	$\Delta\lambda$ (nm) = $\lvert(\lambda_{max}[aq] - \lambda_{max}[mic])\rvert$	λ_{max} (nm) (aqueous)	λ_{max} (nm)	λ_1 (nm)	$\Delta\lambda$ (nm) = $\lvert(\lambda_{max}[aq] - \lambda_{max}[mic])\rvert$
			SDS				
Thionine	634	520	36	598	601	564	3
Azure C	620	570	0	620	620	–	0
Azure A	634	593	4	630	634	–	0
Azure B	648	591	2	646	645	600	1
Methylene Blue	661	604	0	661	658	612	3
			AOT				
Thionine	598	564	0	598	598	564	0
Azure C	618	570	2	620	618	–	2
Azure A	634	591	4	630	634	591	4
Azure B	646	512	0	646	646	580	0
Methylene Blue	661	608	0	661	661	614	0

Coomassie brilliant blue G-250 (CBB) dye as a probe. They found the cmc values very close to the other literature values. Huang et al. [23] also described a method of cmc determination by measuring surfactant catalyzed redox reaction rate between H_2O_2 and bromopyrogallol red (BPR), a triphenylmethane dye. They used two cationic surfactant, viz. cetylpyridinium bromide (CPB) and cetyltrimethylammonium bromide (CTAB) for their experiment.

The association of a substrate or a probe (dye) molecule with a surfactant micelle can be described by the following equilibrium [190]:

$$D_w + S_m \underset{}{\overset{K_{ass}}{\rightleftharpoons}} D_m \qquad (4.17)$$

for which the equilibrium or association constant, K_{ass} is given by the expression

$$K_{ass} = \frac{[D_m]}{[D_w][S_m]} \qquad (4.18)$$

where $[D_w]$ and $[D_m]$ denote the concentrations of probe in aqueous and micellar phase respectively, and $[S_m]$ is related to the total surfactant concentration, $[S_t]$ by the relation

$$[S_m] = [S_t] - \text{cmc} \qquad (4.19)$$

It has been already pointed our that the shape of the visible absorption spectra of thionine dyes are greatly influenced in the presence of submicellar concentration of SDS and AOT due to strong electrostatic interaction between the surfactant and dye molecule. However, when the surfactant concentration reaches cmc value, at the onset of homogeneous micelle formation, the spectral feature is restored, but the absorbances at λ_{max} is greatly enhanced as compared to the values observed in the pure aqueous solution of the corresponding dye. From this marked change in the spectral intensity of the dye below and above cmc of the surfactant, the dye-surfactant association constant (K_{ass}) and critical micelle concentration (cmc) of SDS and AOT at 303K have been determined based on the methods of Nigam et al [190] and Datta et al. [192]. Considering the equilibrium 4.18 and the mass balance variation 4.19 one can easily derive the following equation [22,192]:

$$\frac{(d_0 - d)}{(d - d_m)} = -K_{ass}.cmc + K_{ass}[S_t] \qquad (4.20)$$

where d_0, d and d_m are the absorbances of the dye in absence of surfactant, in presence of post-cmc surfactant concentration $[S_t]$, and in excess of surfactant respectively at a fixed wavelength of the band where absorbance increases with the concentration of the added surfactant. A plot of $(d_0 - d)/(d - d_m)$ versus $[S_t]$ is linear with slop equal to K_{ass} and the intercept of the abscissa equal to cmc. The plots of $(d_0 - d)/(d - d_m)$ vs. $[S_t]$ for different dye surfactant systems are shown in Figures 4.13 - 4.21.

Table 4.2

Spectroscopically determined cmc of SDS and AOT with Gibbs free energy (ΔG^0) and the corresponding association constant (K_{ass}) of dye-surfactant at 303K

Surfactant	Dye	cmc /(mol.dm^{-3}×10^3)	K_{ass} /(dm^{-3}.mol)	$-\Delta G^0$ /(kJ.mol^{-1})
SDS	Thionine	8.82 (7.60)	285.2	14.24
	Azure C	8.72 (8.40)	173.6	12.99
	Azure A	9.02 (8.20)	121.4	12.09
	Azure B	8.80 (8.50)	109.0	11.82
	Methylene Blue	8.40 (8.50)	96.5	11.51
AOT	Thionine	2.65 (2.80)	90.6	11.35
	Azure C	2.82 (2.60)	70.3	10.71
	Azure A	2.87 (2.50)	60.1	10.32
	Azure B	3.01 (3.00)	50.1	9.86
	Methylene Blue	2.85 (3.10)	48.3	9.77

The plots are linear which indicates the validity of the equation (4.20). Present method yields cmc values much easily compared to other spectroscopic methods using probes [191]. The values of $[S_t]$ corresponding to the point where the straight line meets the abscissa, gives cmc of the surfactant. The points for $[S_t]$ below cmc fall on the abscissa due to the absence of micelles in the system. The inflexion points of the plots of absorbances as a function of surfactant concentrations (Figure 4.22 - 4.27) also correspond very nearly (but not exactly) to the cmc value of the surfactants. The

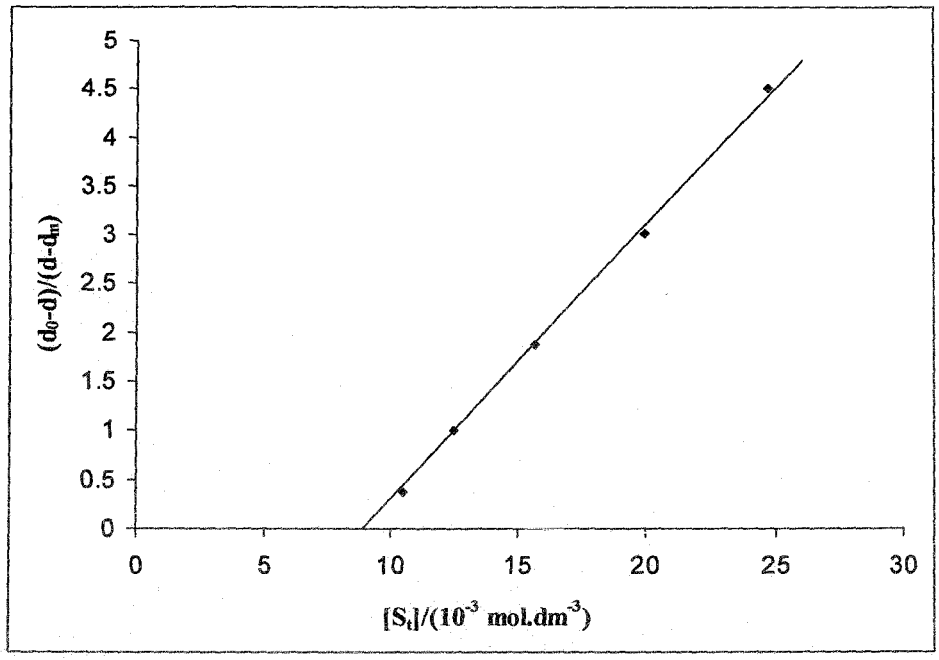

Figure 4.13 $(d_0-d)/(d-d_m)$ vs. concentration (SDS) for Thionine-SDS system having dye concentration 1.50 x 10^{-5}(M) at 303K.

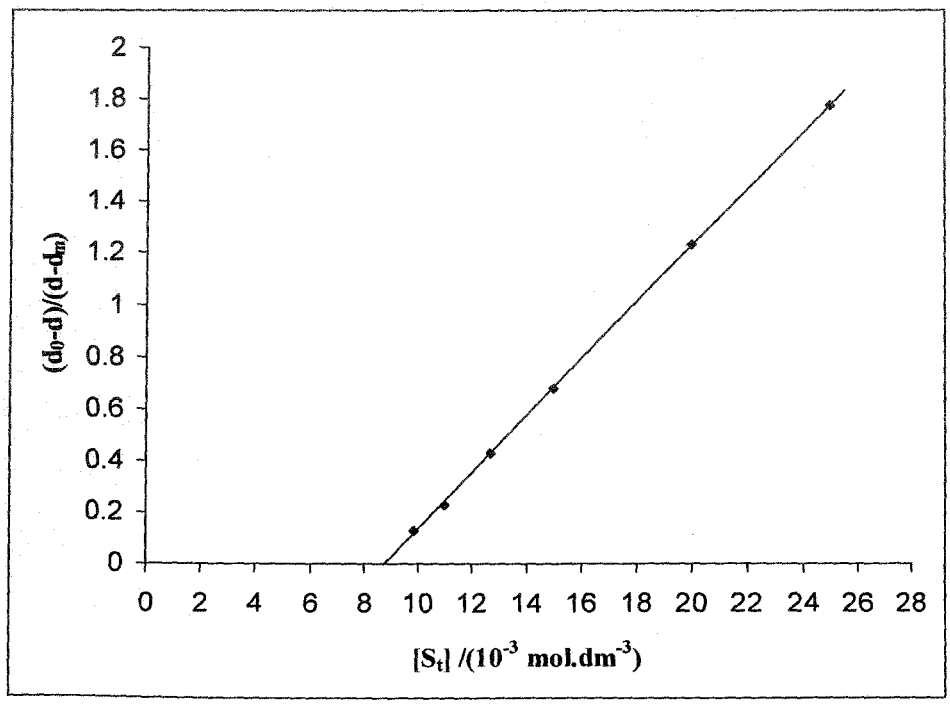

Figure 4.14 $(d_0-d)/(d-d_m)$ vs. concentration (SDS) for Azure B-SDS system having dye concentration 1.20 x 10^{-5}(M) at 303K.

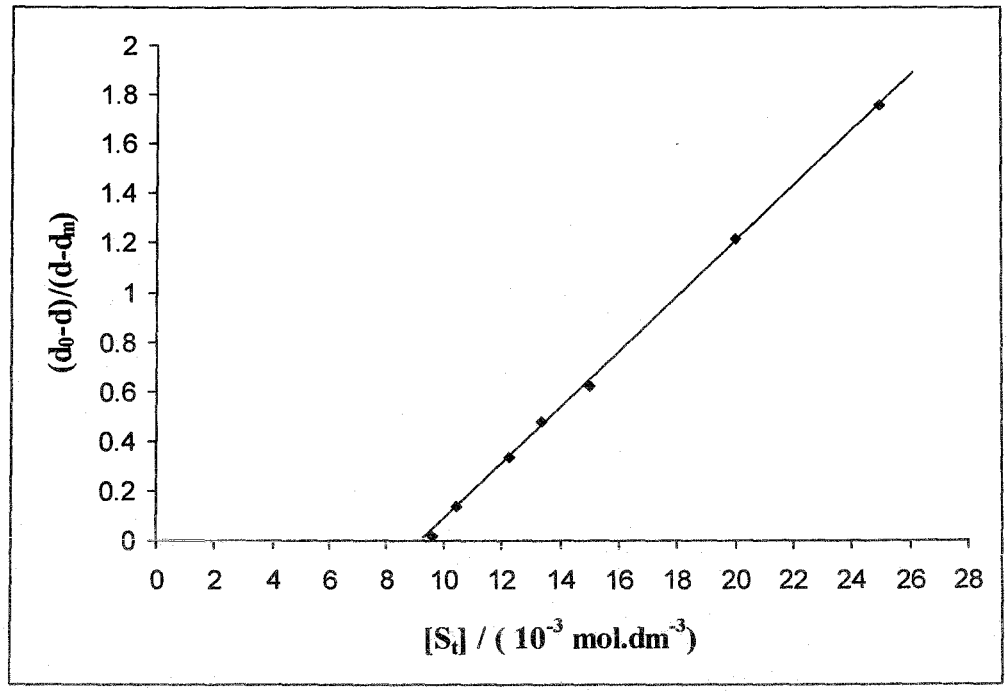

Figure 4.15 (d_0-d)/(d-d_m) vs. concentration (SDS) for Azure A-SDS system having dye concentration 2.1 x 10^{-5}(M) at 303K

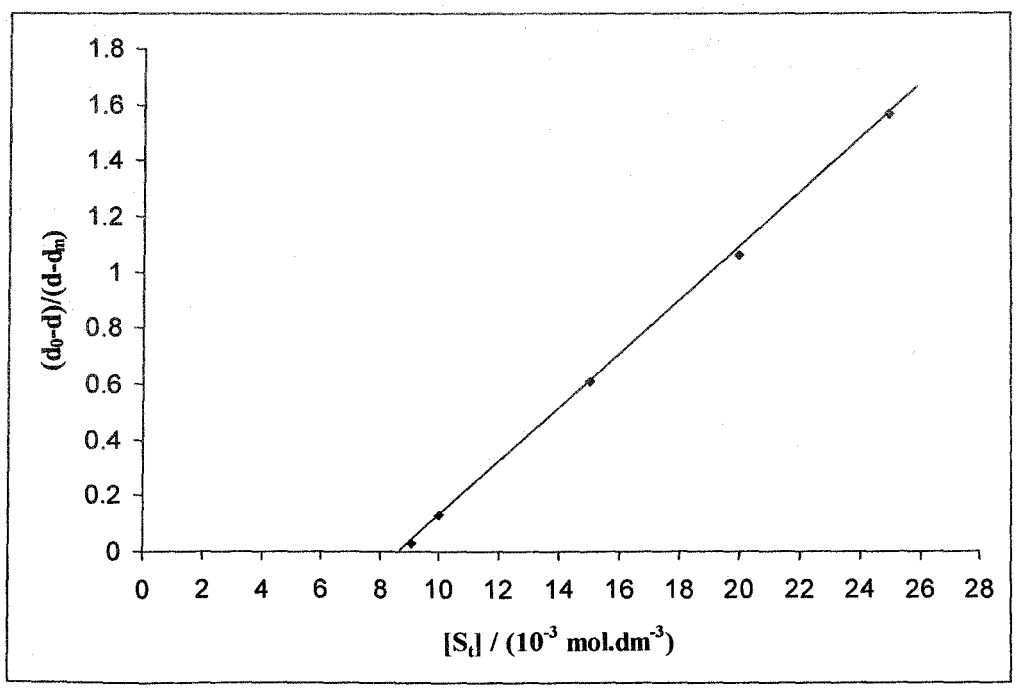

Figure 4.16 (d_0-d)/(d-d_m) vs. concentration (SDS) for Methylene Blue-SDS system having dye concentration 1.17 x 10^{-5}(M) at 303K.

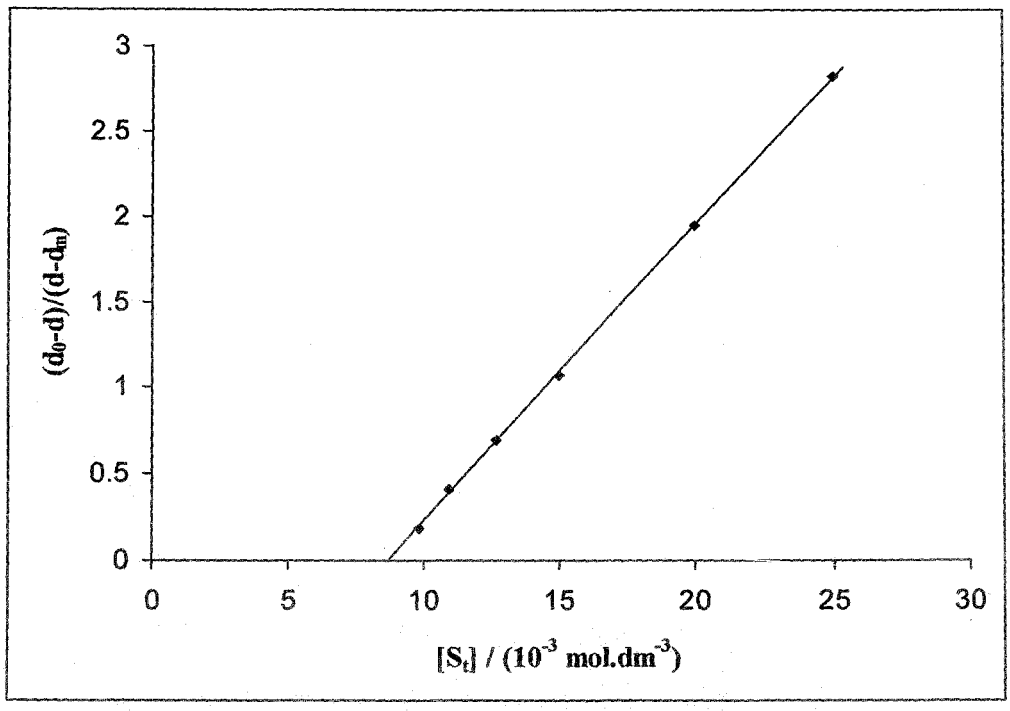

Figure 4.17 $(d_0-d)/(d-d_m)$ vs. concentration (SDS) for Azure C-SDS system having dye concentration 1.50 x 10^{-5}(M) at 303K.

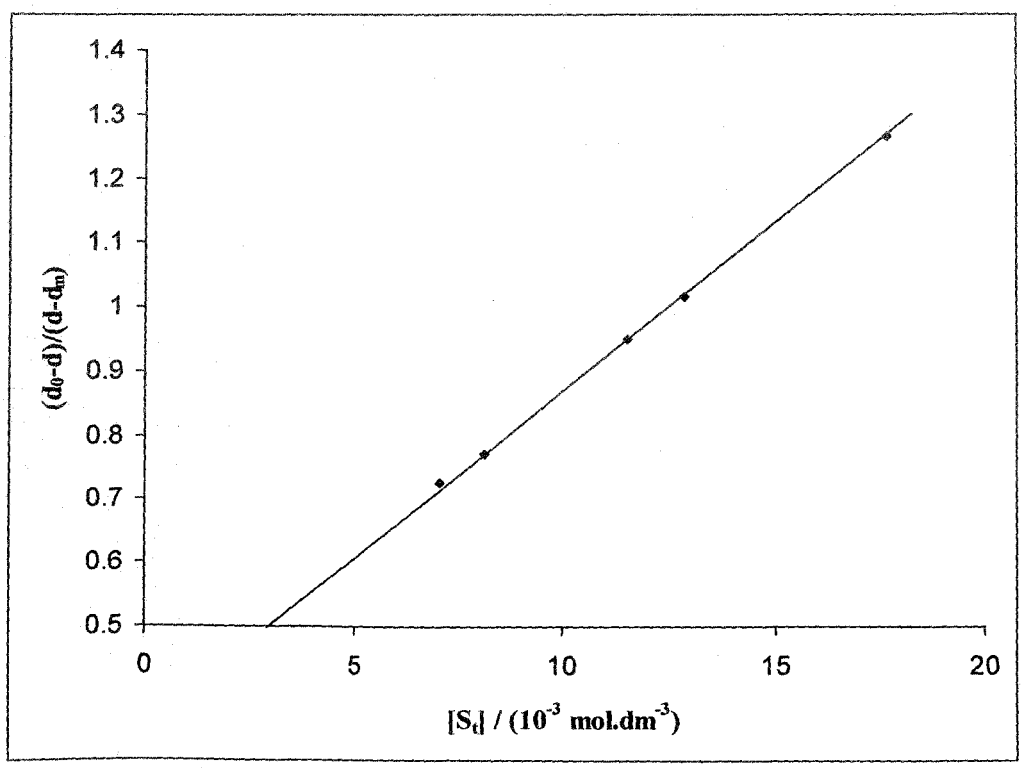

Figure 4.18 $(d_0-d)/(d-d_m)$ vs. concentration (AOT) for Azure B-AOT system having dye concentration 1.20 x 10^{-5}(M) at 303K.

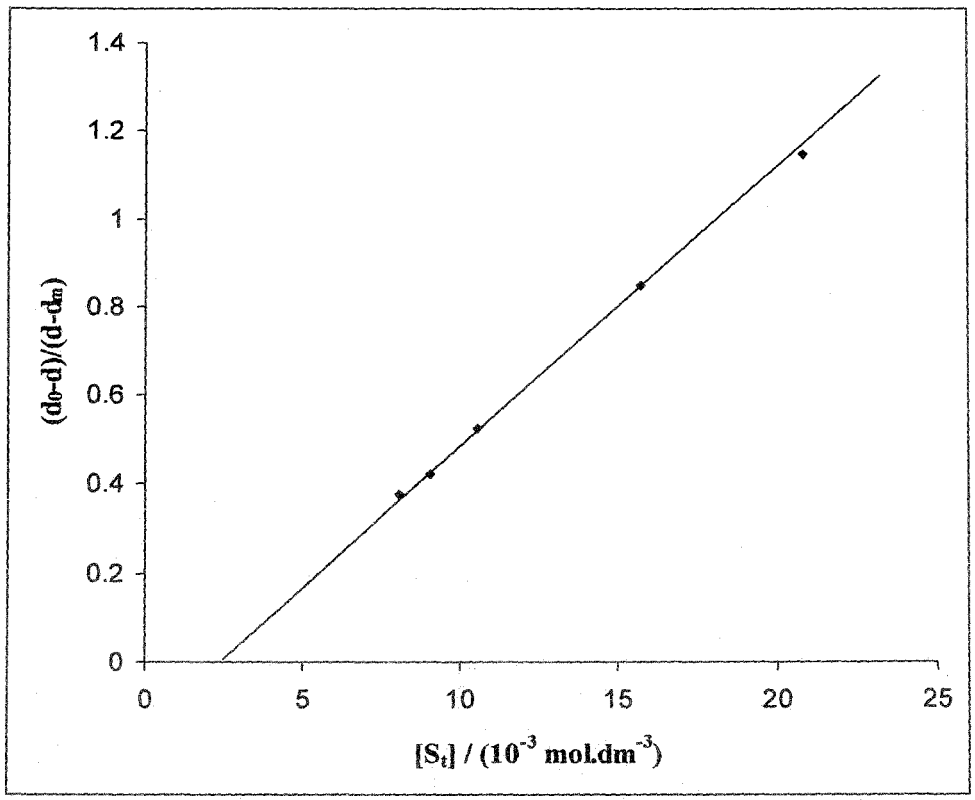

Figure 4.19 $(d_0-d)/(d-d_m)$ vs. concentration (AOT) for Azure A-AOT system having dye concentration 2.10 x 10^{-5}(M) at 303K.

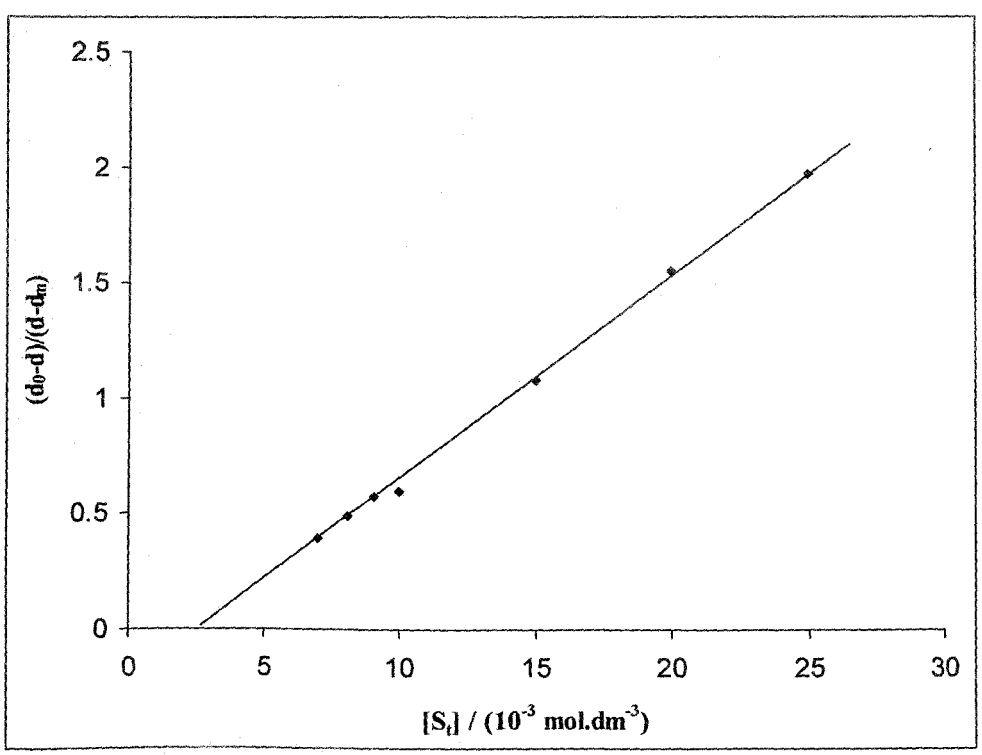

Figure 4.20 $(d_0-d)/(d-d_m)$ vs. concentration (AOT) for Thionine-AOT system having dye concentration 1.50 x 10^{-5}(M) at 303K.

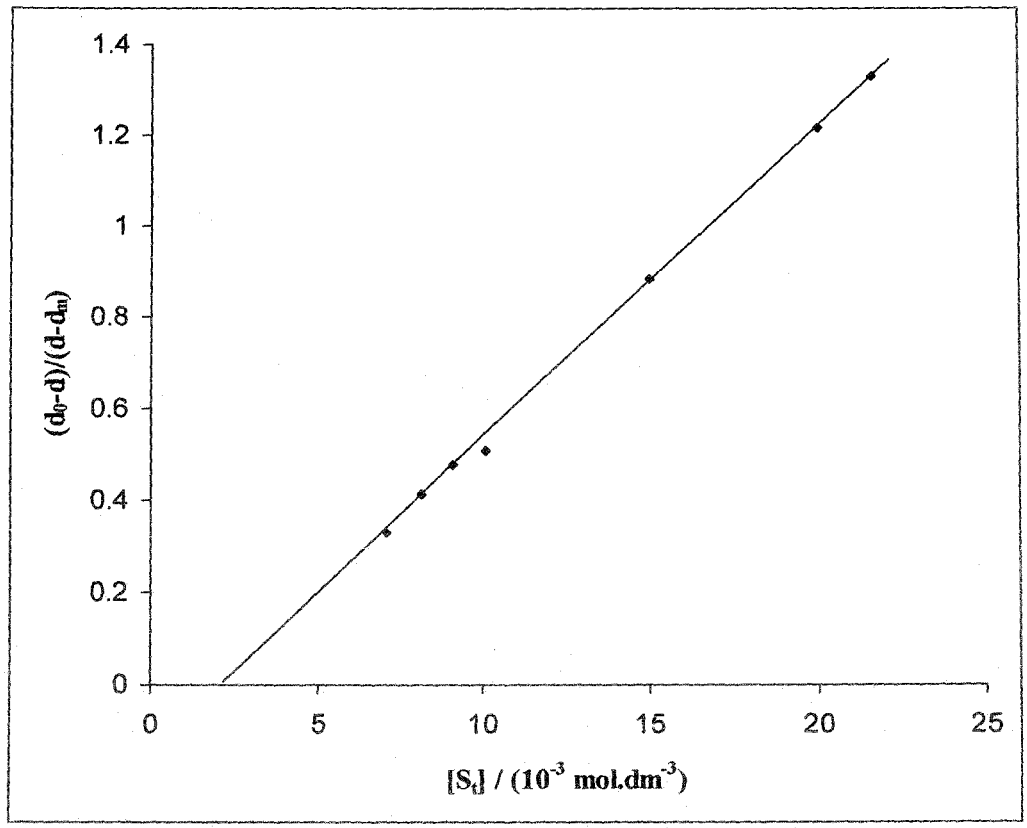

Figure 4.21 $(d_0-d)/(d-d_m)$ vs. concentration (AOT) for Azure C-AOT system having dye concentration 1.24 x 10^{-5}(M) at 303K.

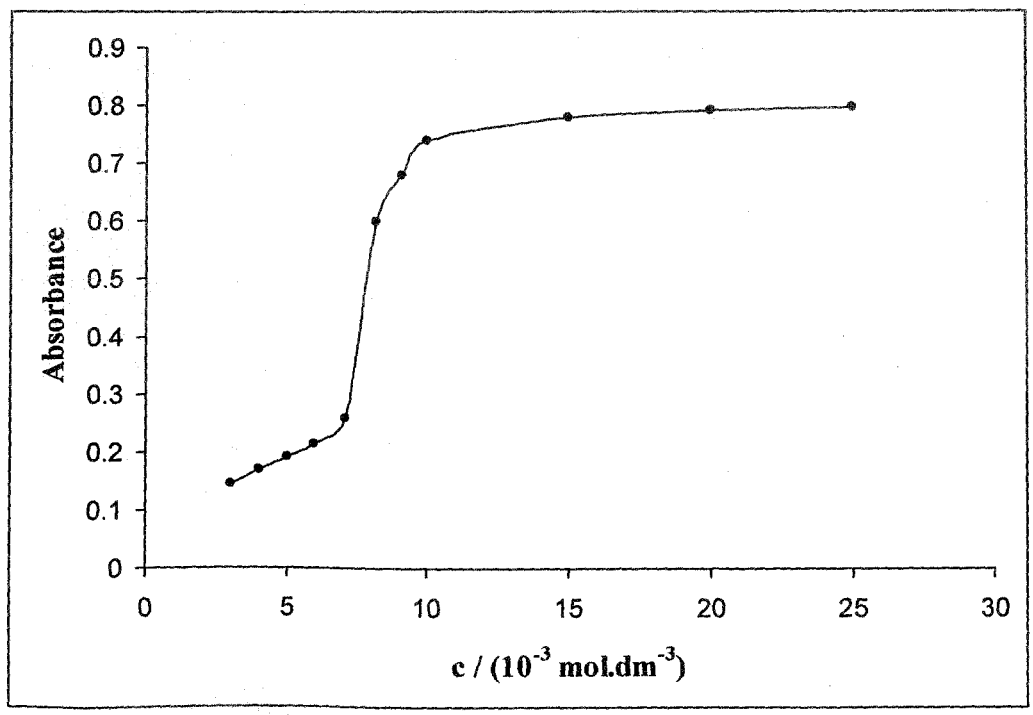

Figure 4.22 Absorbance (λ = 600 nm) vs. concentration (SDS) for Thionine-SDS system with the dye concentration 1.50 x 10^{-5}(M) at 303K.

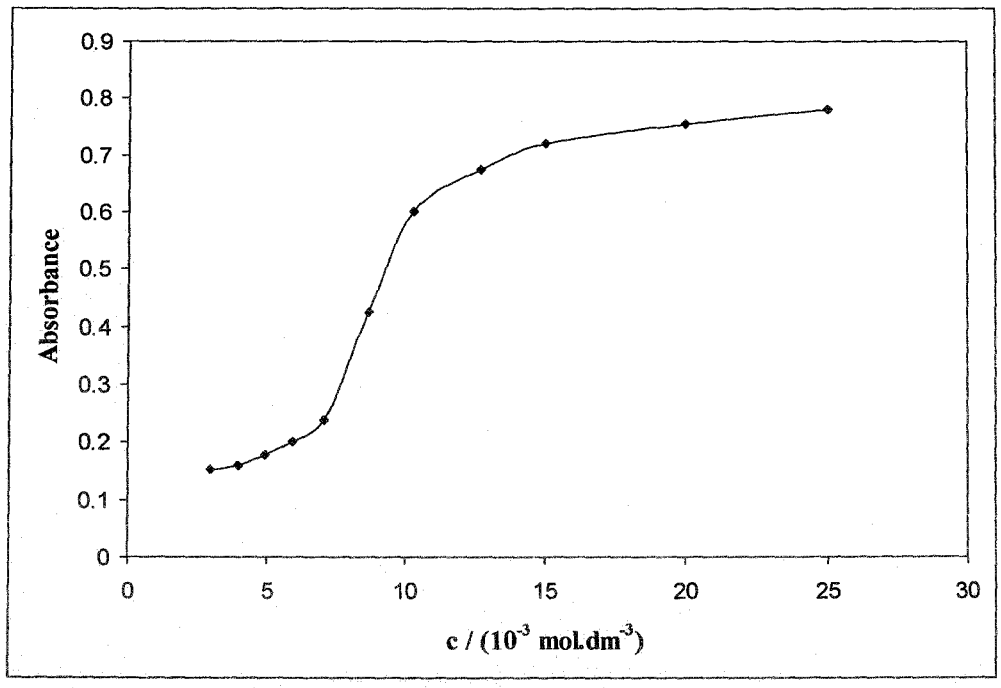

Figure 4.23 Absorbance (λ = 645 nm) vs. concentration (SDS) for Azure B-SDS system having dye concentration 1.20 x 10^{-5}(M) at 303K.

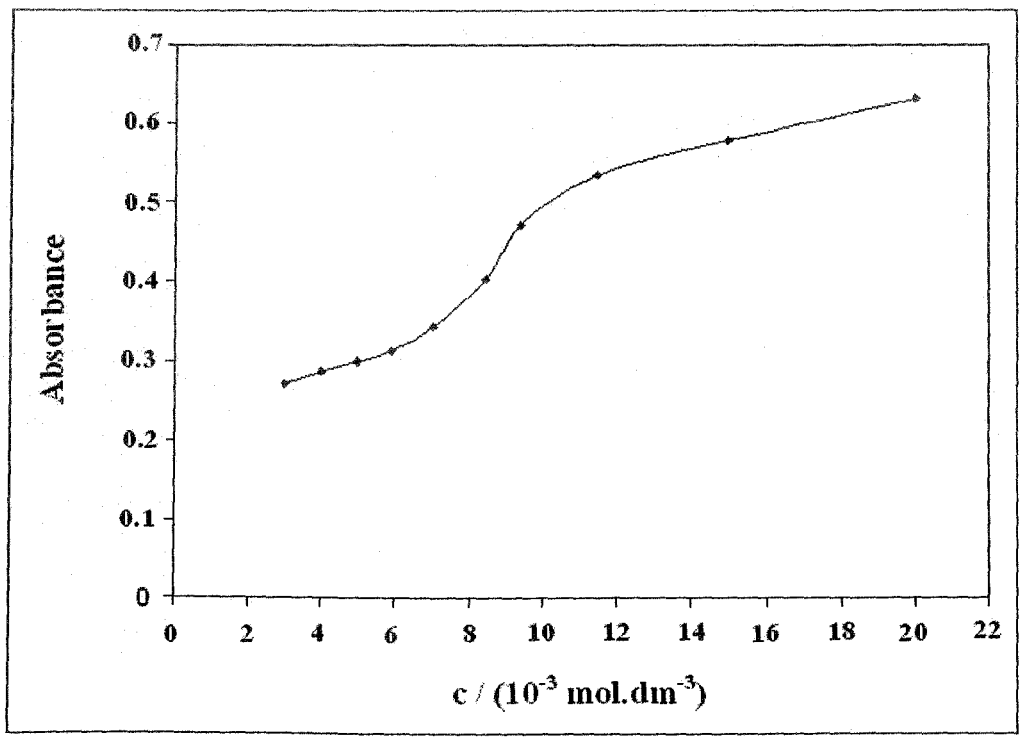

Figure 4.24 Absorbance (λ = 634 nm) vs. concentration (SDS) for Azure A-SDS system having dye concentration 2.10 x 10^{-5}(M) at 303K.

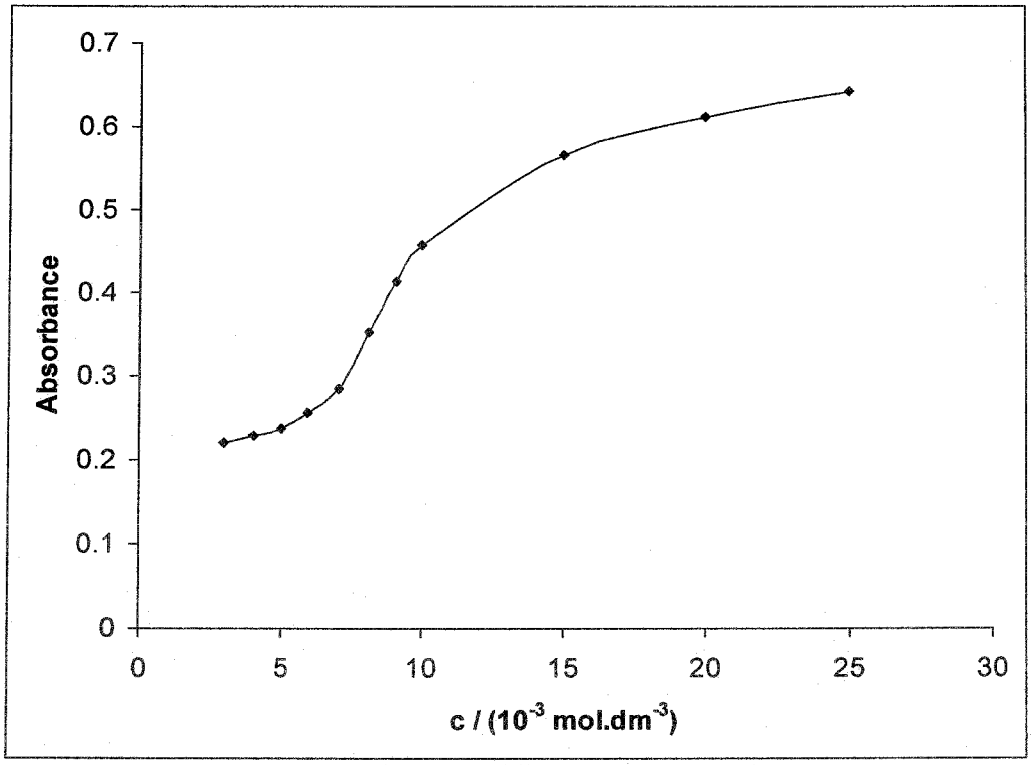

Figure 4.25 Absorbance (λ = 660 nm) vs. concentration (SDS) for Methylene Blue-SDS system having dye concentration 1.17 x 10^{-5}(M) at 303K.

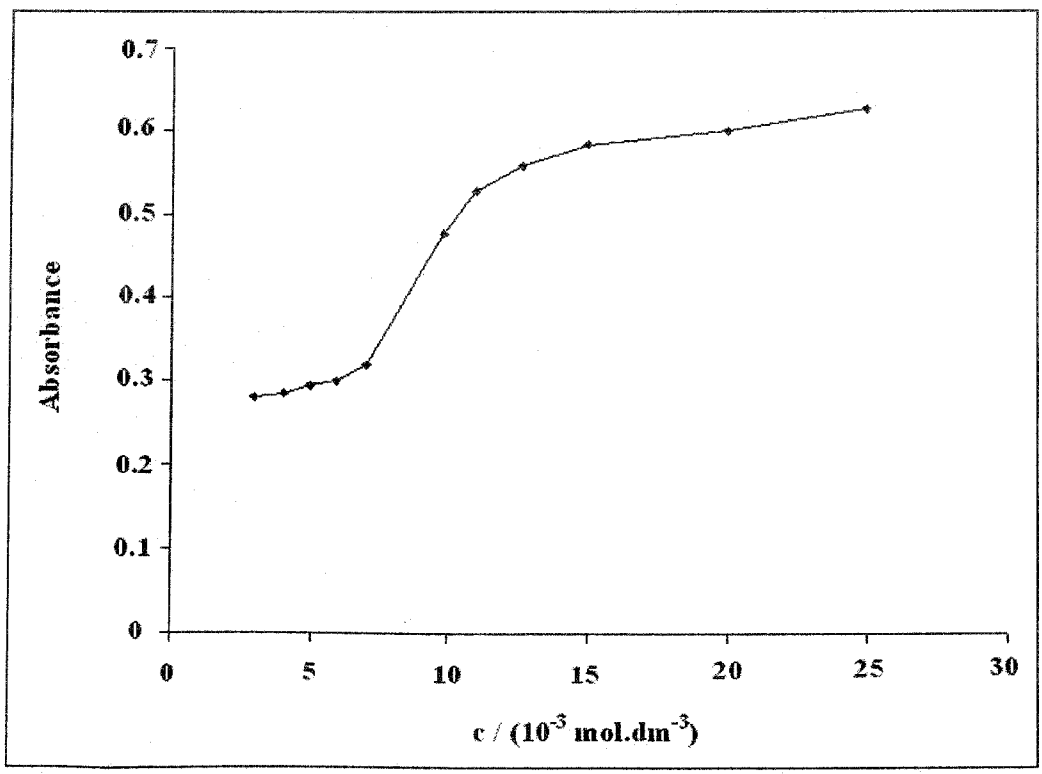

Figure 4.26 Absorbance (λ = 620 nm) vs. concentration (SDS) for Azure C-SDS system having dye concentration 1.24 x 10^{-5}(M) at 303K.

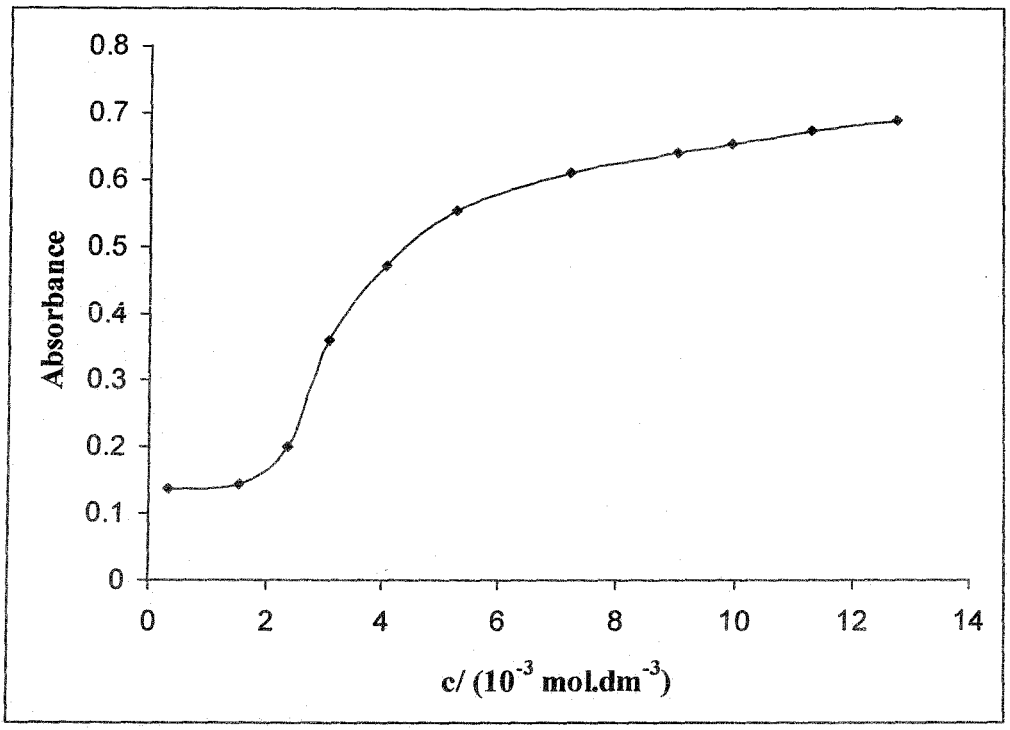

Figure 4.27 Absorbance (λ = 646 nm) vs. concentration (AOT) for Azure B-AOT system having dye concentration 1.20x 10^{-5}(M) at 303K.

inflexion points of these plots are shown in Table 4.2 in the brackets against the corresponding cmc values measured from the plot of equation 4.20. The cmc values obtained by the present method are slightly different from those obtained by other methods as shown in chapter 3. However, it should be noted that premicellar interaction between dye molecules and the surfactant unimers must affect the experimental cmc as determined above and this has already been discussed.

The free energy change, ΔG^0 for the dye-surfactant interaction is determined from the thermodynamic relation, $\Delta G^0 = - RTlnK_{ass}$. It was previously reported that K_{ass} was dependent on the pH, therefore in the present study pH is mentained constant throughout. Measured values of cmc, K_{ass} and ΔG^0 for different dye-surfactant systems are summarized in Table 4.2. Though García-Río et al. [2] claimed exactly same value of cmc of SDS by UV-vis spectrophotometry with crystal violet (CV), as compared other standard methods, it should be noted that apart from the submicellar dye-surfactant interaction the charged dye particle may also change the microenvironment of micellar pseudo-phase resulting in the slight modification of cmc value. The association constants for each pair of dye-surfactant system shows a general trend. It has been observed from Table 4.2 that thionine stacked most strongly with each of the two surfactants followed by other dyes in the order AzC>AzA>AzB >MB. It suggests that the dye-surfactant coulombic interaction between the charged part of the dye molecule and the ionic head of the amphiphile plays a key role in the interaction at the postmicellar concentration of surfactant along with the hydrophobic interaction between the micellar core and the aromatic moiety of the dye. The large negative ΔG^0 values also support the view in favour of the above electrostatic interaction.

4.3.3 Studies on Monomer-dimer Equilibrium of Progressively Alkylated Thiazine Dyes in Aqueous and Microemulsion Media

As discussed in the experimental section the microemulsions are prepared with a cationic surfactant, cetylpyridinium bromide (CPB) in a 1:1 (volume/volume) mixture of n-heptane and chloroform by mixing appropriate amount of water. The reason for choosing the particular microemulsion for the present study is two fold. Firstly, the cationic surfactant like CPB, restricts the possibility of the entry of cationic thiazine dyes in the interfacial region of the microemulsion and ensures the location

in the water-pools. Secondly, in the presence of dye molecules above microemulsion offers a very stable and well-behaved system for studying monomer-dimer equilibrium in water-pools of microemulsion. Further, it can be said that in microemulsion the compartmentalized water dipoles must be firmly associated with the positively charged inner surface of the aggregate. Dyes used for the present study are highly soluble in water but completely insoluble in both chloroform and n-heptane. When dissolved in microemulsion, optically clear solutions are obtained. It is also obvious that due to strong columbic repulsion between the dye molecules and charged monolayer of the interior of microemulsion, the dyes essentially exist in the water-pool.

The representative spectra of five thiazine dyes in microemulsion (recorded in 1 mm path length cell) are shown in Figure 4.28 – 4.32. As expected, the spectra show considerable changes with the variation of dye concentrations in microemulsion water-pool due to the presence of aggregation equilibrium. With the change of concentration of dye in the compartmentalized water for a particular system the dimension of the pool (ω) also change to some extent. It is, however, assumed that in the present experiments, small variation of ω value (22.0 – 38.3) does not affect the microenvironment of the pool to any great extent. Relatively large water-pools of the microemulsion offer an ideal media (size variation is small) to study the aggregation equilibria of dyes in microemulsion media where confinement of dye molecules in the pool is ensured by electrostatic interactions between dye molecules and the interface as already pointed out. To avoid the possibility of formation of trimer and higher aggregates the concentrations are kept within a narrow range (1.35×10^{-4} to 7.28×10^{-4}) for each dye.

Depending upon the pH of the system the thiazine dyes can exists in two forms, viz. Th^+, AzA^+, AzB^+, AzC^+, MB^+ and their corresponding protonated forms in aqueous solution [195]. Different researchers have also calculated the equilibrium constants of acid and basic form of dyes [195-197]. However, when these dyes are dissolved in water the pH of the solution remains within a small range 6.8 ± 0.5 where the dyes exist as their cationic form. In the present investigation spectra of each dye (Figure 4.28 – 4.32) show a clear isobestic point when recorded as a function of concentration. This supports the existence of two chemical species in each of dye system viz., monomer and the dimer species. Thionine shows an isobestic point at

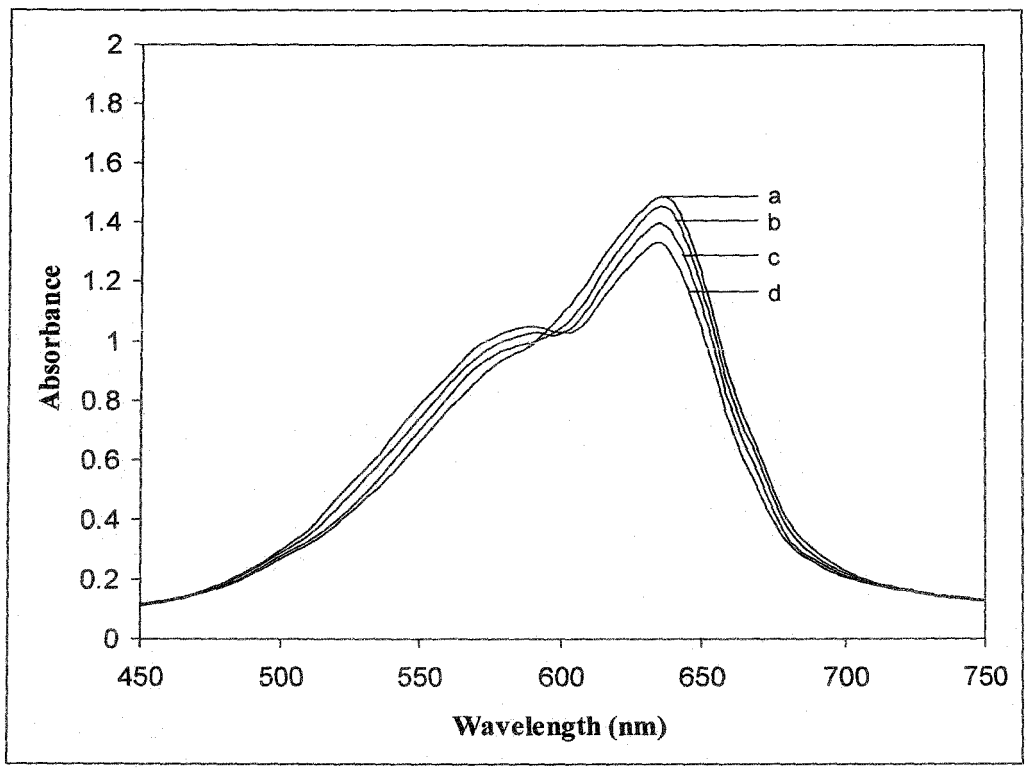

Figure 4.28 Absorption spectra of Azure A [(a) 5.34 x 10^{-4}, (b) 5.75 x 10^{-4}, (c) 6.03 x 10^{-4}, (d) 6.56 x 10^{-4} M] in microemulsion (water-in-oil) at 303K.

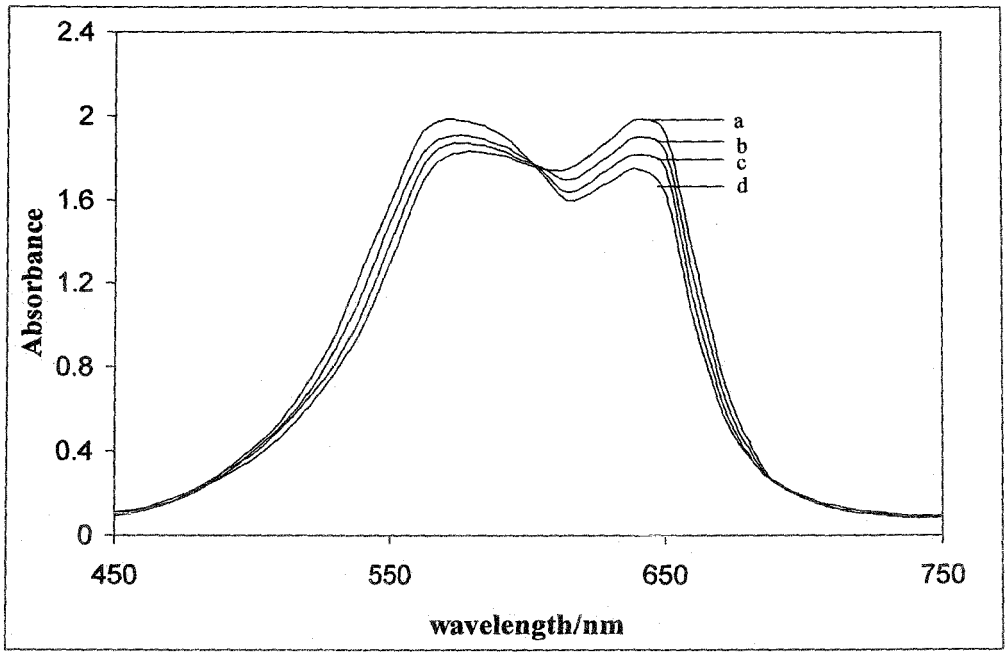

Figure 4.29 Absorption spectra of Azure B [(a) 5.00 x 10^{-4}, (b) 5.65 x 10^{-4}, (c) 6.13 x 10^{-4}, (d) 6.70 x 10^{-4} M] in microemulsion (water-in-oil) at 303K.

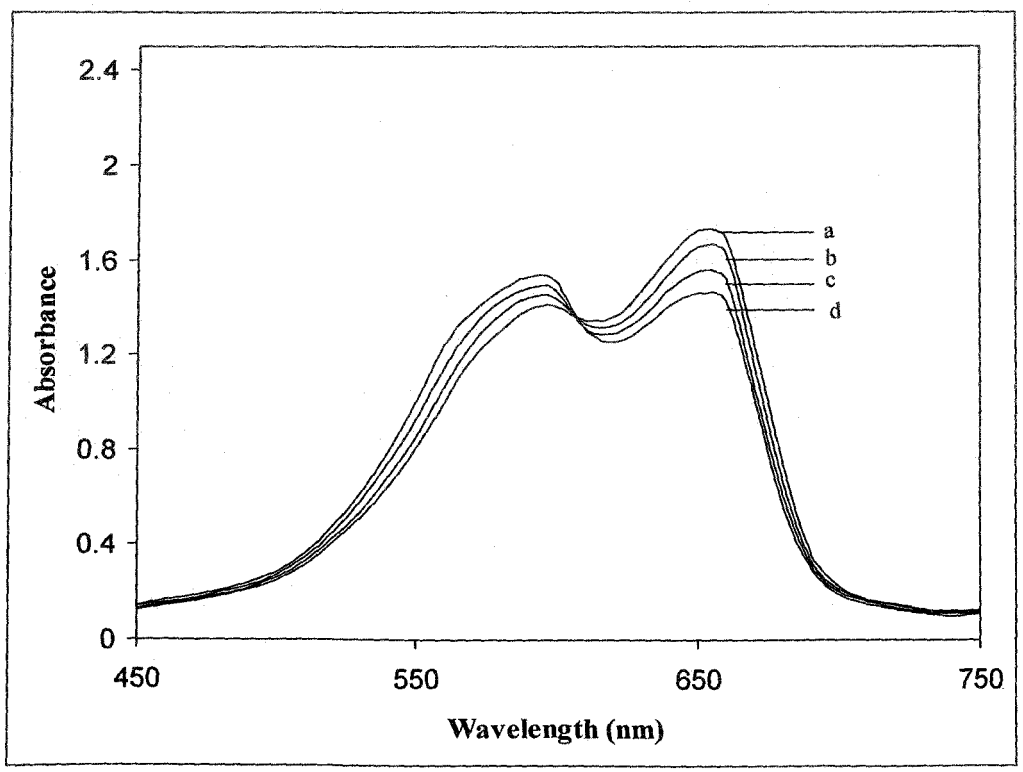

Figure 4.30 Absorption spectra of Methylene Blue [(a) 6.20 x 10^{-4}, (b) 6.55 x 10^{-4}, (c) 6.90 x 10^{-4}, (d) 7.23 x 10^{-4} M] in microemulsion (water-in-oil) at 303K.

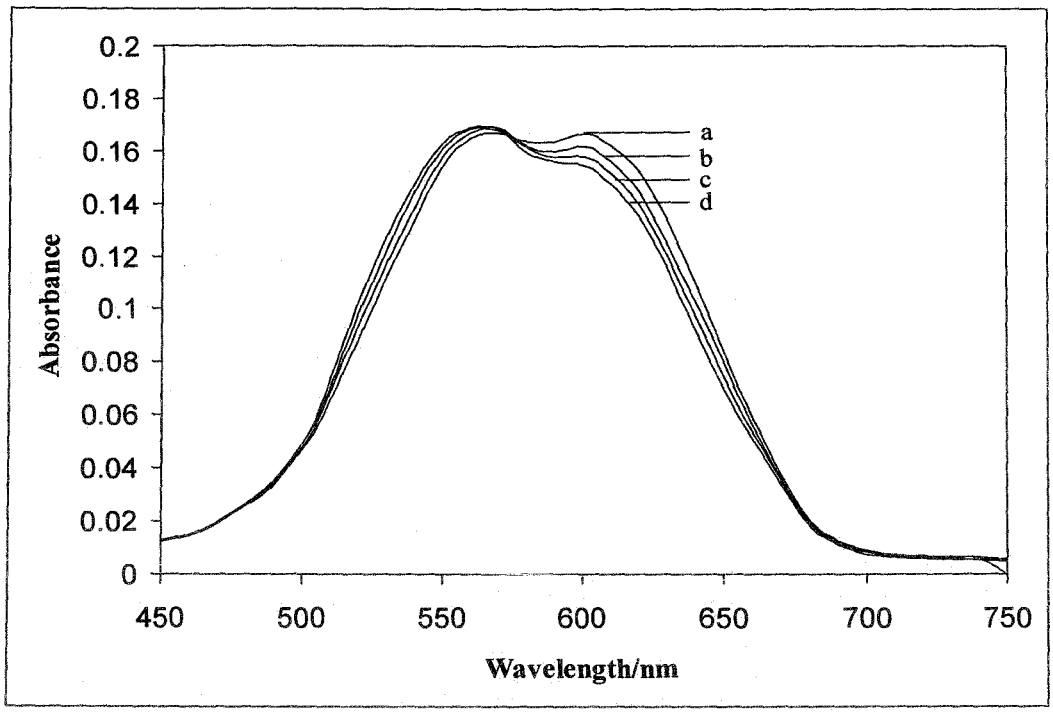

Figure 4.31 Absorption spectra of Thionine [(a) 1.35 x 10^{-4}, (b) 1.67 x 10^{-4}, (c) 1.90 x 10^{-4}, (d) 2.56 x 10^{-4} M] with different sizes of microemulsion (water-in-oil) at 303K

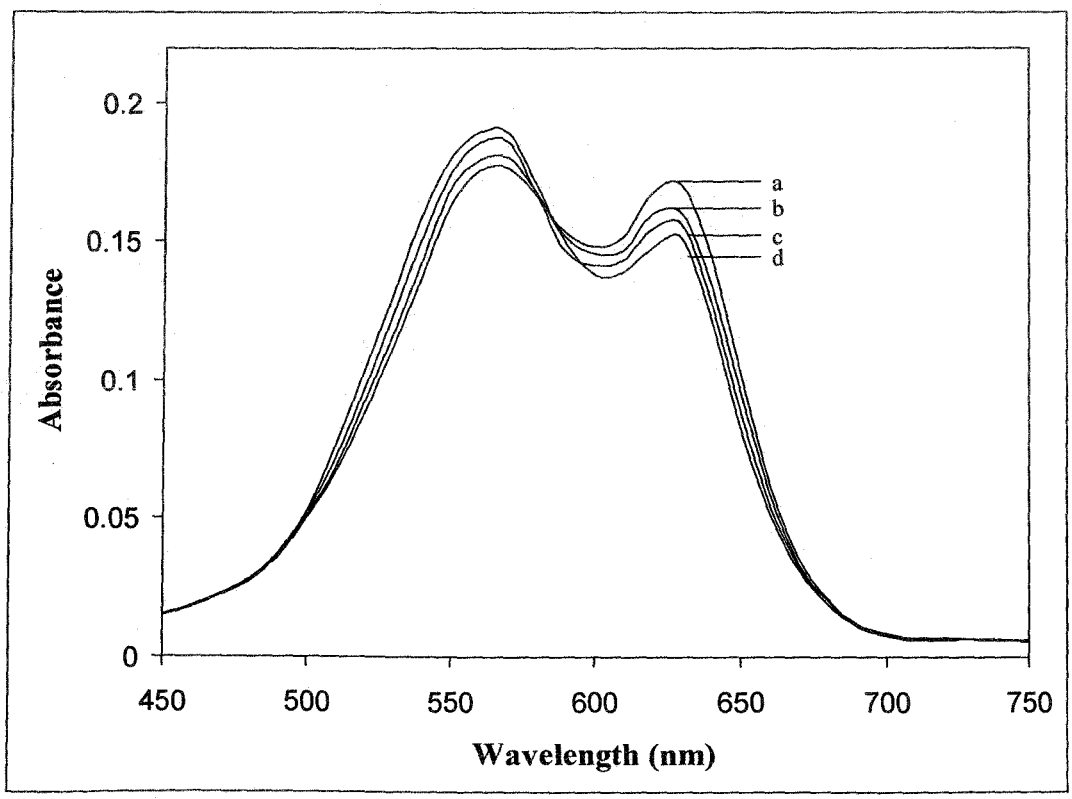

Figure 4.32 Absorption spectra of Azure C [(a) 5.45 x 10^{-4}, (b) 5.63 x 10^{-4}, (c) 5.90 x 10^{-4}, (d) 6.32 x 10^{-4} M] with different sizes of microemulsion (water-in-oil) at 303K

576 nm and the other dyes, viz, AzA, AzB, AzC and MB display their isobestic points at 600, 605, 585 and 606 nm respectively. These two species viz., monomer and the dimer species correspond to those appeared in the aqueous phase also because the spectra obtained in present microemulsion system are apparently similar to those observed in the aqueous solution; the only difference is in their absorbance intensity.

The dimension of microemulsions bearing water-pools of the microemulsion depends upon the [water]/[CPB] mole ratio, ω. For the present systems, CPB is present at a fixed concentration of 0.1512M with appropriate amount of water to prepare microemulsions such that ω may have values within a range of 22.0 to 38.3. For each dye, the spectra show an intense peak in similar wavelength as observed in case of pure dilute aqueous solution. It is well known that the compartmentalized water in microemulsion is much different in character compared to bulk water with respect to the physical nature, viz. polarity, viscosity, acidity etc. [200,201] due to its restricted mobility and very low dielectric constant at the interface. It has been observed that in the absence of the complication of highly polarisable groups such as ester, amides, nitriles and aromatic moieties in the solvent, the spectra of dyes may be correlated directly with the dielectric constant of the surrounding medium [202].

Interpretation of measurements on micellar solutions is largely predicted on the oil-drop picture of a micelle, with a hydrocarbon-like interior of local dielectric constant ~2. There must be a transition between that small value and that of the bulk solvent, approximately 80, as the head group region is traversed. Indeed a radically varying dielectric constant, highly dependant upon position and microenvironment is anticipated, and this is suggested by the discrepancies between the results of various types of solubilized probe studies on identical micellar solution. The value of dielectric constant also shows temperature dependency for every surfactant. In case of CPB the dielectric constant at 303K was measured as 24.0 at the micelle-water interface [203].

However, it was observed that in microemulsion at low water levels ($\omega < 7$-10), the radii of inner water-pools are typically 0.8-1.6 nm, and most of the water molecules are utilized to form the hydration sphere around the polar surfactant head groups and counter-ions [204]. Beyond $\omega > 10$, the radii of the inner water-pools increase substantially and the properties of the inner water-pool tend towards those of ordinary bulk water. However, for the present purpose as the concentration of dye

increases, the peak that supports the presence of monomer, shows lower absorbance while another peak (supports the existence of aggregates) increases. The dimerization constant of monomer-dimer equilibrium for each system is calculated by using the technique of Sabaté et al. [205]

The monomer-dimer equilibrium of dye molecules in aqueous or microemulsion media may be represented as follows:

$$M + M \rightleftharpoons D \tag{4.21}$$

where M and D stands for monomer and the dimer respectively. This equilibrium may be described by the dimerisation constant K_D, which is given by the ratio between the molar concentrations of dimers, C_D, and the monomers, C_M, at equilibrium at a constant temperature and can be expressed as

$$K_D = \frac{C_D}{C_M^{\,2}} \tag{4.22}$$

Thus, it is necessary to know the value of C_D and C_M, which can be determined from the molar absorptivity obtained from the spectral bands of monomeric and dimeric species.

The total absorbance (A_λ) of a dye solution at a given wavelength λ is

$$A_\lambda = \varepsilon_M(\lambda).C_M + \varepsilon_D(\lambda).C_D \tag{4.23}$$

where ε_M and ε_D represent the molar absorption coefficients of monomeric and dimeric species respectively of any band at a wavelength λ.

Considering the mass balance of dye in the dispersed volume the monomer and dimer concentrations can be calculated from equation 4.22

$$C = C_M + 2C_D \tag{4.24}$$

where C is the total analytical concentration of dye.

Replacing C_M and C_D with the total concentration term, equation 4.23 can be rewritten as:

$$A_\lambda = \varepsilon_D(\lambda)\left(\frac{C}{2} - \frac{-1 \pm \sqrt{1+8CK_D}}{8K_D}\right) + \varepsilon_M(\lambda)\left(\frac{-1 \pm \sqrt{1+8CK_D}}{4K_D}\right) \tag{4.25}$$

Now, from the plot of the measured absorbances as a function of dye concentration at any wavelength, the molar absorption coefficient of monomers, $\varepsilon_M(\lambda)$ and dimers, $\varepsilon_D(\lambda)$ along with the dimerisation constant K_d, are calculated using a nonlinear least-square fitting routine (Microsoft Excel Solver) [205]. The resolved monomer and dimer spectra are drawn for the corresponding values of $\varepsilon_M(\lambda)$ and $\varepsilon_D(\lambda)$ as a function of λ.

Spectral features of progressively alkylated thiazine dyes applied in the present study in aqueous medium were reported by previous researchers [179,206]. The deconvoluted monomer and dimer absorption spectra, calculated using the equation 4.25, of all the five dyes both in aqueous and in microemulsion, are shown in Figures 4.33 - 4.42. Some charecterestic features of monomer resolved spectra in aqueous and microemulsion media are listed in Tables 4.3 and 4.5 respectively. The resolved dimer spectra are, however composed of two bands of monomer with their maxima at greater and smaller energy than the monomer maximum respectively [173]. Some of the characteristics of dimer spectra along with their respective dimerization constants are listed in Table 4.4 and 4.6. If we compare the charecterestics of monomer spectra in aqueous media with that of microemulsion media it is seen that the absorption peak (λ_{max}) are more or less remain unaltered except thionine and azure C. The λ_{max} of visible absorption spectra of thionine and azure C are red shifted through 7.0 and 5.0 nm respectively. However, the molar absorptivities (ε's) of resolved monomer spectra have displayed a very great change for all the five thiazine dyes. In the water-pools of microemulsion the molar absorptivities of the monomer are decreased to a great extent relative to bulk water.

Under the present experimental conditions (303K temperature), in aqueous medium, the K_d values obtained, are 1.761×10^3, 2.350×10^3, 3.381×10^3, 6.258×10^3 and 3.658×10^3 lit/mol for Th, AzC, AzA, AzB and MB respectively in aqueous medium. The K_d values indicate that the increased hydrophobicity in the dye molecule upon methylation increases dimerization tendency, which in turn minimizes the contact area of the dyes with water. In case of methylene blue, steric hindrance is probably very high and the dimerization constant is less. In microemulsion media, on the other hand, the K_d values are 2.214×10^3, 1.760×10^3,

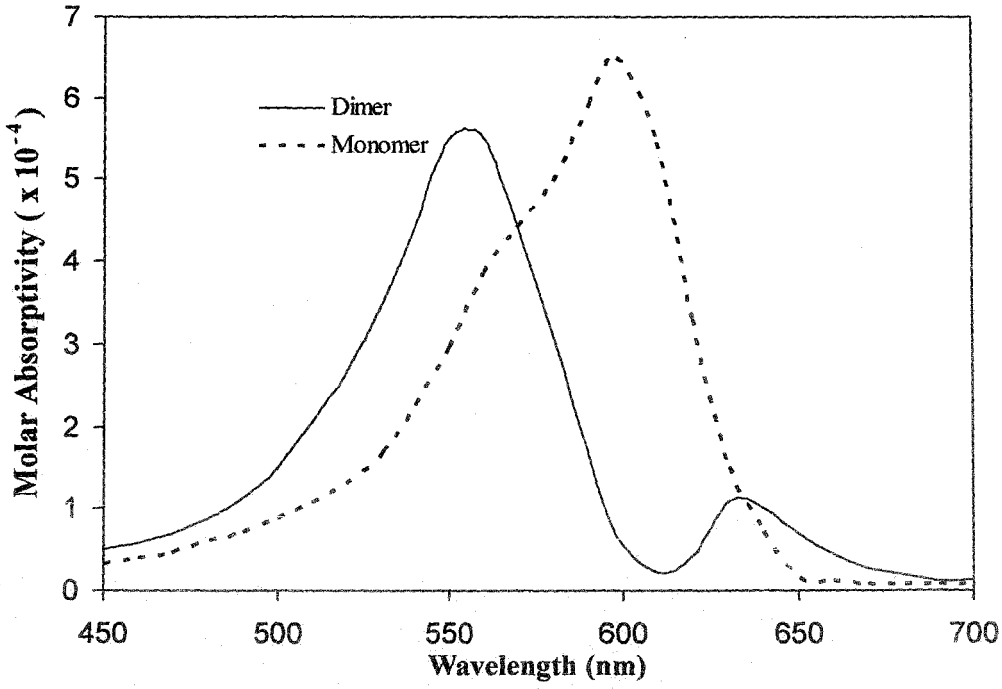

Figure 4.33 Absorption spectra of Thionine in water

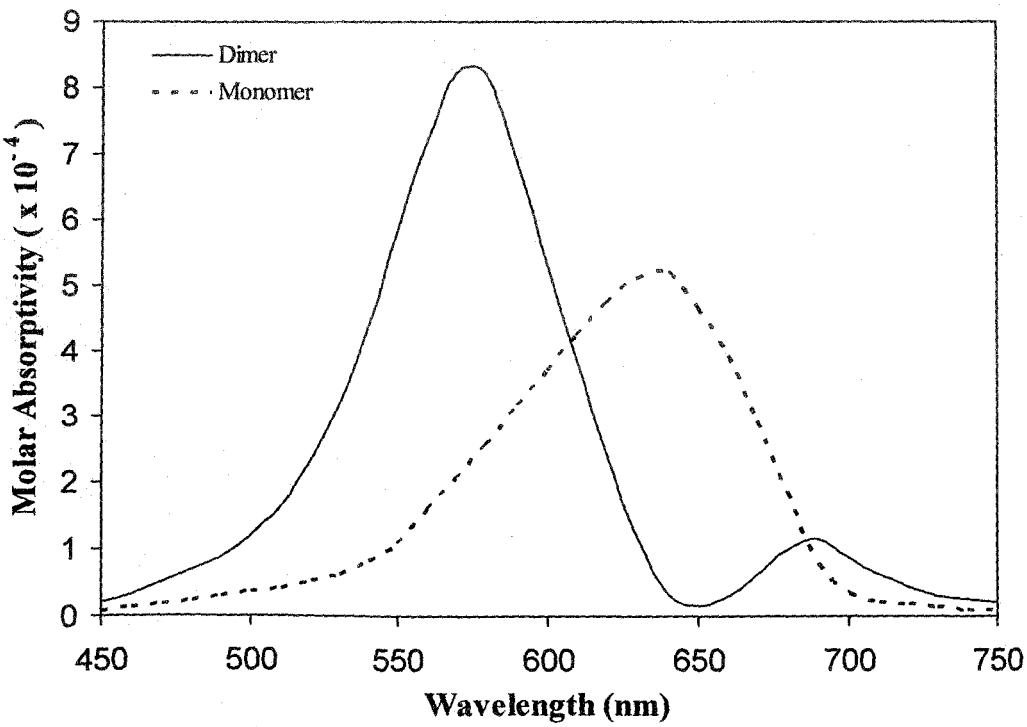

Figure 4.34 Absorption spectra of Azure A in water

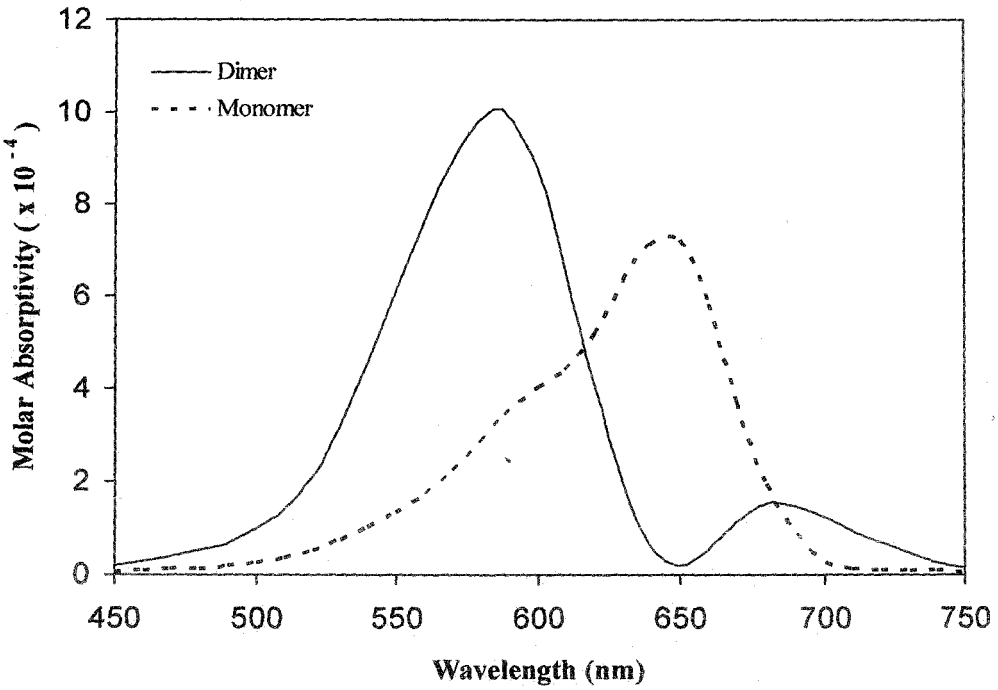

Figure 4.35 Absorption spectra of Azure B in water

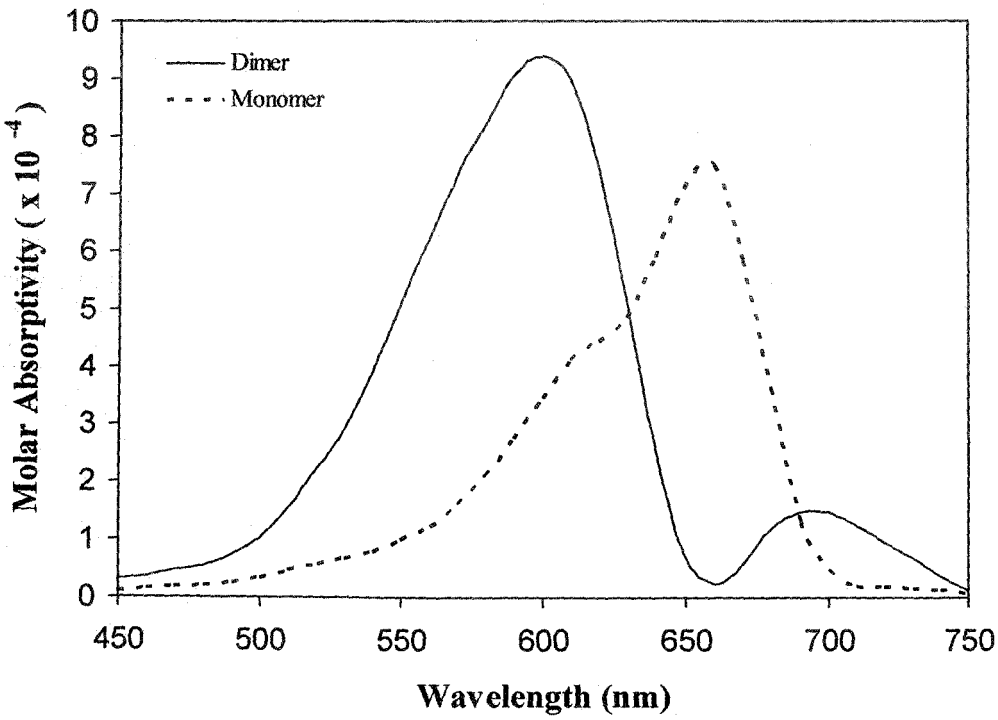

Figure 4.36 Absorption spectra of Methylene Blue in water

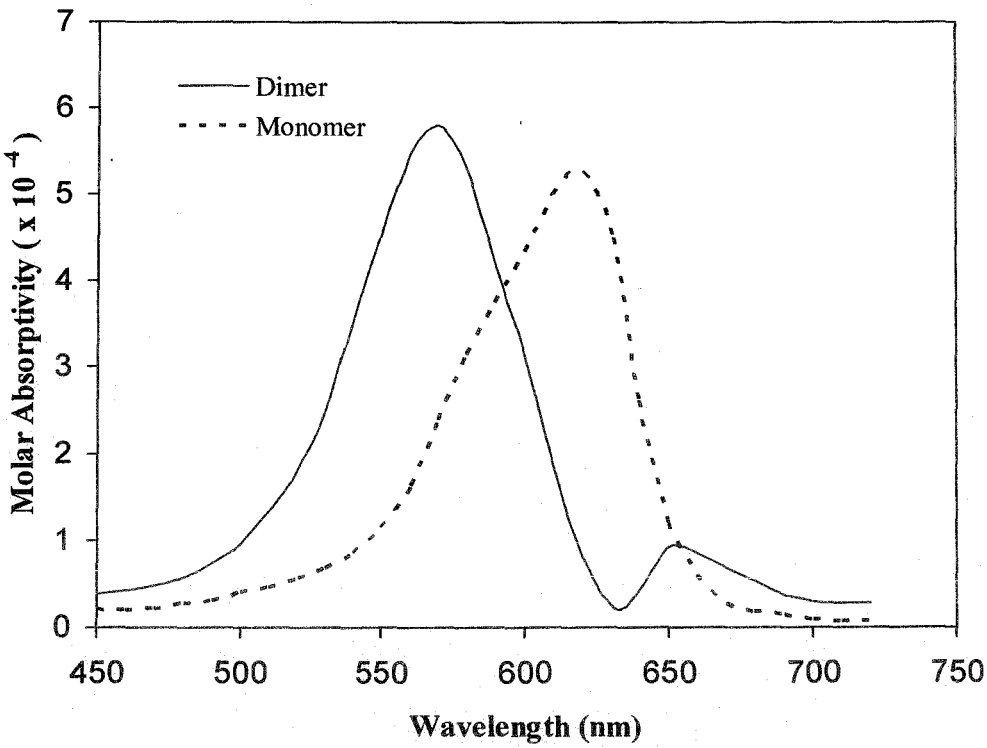

Figure 4.37 Absorption spectra of Azure C in water

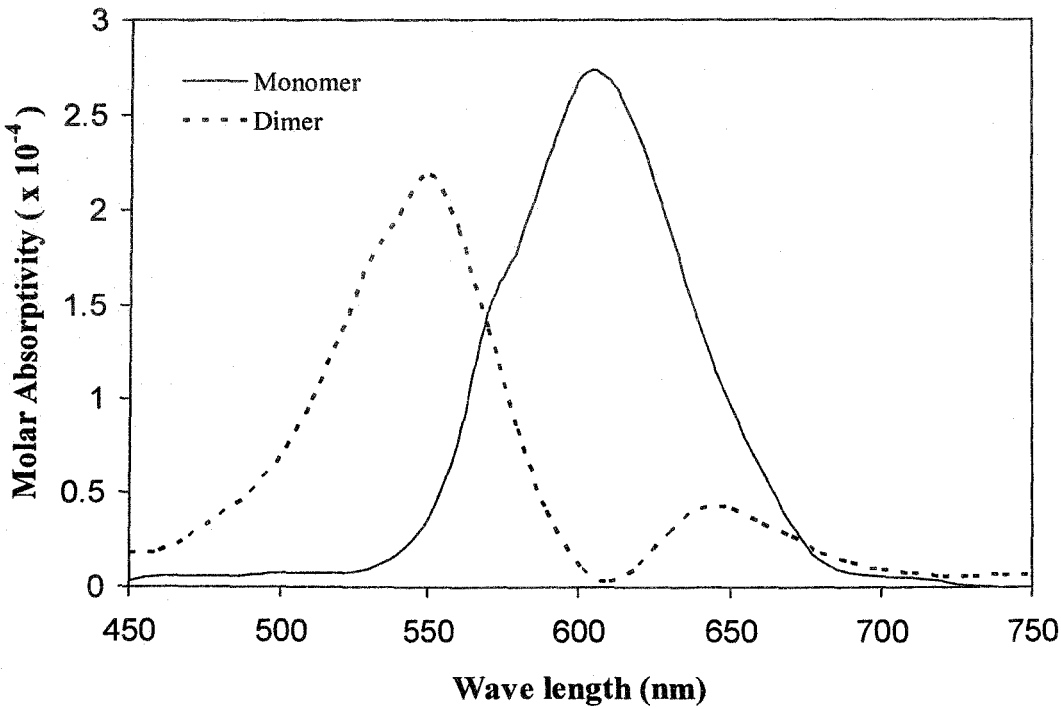

Figure 4.38 Absorption spectra of Thionine in microemulsion

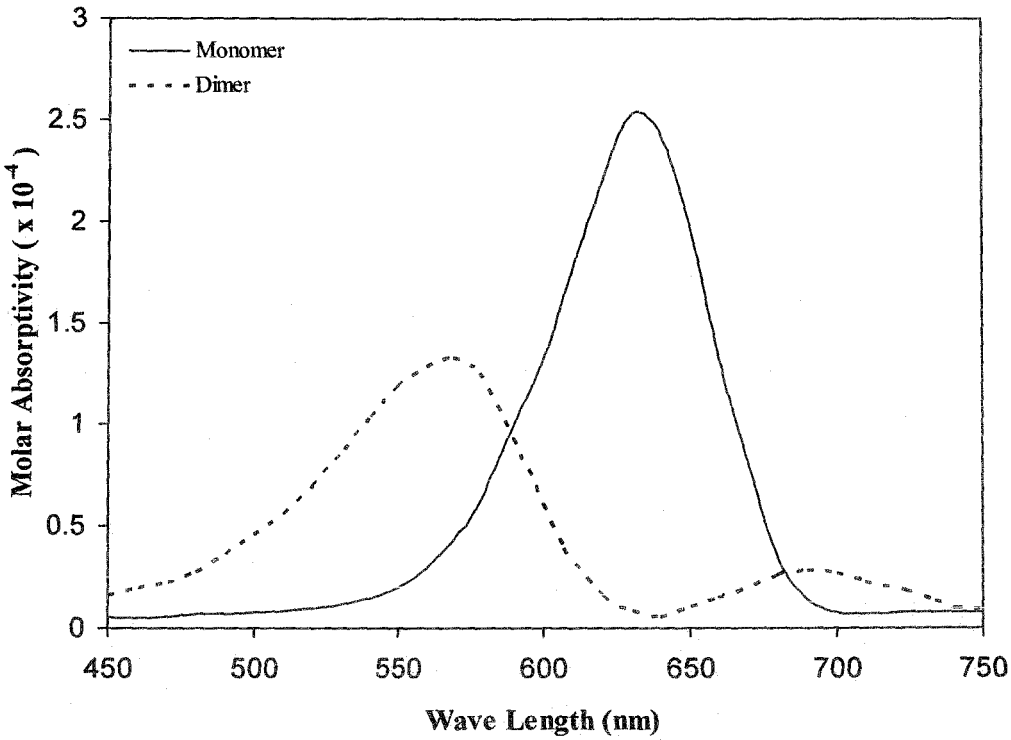

Figure 4.39 Absorption spectra of Azure A in microemulsion

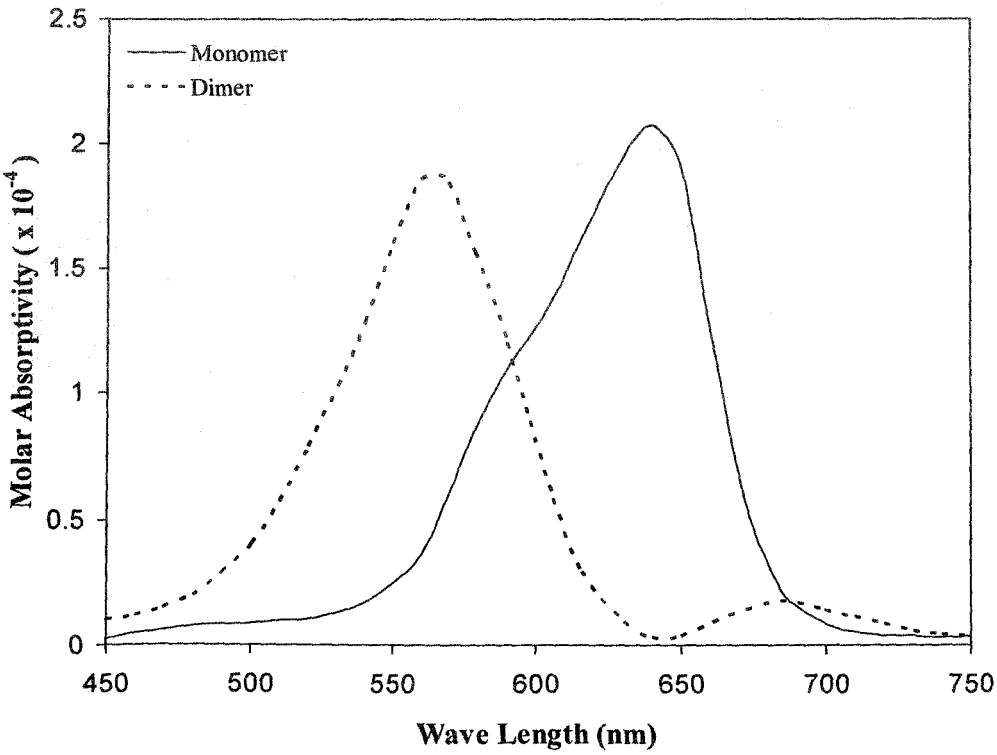

Figure 4.40 Absorption spectra of Azure B in microemulsion

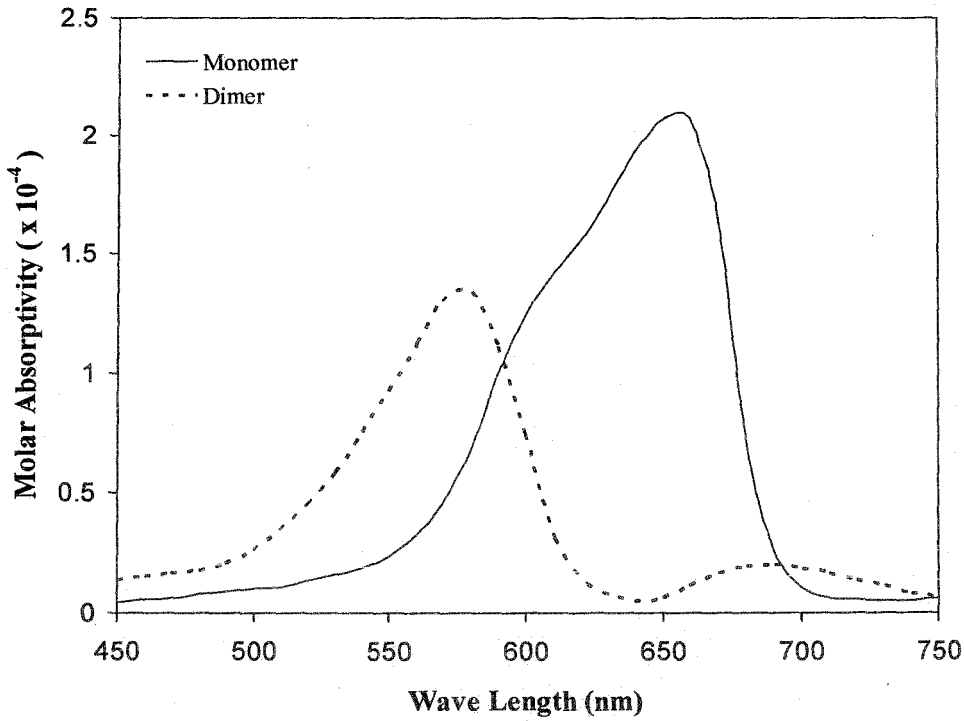

Figure 4.41 Absorption spectra of Methylene Blue in microemulsion

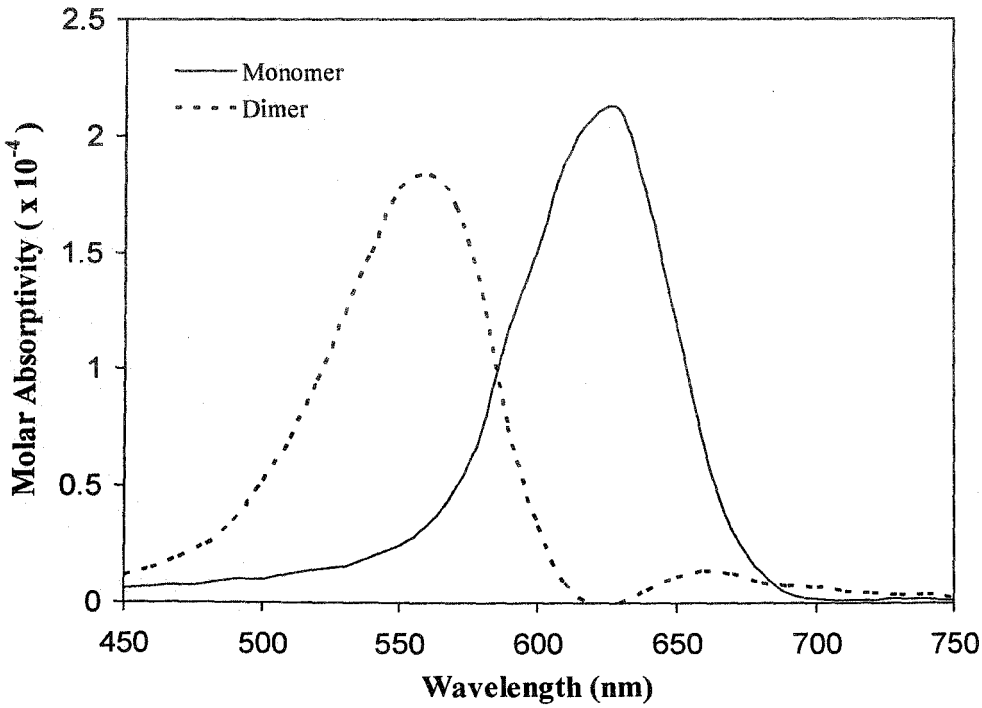

Figure 4.42 Absorption spectra of Azure C in microemulsion

Table 4.4

Dimerizatin parameters (K_d, ΔG^0) and some characteristics of dimer spectra of the dyes in aqueous solution

Dye	$K_d \times 10^{-3}$ (lit.mol^{-1})	$-\Delta G^0$ (kJ.mol^{-1})	λ_1(nm)	λ_2(nm)	$\varepsilon_1 \times 10^{-4}$	$\varepsilon_2 \times 10^{-4}$
Thionine	1.761	18.83	555	630	5.64	1.11
Azure C	2.350	19.56	571	651	5.75	0.96
Azure A	3.381	20.47	575	687	8.17	1.16
Azure B	6.258	22.02	588	682	10.11	1.50
Methylene Blue	3.658	20.67	600	691	9.27	1.03

Table 4.3

Some characteristics of monomer spectra of the dyes in aqueous solution

	Thionine	Azure C	Azure A	Azure B	Methylene Blue
λ_{max}(nm)	598	620	634	646	661
$\varepsilon \times 10^{-4}$	6.16	4.96	5.18	6.90	7.20

Table 4.5

Some characteristics of monomer spectra of the dyes in microemulsion

	Thionine	Azure C	Azure A	Azure B	Methylene Blue
λ_{max}(nm)	605	625	634	646	661
$\varepsilon \times 10^{-4}$	2.71	0.71	2.54	2.07	2.10

3.504×10^3 and 4.112×10^3, 1.501×10^3 lit/mol for Th, AzC, AzA, AzB and MB respectively, which do not follow the regular trend like that in aqueous medium. It is therefore evident that along with the structure of the dye molecules, nature of the solvent along with the electrostatic interactions (repulsion) between the similarly charged dye molecules and the inner phase of microemulsion may also play important role on the strength of aggregation. The ΔG^0 for dimerization processes of five thiazine dyes are negative and do not differ very much upon progressive methyl substitution. As expected there is no general trend but in most cases, ΔG^0 displays slightly higher negative value on methylation in aqueous and micro-emulsion media.

Table 4.6

Dimerizatin parameters (K_d, ΔG^0) and some characteristics of dimer spectra of the dyes in microemulsion

Dye	$K_d \times 10^{-3}$ (lit.mol^{-1})	$-\Delta G^0$ (kJ.mol^{-1})	λ_1(nm)	λ_2(nm)	$\varepsilon_1 \times 10^{-4}$	$\varepsilon_2 \times 10^{-4}$
Thionine	2.214	19.40	550	640	2.18	0.41
Azure C	1.760	18.83	559	660	0.61	0.05
Azure A	3.504	20.56	570	690	1.33	0.28
Azure B	4.112	20.96	563	684	1.86	0.18
Methylene Blue	1.501	18.42	580	685	1.34	0.21

4.3.4 Analysis of Monomer Spectra in Aqueous and Microemulsion Media in terms of Vibronic Exciton Model

The monomer spectra of five thiazine dyes at 303K, as resolved from deconvolution calculations are shown in Figures 4.33 - 4.42. Monomers which are present in equilibrium with dimers in aqueous and microemulsion media have shown some striking features depending upon the medium. All the monomer spectra were analyzed in detail in terms of their vibronic bands in order to understand these features. In this analysis, it is assumed that the force constant of the ground and excited states are same and the vibronic transition can be described satisfactorily by a Gaussian band shape. The simplest physical model in dealing with a vibronic progression is that of a displaced harmonic oscillator with Gaussian bands of constant band width requiring five adjustable parameters. Background of the method of such an analysis is given below [208,209].

Molecules of many atoms posses a number of vibrational modes and their electronic transition may be accompanied by simultaneous changes in the vibrational quanta of various fundamentals. However, of the large number of possible "vibronic bands" only a few will occur with large probability, in general. Application of Born-Openheimer approximation and symmetry considerations show that an allowed electronic transition is dominated by totally symmetric vibrational progressions. For aromatic molecules the dominant totally symmetric vibration is the ring "breathing". Moreover, since vibrational spacings are of the order of 1000 cm^{-1}, the number of vibrationally excited molecules at room temperature is negligibly small. It follows

that an allowed electronic transition of large planner (aromatic) molecule in solution may be taken to consist of a single progression in absorption spectrum.

In the present investigation, the spectra of the five thiazine dye monomers have been analyzed in terms of their vibronic bands b_g adopting the following assumption.

(i) Only one fundamental vibrational mode need to be considered.

(ii) The difference in the force constants of the ground state and excited state oscillators may be disregarded;

(iii) The harmonic approximation applies;

(iv) The vibronic transition may be described satisfactorily by a Gaussion band shape;

The assumptions lead to single formulae for analyzing the absorption spectra of the monomers. The simplest physical model as described, to apply in dealing a vibronic progression is that of a displaced harmonic oscillator with Gaussian bands of constant band width requiring just five adjustable parameters in accordance with the formulae

$$I(\bar{\nu}) = I_{00}\sum_{m}\frac{X^m}{m!}\left(1+\frac{mV}{\bar{\nu}_{00}}\right)\exp\left\{\left(-\frac{4\ln 2}{b_g^2}\right)(\bar{\nu}-\bar{\nu}_{00}-mV)^2\right\} \qquad (4.26)$$

where , I_{00} is the intensity, $\bar{\nu}_{00}$ is the position of the (0,0) band, b_g is the Gaussion band width, X is the ratio of (1,0) to (0,0) band intensities and ν, the separation between the bands.

In general intensity distribution within an electronic band is represented well by Gaussion model. It is described accordingly, each vibronic band, (m,0) by the formula.

$$I_m(\bar{\nu}) = A_{m_1}\exp\left(-A_{m_3}\left(\bar{\nu}-A_{m_2}\right)^2\right) \qquad (4.27)$$

Where $I_m(\bar{\nu})$ is the band intensity at wave number $(\bar{\nu})$, Am_1 is the peak height, Am_2 is the position of the band centre, and $A_{m_3} = \ln 2/b_g^2$ with $2b_g$ as the

width of the band at half maximal intensity. The band width may be taken to be constant within a progression, so that one writes $A_{m_3} = A_3$

It is also assumed that the ground and excited states are adequately described as displaced harmonic oscillators with the same force constant which has the following consequences:

i) the band centers are separated by a constant distance V, so that

$$Am_2 = Ao_2 + mV$$

ii) the intensity of the band obey a modified poisson distribution.

In particular, in the case of Gaussian bands the integrated intensities are proportional to the peak height Am_1 and these are related to one another through a parameter X which, in turn, is a measure of the displacement of the normal co-ordinate of vibration(s)

$$Am_1 = \frac{X^m}{m!} A_{o1} \frac{A_{m2}}{A_{o2}} \tag{4.28}$$

The complete progression may thus be defined in terms of five molecular parameters x, v, Ao_1, Ao_2 and A_3 as follows

$$I(\bar{\nu}) = \sum_m \frac{X^m}{m!} Ao_1 \left(1 + \frac{mV}{Ao_2}\right) \exp\left\{-A_3^2(\bar{\nu} - Ao_2 - mV)^2\right\} \tag{4.29}$$

Replacing the symbols of the above parameters by more common symbols and after minor rearrangement the equation 4.29 takes the form of equation 4.26, as already described.

The $\varepsilon(\lambda)$ values recovered were plotted as a function of wave number $(1/\lambda)$ are shown in Figure 4.43 – 4.52 reproduce the experimental monomer spectra and the fitted monomer spectra ($\varepsilon(\lambda)$ vs. wave number, $1/\lambda$) of five thiazine dyes both in aqueous and microemulsion media. The spectra were fitted to the above 'five parameter Gaussion equation'. This has been done on a computer by means of a general non-linear curve-fitting program, KINFIT (updated) [209] properly adopted in the present system. Satisfactory results were obtained by truncating the summation after six bands. Results of fitting indicate that the present physical model describing a vibronic progression of a displaced harmonic oscillator with Gaussian

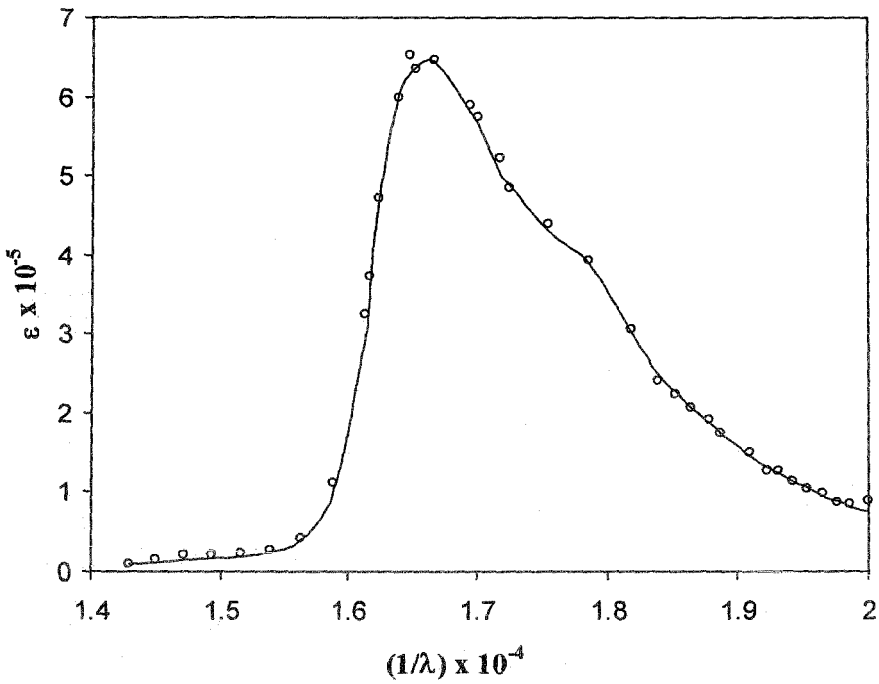

Figure 4.43 Absorption spectra of Thionine monomer in aqueous medium. Solid line represents the experimental spectrum and circles correspond to calculated points.

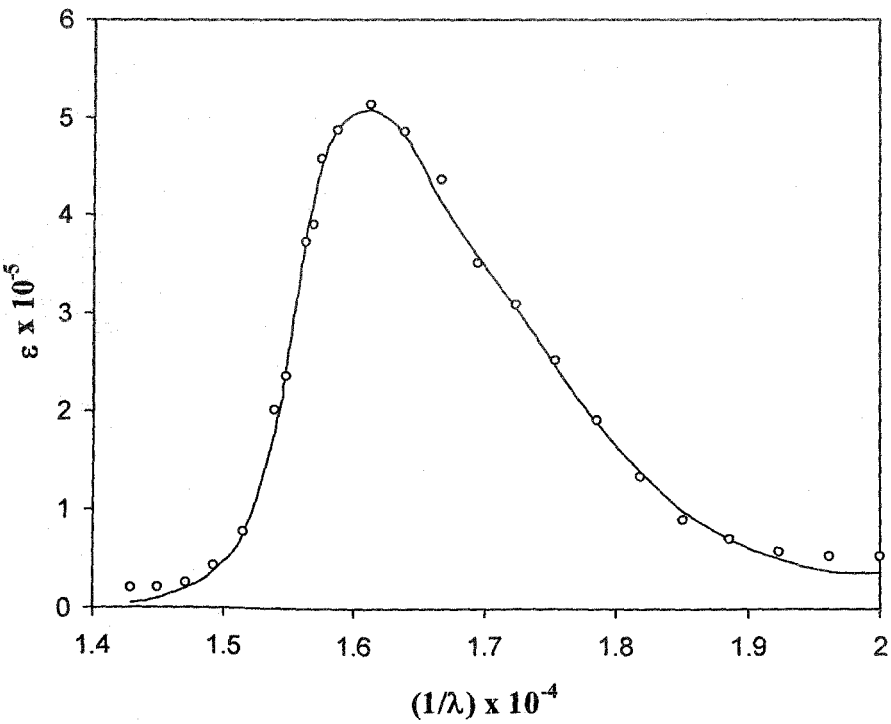

Figure 4.44 Absorption spectra of Azure C monomer in aqueous medium. Solid line represents the experimental spectrum and circles correspond to calculated points.

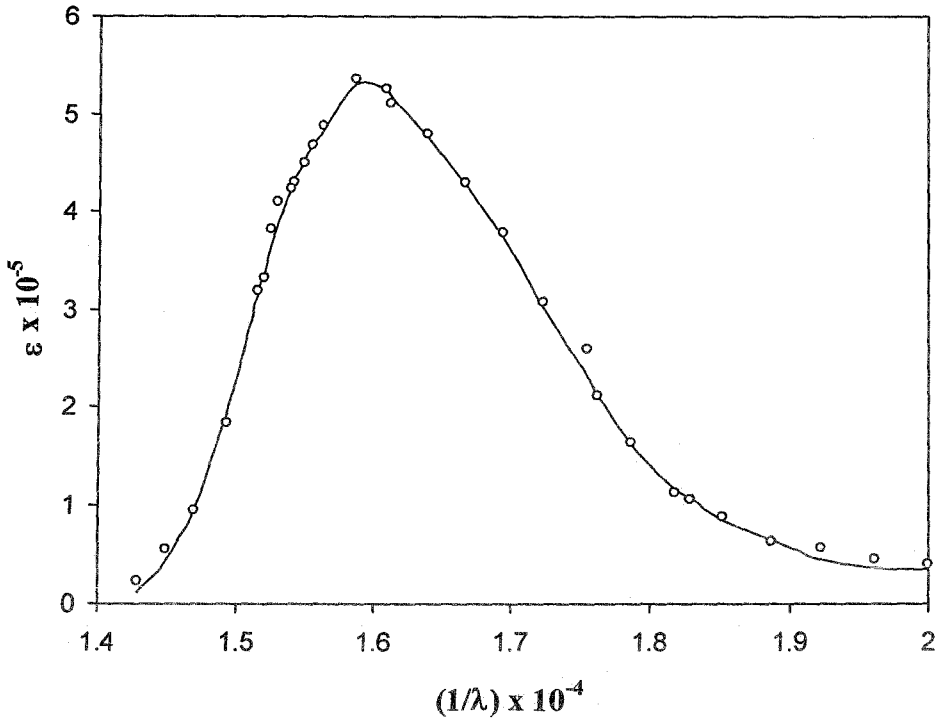

Figure 4.45 Absorption spectra of Azure A monomer in aqueous medium. Solid line represents the experimental spectrum and circles correspond to calculated points.

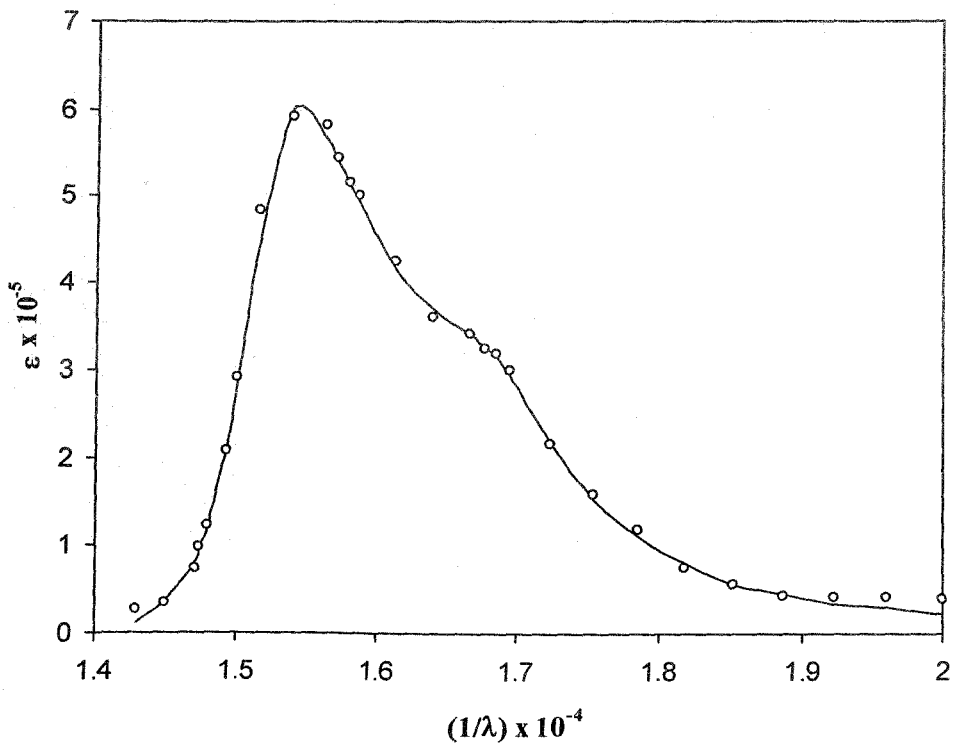

Figure 4.46 Absorption spectra of Azure B monomer in aqueous medium. Solid line represents the experimental spectrum and circles correspond to calculated points.

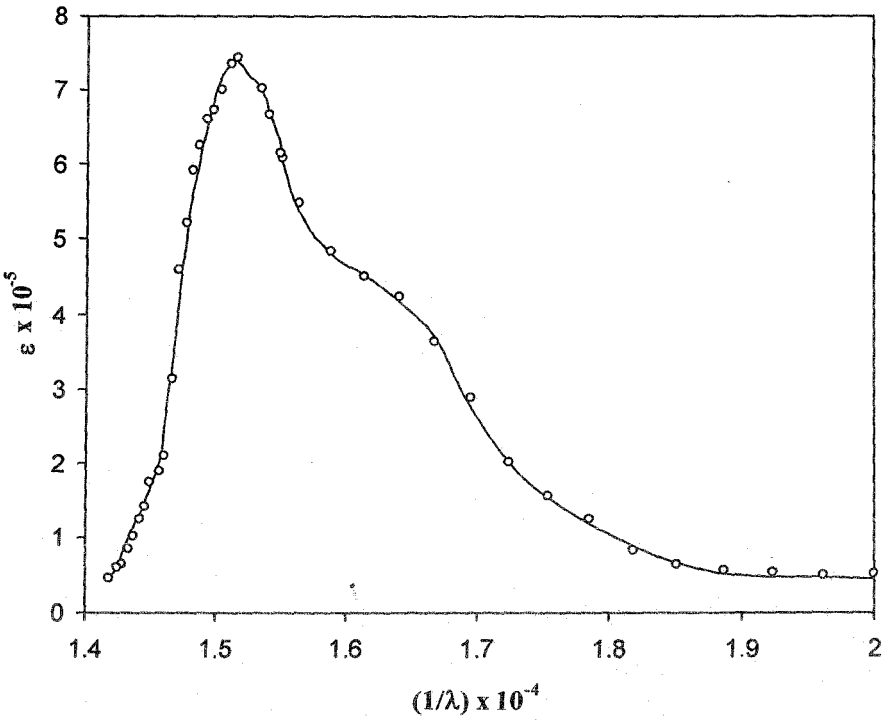

Figure 4.47 Absorption spectra of Methylene Blue monomer in aqueous medium. Solid line represents the experimental spectrum and circles correspond to calculated points.

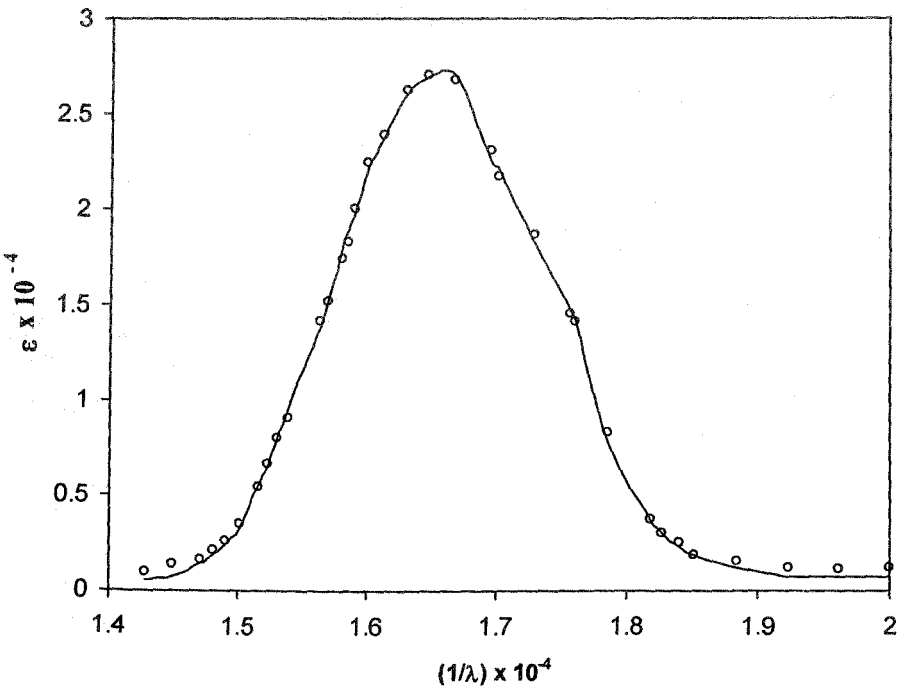

Figure 4.48 Absorption spectra of Thionine monomer in microemulsion. Solid line represents the experimental spectrum and circles correspond to calculated points.

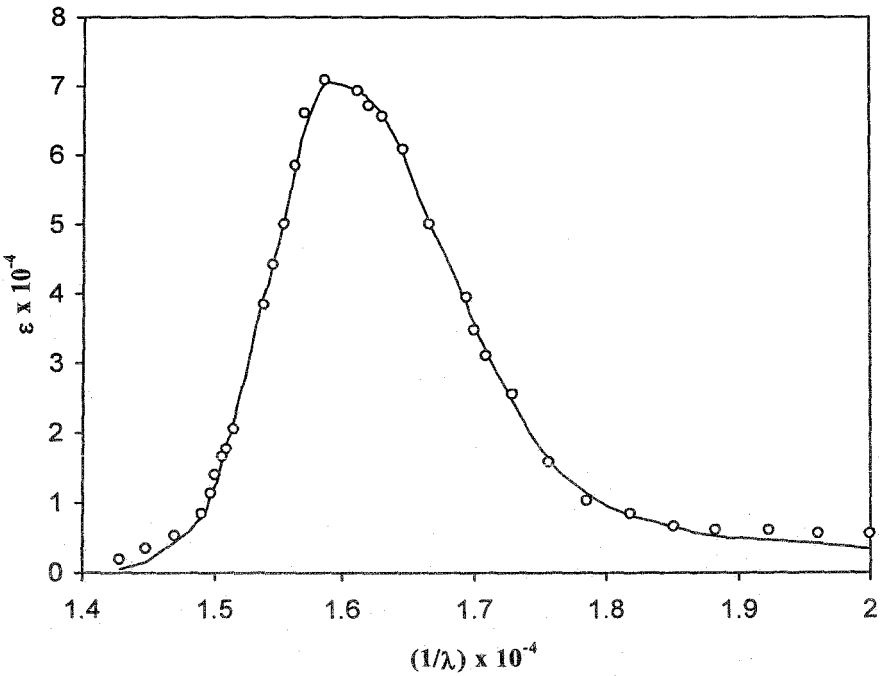

Figure 4.49 Absorption spectra of Azure C monomer in microemulsion. Solid line represents the experimental spectrum and circles correspond to calculated points.

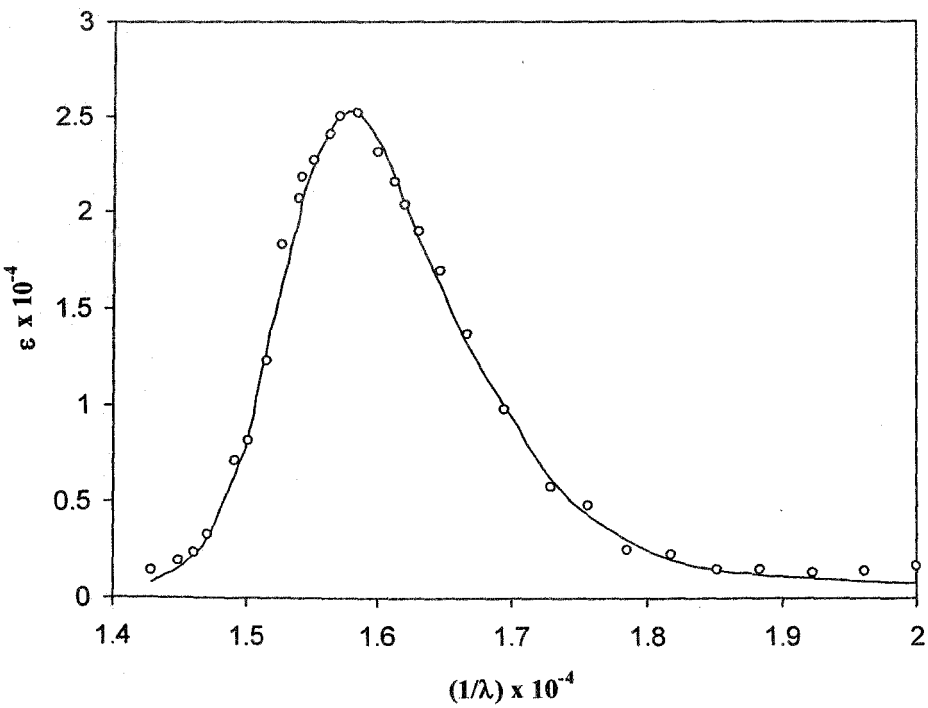

Figure 4.50 Absorption spectra of Azure A monomer in microemulsion. Solid line represents the experimental spectrum and circles correspond to calculated points.

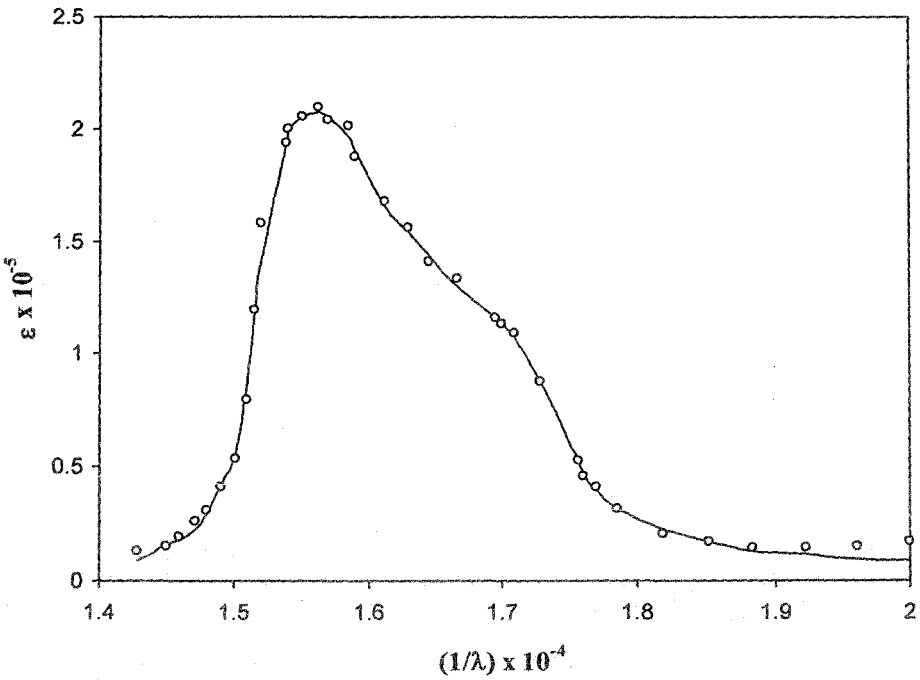

Figure 4.51 Absorption spectra of Azure B monomer in microemulsion. Solid line represents the experimental spectrum and circles correspond to calculated points.

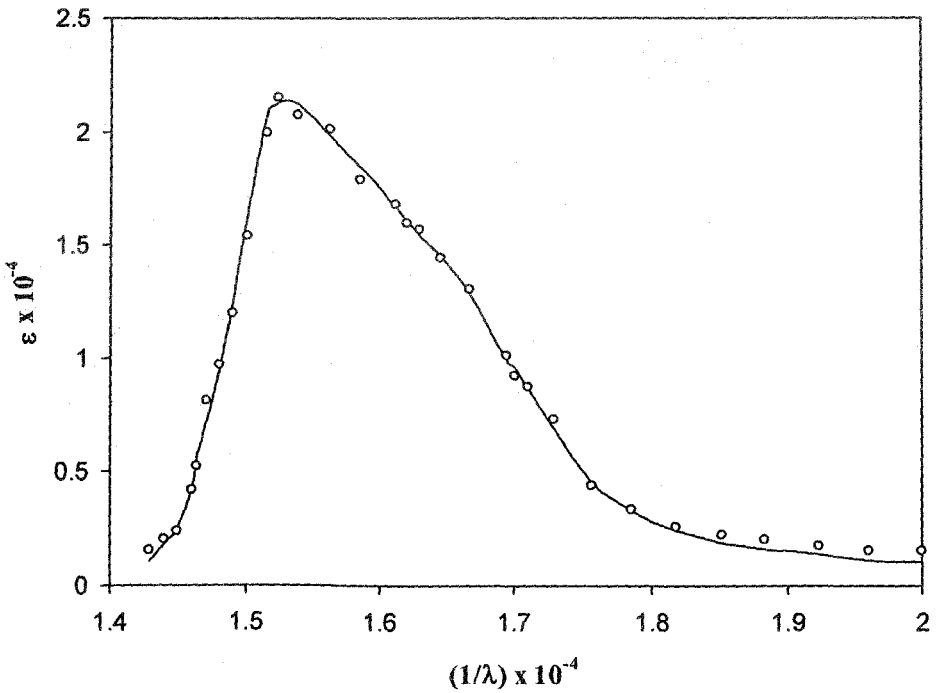

Figure 4.52 Absorption spectra of Methylene Blue monomer in micro-emulsion. Solid line represents the experimental spectrum and circles correspond to calculated points.

bands of constant band width is well applicable in the present systems under investigation.

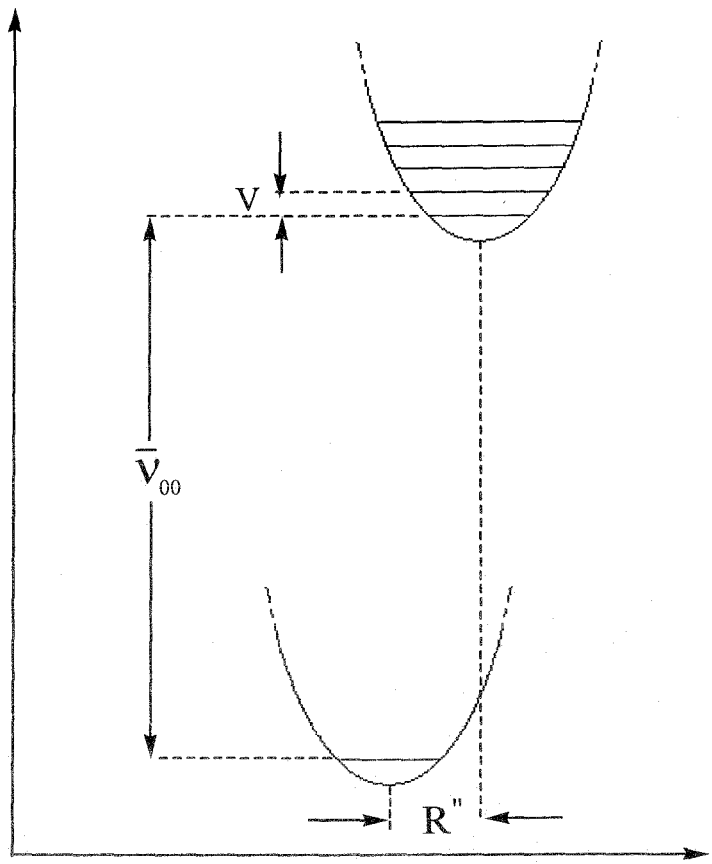

Figure 4.53 Schematic potential energy diagram in absorption

The parameter X which is the ratio of the (1, 0) to (0, 0) band intensities is related to the equilibrium nuclear conformation in the two electronic states. It is thus related to the displacement of the normal coordinate of vibration R, through the formula $X = (2\pi^2 c' V\mu) R^2$, where μ is the reduced mass of the oscillator, c' is the velocity of light and R is the displacement of normal coordinate of vibration, i.e., change in bond lengths between the atoms of the aromatic ring system.

Values of all five parameters of the progressively alkylated thiazine dyes in aqueous and microemulsion are listed in Table 4.7 and 4.8 respectively. Substantial change in the intensity I_{00} and the ratio of (1,0) to (0,0) band intensities i.e. X in most of the dyes have been observed which are intriguing. As has been mentioned above there are some evidences and justification in favour of an assertion that the parameter I_{00} and X are correlated. While the exact reason for the observed variation

of V with progressive methylation of dye or with the salvation media is not certain, above variation must have influenced vibronic characteristics of the dye molecules.

Table 4.7

Monomer (in aqueous solution) parameters for the five thiazine dyes with standard deviation

Dye	I_{00}	ν_{00} (cm^{-1})	V (cm^{-1})	X	b_g (cm^{-1})
Thionine	28424±913	16669±26	1072±47	0.587±0.038	1171±45
Azure C	26130±780	16065±25	1190±43	0.533±0.036	1173±46
Azure A	25584±984	15705±39	1361±52	0.626±0.056	1120±49
Azure B	23520±732	15522±19	1053±35	0.547±0.028	1162±36
Methylene Blue	24560±836	15288±54	1078±19	0.649±0.014	1143±34

Table 4.8

Monomer (in microemulsion) parameters for the five thiazine dyes with standard deviation

Dye	I_{00}	ν_{00} (cm^{-1})	V (cm^{-1})	X	b_g (cm^{-1})
Thionine	25205±880	16265±11	1193±36	0.403±0.031	1011±31
Azure C	24750±750	15920±57	1228±71	0.396±0.066	969±11
Azure A	24525±525	15739±23	1261±36	0.298±0.034	1134±68
Azure B	20760±480	15600±17	1019±30	0.470±0.028	1019±35
Methylene Blue	21980±520	15384±33	1068±57	0.620±0.052	1065±52

The rationale behind the observed variation of X for the thiazine dyes lie in the fact that though both the salvation media are water, the difference in physical characteristics (water mobility, dielectric constant, etc.) of bulk water with that of the water-pool of miocroemulsion also influences dimer geometry in solution and that in presence of a dynamic equilibrium which exists between monomers and the dimers, the electronic distribution of dye molecules are influenced and which is manifested in the variation in X value. This point will be discussed further during considering dimer spectra of the thiazines. The I_{00} values i.e., intensity of (0,0) band

also experience considerable loss in moving the medium from bulk water to microemulsion water-pool.

4.3.5 Analysis of Dimer Spectra in terms of Molecular Exciton Model

An important theoretical tool by which different types of dye aggregates (H, J or intermediate) could conveniently be analyzed is the molecular exciton theory of dipole-dipole coupling. According to this model, parallel aggregates (H - aggregates) absorb at shorter wave length and head to tail aggregates (J aggregates) show absorption at longer wave lengths compared to monomer. Intermediate geometries give rise to band splitting, where the monomer units are thought to be arranged parallely (Model I) or obliquely (Model II). In the above geometries the excited states of the dimer are described by exciton states in which the excitation is delocalised over both monomer units. This model describes the resonance interaction of excited states of molecular aggregate systems and neglect vibronic interactions. The model thus applies to aggregates of molecules which have intense or strongly allowed singlet-singlet interaction, with strong 0-0 vibronic bands. On the other hand, Fulton and Gouterman [211] described a model where the degenerate exciton interaction in the dimer corresponds to the vibronic coupling phenomena. Kurucsev applied the model of Fulton and Gouterman to dimer species of a number of dyes [212-214]. Although the vibronic exciton model has been claimed to be based on more recent development in exciton theory, the so called "non-vibronic" model is simpler and works surprisingly well in explaining dimer spectra of many organic dye systems. The splitting of dimer spectra for the so called "intermediate geometries" leads to compute the angle θ between monomer units and intermolecular separation of the monomer molecules in the dimer.

Resolved dimer spectra of dyes are shown in Figures 4.33 - 4.42. As expected each dimer spectrum is decomposed into two bands characteristics of which are given in Table 4.4 and 4.6 in both aqueous and microemulsion media. The decomposition of the dimer spectrum into two bands shows that the monomer visible spectrum corresponds to an electronic transition with two vibronic bands and not two electronic transitions. As mentioned earlier in the exciton model the point dipole - point dipole approximation of the point multiple expression of the theory of moleculer exciton coupling can be extended and applied to all thiazine dimers in

concentrated solutions. Briefly, using the values of the oscillators' strength of the low (f_1) and high (f_2) frequency components (the J-band and H-band respectively) of the dimer spectra, the angle θ between the main oscillators of the two molecules can be determined by the expression [215].

$$f_1/f_2 = \tan^2\{(180-\theta)/2\} \tag{4.30}$$

On the other hand, the distance (R) betweens the centers of the two molecules can be calculated from the resonance interaction energy, U, (a term which is equal to half the separation between the electronic band maxima of the splitted dimer spectrum).

(U has been designated as $\mathscr{E}$ in Figure 4.2)

The relationship between the interaction energy, strength of transition dipole and the geometry of the dimer is given by the general equation

$$U = \frac{|M|^2}{R^3}\left(\cos\theta + 3\cos^2\phi\right) \tag{4.31}$$

Where $|M|^2$ is the square of the transition moments of the monomer, θ is the angle between polarization axes for the monomer and ϕ is the angle between the polarization direction and the line joining the centers of the two component molecules. The following equation can be used directly to determine oscillator strength of a derivative spectrum.

$$f = 4.32 \times 10^{-9} \int \varepsilon(\nu)\, d\nu \tag{4.32}$$

However, it is more convenient to modify the equation to make it easier to analyze spectra measured a function of a wave length instead of frequency. If the dispersion relationship $C = \lambda\nu$ is used to substitute for ν in the above equation, the alternative relationship

$$f = (0.0432 / \lambda_0^2) \int \varepsilon\ (\lambda)\, d\lambda. \tag{4.33}$$

may be derived. In this expression $\varepsilon(\lambda)$ has units of lit/mol-cm and λ in nm, λ_0 is the wave length at the peak of a smoothed envelops containing the spectrum.

The angle θ calculated for the dimers are presented in Table 4.11 and 4.12. For the calculations of f_1 and f_2 values for each dimer spectrum, measurement of the area

under the J and H-bands of the spectra was done by using Microcal Origin 6.0 software. The transition moment M is calculated using the relationship

$$f = 4.704 \times 10^{29} \bar{\nu} M^2 \tag{4.34}$$

in cm^{-1} of the dimer at maximum ε in the dimer spectrum.

The distance (R) between monomers in a dimer is model dependent, i.e., it depends on the geometric disposition. To explain dimer band splitting, two models allowing the two transitions are possible. In model I, the monomers are in parallel planes with a twist angle θ while in model II, they are in the same plane forming angle θ. The interaction energy in these models is as follows [158,159].

Model I: ($\theta = \theta$ and $\phi = 90^0$; Sandwitch dimer with a Twist angle θ)

$$U = -\frac{|M|^2 \cos\theta}{R_I^3} \tag{4.35}$$

Model II: ($\theta = \theta$ and $\phi = \theta$; Co-planar inclined angle dimer)

$$U = -\frac{|M|^2}{R_{II}^3}\left(\cos\theta + 3\cos^2\phi\right) = -\frac{|M|^2}{R_{II}^3}\left(\cos\theta + 3\sin^2\theta/2\right) \tag{4.36}$$

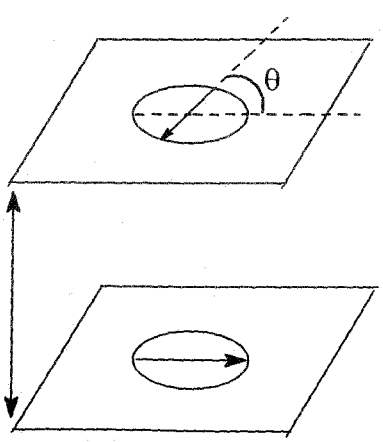

Model - I

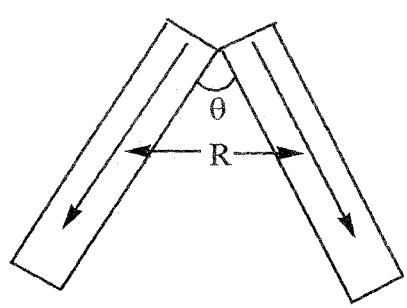

Model - II

Where R_I and R_{II} are the distances between the monomers in the dimers in model I and II respectively. Model I refers to the case of non-planar transition dipoles where the molecules are arranged in a sandwich dimer (card pack) oriented with angle θ the angle of skew between the polarization direction of the absorption oscillators of each dye molecule. Model II refers to the "coplanar inclined angle dimer" of the

"oblique" arrangement where θ is the angle between the planes of the aromatic ring. The twist angles θ (for model I) and the oblique angle θ (for model II) and the distance (R) between the centers of the monomer units in a dimer have been calculated for all the thiazine dyes under investigation.

The calculated oscillators strength of the dimers are listed in Table 4.9 and 4.10. The excitonic parameters of thiazine dimers and values of transition moments and twist angles are shown in Table 4.11 and 4.12 respectively in aqueous and microemulsion media.

Table 4.9

Oscillators strength in aqueous medium

Dye	Oscillator strength of monomer (f_m)	Oscillator strength of the low frequency band (J-band) f_2 of dimer)	Oscillator strength of the high frequency band (H-band) f_1 of dimer
Thionine	0.603	0.048	0.532
Azure C	0.451	0.043	0.581
Azure A	0.552	0.050	0.863
Azure B	0.641	0.075	0.980
Methylene Blue	0.610	0.073	0.972

Table 4.10

Oscillators strength in microemulsion medium

Dye	Oscillator strength of monomer (f_m)	Oscillator strength of the low frequency band (J-band) f_2 of dimer)	Oscillator strength of the high frequency band (H-band) f_1 of dimer
Thionine	0.382	0.032	0.307
Azure C	0.101	0.025	0.280
Azure A	0.202	0.029	0.250
Azure B	0.280	0.030	0.299
Methylene Blue	0.191	0.024	0.231

The twist angle for the thionine (34.8^0) is found to be largest among all the dyes and Az C shows smallest twist angle of 28.4^0 when dimers are formed in aqueous medium. But in microemulsion Az B gives the least value of twist angle among all the dyes. As discussed earlier the variation of physico-chemical characteristics of the

water in the water-pool to that of the bulk water also plays important role to the dimer geometry.

Table 4.11

Excitonic parameters of the dimers of thiazine dyes in aqueous media

Dye	Twist angle (θ /deg.)	Square of the transition moments $(\|M\|^2 x10^{36})$ /esu	Interaction energy (U /cm^{-1})	Intermolecular distance (Å)	
				R_I	R_{II}
Thionine	34.8	56.23	1072.5	6.01	6.61
Azure C	28.4	63.20	1076.5	6.38	6.80
Azura A	28.5	67.23	1417.5	5.95	6.75
Azura B	30.2	59.96	1172.0	6.06	6.65
Methylene Blue	31.7	78.81	1097.5	6.76	7.30

Table 4.12

Excitonic parameters of the dimers of thiazine dyes in microemulsion media

Dye	Twist angle (θ /deg.)	Square of the transition moments $(\|M\|^2 x10^{36})$ /esu	Interaction energy (U /cm^{-1})	Intermolecular distance (Å)	
				R_I	R_{II}
Thionine	35.7	35.89	1515.1	3.70	5.59
Azure C	28.1	29.57	1465.9	4.65	5.88
Azura A	30.9	30.19	1541.0	4.42	5.35
Azura B	25.3	23.69	1682.2	4.12	5.01
Methylene Blue	28.2	33.43	1374.3	4.97	6.26

While the twist angles displayed by all the five dyes are close to each other, no systematic variation is observed on progressive alkylation of the dye molecule. However, except methylene blue, progressive alkylation decreases the twist angle to some extent. It seems apparent that apart from the steric effect due to the addition of successive methyl groups in the dye molecule, hydrophobic as well as electron donating nature of methyl groups are also involved. Apparently the increased hydrophobic interaction due to methyl substitution as well as for their electron donating nature, a stronger field is created such that the dipoles tend towards parallel alignment resulting in decrease in θ upon introduction of methyl groups successively in the thionine molecule. In other wards a better $\pi - \pi$ interaction

between two monomer molecules as a result of successive addition of methyl groups may cause the observed alignment. Further substitution of methyl groups probably increase stetric hindrance resulting in the increase of the angle, θ, between dipoles in the case of methylene blue. But in microemulsion due to the effective electrostatic repulsion between the similarly charged dimers and inner layer of microemulsion, the dimers give relatively lower twist angle between the dipoles when compared to that in bulk water.

It should be mentioned in this context that the angle between the transition moments of two monomers of methylene blue as reported by Bergmann and O'Konski [147] was only 13^0. The twist angle calculated for the present study is much higher than that reported by above authors. However, the present analysis is based on more recently developed theories, which showed consistency in recent study for a number of dye systems [216]

On the other hand, intermolecular distance between two monomer molecules in a dimer as calculated according to model I varies from 5.59 to 6.76 Å; while the same varies from 6.61 to 7.30 Å when calculated according to model II for aqueous medium. In microemulsion media, however the distance lie between 3.70 to 4.97 Å for model I and 5.01 to 6.26 Å for model II.

It is interesting to note that due to the location of dyes in the relatively confined space and also due to the electrostatic interactions and low dielectric constant of the medium, distance between monomers in the dimer is decreased considerably in water-pools of microemulsion. This is due to stronger excitinic band splitting of dimer spectra in microemulsion relative to bulk water. The distances between the transition dipoles in the dimers as revealed in the present systems are somewhat higher than observed previously for fluorescein and rhodamine dyes. But the values calculated according to model I are somewhat less. In view of this and the observation of the previous workers on a number of dyes it may be argued that model I might be appropriate. On the other hand, more recent work argued in favour of model II [209]. However, these models represent only the ideal cases and the real structure may only approximate to one of them. It is noteworthy that although the exciton theory as applied in the present systems is over simplification for the problem of dye aggregation, the interdipole distances computed therefrom appears to be reasonable if proper geometry of the aggregate is taken into consideration.

References

1. Rafati, A.A; Gharibi, H.; Rezaie Sameti M. *J. Mol. Liq.* **2004**, *111*, 109.
2. García-Río, L.; Hervella, P.; Mejuto, J.C.; Parajó, M. *Chem. Phys.* **2007**, *335*, 164.
3. Tehrani Bagha, A.R.; Bhrami, H.; Movassagh, B.; Arami, M.; Menger, F.M. *Dyes Pigments* **2007**, *72*, 331.
4. Hartley, G.S. *Trans. Faraday Soc.* **1934**, *30*, 44.
5. Savvin, S.B.; Chernova, R.K.; Shtykov, S.N. *Zh. Analit. Khim.* **1978**, *33*, 865.
6. Rosendorfova, J.; Cermakova, L. *Talanta* 1980, *27*, 705.
7. Minch, M.J. and Sadiq-Shah, S. *J. Org. Chem.* **1979**, *44*, 3253.
8. Buwalda, R.T., Engberts, J.B.F.N. *Langmuir* **2001**, *17*, 1054.
9. Karukstis, K.K.; Savin, D.A.; Loftus, C.T.; D'Angelo, N.D.; *J. Colloid Interface Sci.* **1998**, *203*, 157.
10. He, Q.; Chen, H.; Fresen, J. *Anal. Chem.* **2000**, *367*, 270.
11. Sarkar, M.; Poddar, S. *J. Colloid Interface Sci.* **2000**, *221*, 181.
12. Oliveira, C.S.; Bastos, E.L.; Durate, E.L.; Itri, R.; Baptista, M.S. *Langmuir* **2006**, *22*, 8718.
13. Junqueira, H.C.; Severino, D.; Dias, L.G.; Gugliotti, M.S.; Baptista, M.S. *Phys. Chem. Chem. Phys.* **2002**, *4*, 2320.
14. Chibisov, A.K.; Prokhorenko, V.I.; Gorner, H. *Chem. Phys.* **1999**, *250*, 47.
15. Robinson, B.H.; Löffler, A.; Schwarz, G.; *J. Chem. Soc., Faraday Trans. I* **1973**, *69*, 56.
16. Braswell, E.H. *J. Phys. Chem.* **1984**, *88*, 3653.
17. Rosendorfova, J.; Cermakova, L. *Talanta* **1980**, *27*, 705.
18. Sanh-Medel, Garcia Alonso, A.J.I.; Blanco Gonzalez, E. *Anal.Chem.* **1985**, *57*, 1681.
19. Reeves, R.L.; Maggio, M.S.; Harkaway, S. A. *J. Phys. Chem.* **1979**, *83*, 2359.
20. Kali, K.M.; Cussler, E.L.; Evans, D.F. *J. Phys. Chem.* **1980**, *84*, 593.
21. Corrin, M.L.; Harkins, W.D. *J. Am. Chem. Soc.* **1974**, *96*, 679.
22. Saikia, P.M.; Kalita, A.; Gohain, B.; Sarma, S.; Datta, R.K. *Colloid Surf. A* **2003**, *216*, 21.
23. Huang, X.; Jinghe, Y.; Zhang, W.; Zhang, Z.; An, Z. *J. Chem. Edu.* **1999**, *76*, 93.

24. Samsonoff, C.; Daily, J.; Almog, R.; Berns, D.S. *J. Colloid Interface Sci.* **1986**, 109,325.

25. Sanz-Medel,A.; Camara Rica, C.; Perez Bustamante, J.A. *Anal. Chem.* **1980**, *52*, 1035.

26. Garcia Alonso, J.I.; Sanz-Medel, A. *Quim Anal.* **1986**, *5*, 428.

27. Mukherjee, P.; Mysels, K.J. *J. Am. Chem. Soc.* **1955**, *77*, 2937.

28. Malik, W.V.; Haque, R. *J. Am.Chem. Soc.* **1963**, *67*, 2082.

29. Malik,; W.V.; Jhamb, O.P. *J. Electroanal Chem.* **1970**, *27*, 151.

30. Guha, S.N.; Moorthy, P.N.; Rao, K.N. *Proc. Indian Acad. Sci.* **1982**, *91*, 73.

31. Skarydova, V.; Cermakova, L. *Collection Czech. Chem. Commun.* **1982**, *47*, 776.

32. Savvin, S. B.; Marov, I. N.; Chernova, R.K.; Shtykov, S.N.; Sokolov, A.B. *Zh. Analit. Khim.* **1981**, *36*, 850.

33. Bunton, C.A.; Minch,M. J.; Hidalgo, J.; Sepulveda L. *J. Am. Chem. Soc.* **1973**, *95*, 3262.

34. Bunton, C.A.; Minch, M.J. *J. Phys. Chem.* **1974**, *78*, 1490.

35. Fernandez, M.S.; Fromjertz, P. *J. Phys. Chem.* **1977**, *81*, 1755.

36. Funasaki, N. *J. Phys. Chem.* **1979**, *83*, 1998.

37. Birdi, K.S.; Singh, H.N.; Dolsager, S.V. *J. Phys. Chem.* **1979**, *83*, 2733.

38. Minch, M.J.; Giaccio, M. and Wolff, R. J.Am.Chem.Soc. **97**, 3766, 1975.

39. Chiang, H.C.; Lukton, A. *J. Phys. Chem.* **1975**, *79*, 1935.

40. Stevenson, D.M.; Duff, D.G.; Kirkwood, D.J. *J. Soc. Dyers Colour* **1981**, 97, 13.

41. Biedermann, W.; Datyner, A. *J. Colloid Interface Sci.* **1981**, *82*, 276.

42. Dill, K.A.; Koppel, D.E.; Cantor, R.S.; Dill, J.D.; Bendedouch, D.; Chen, S.H. *Nature*, **1984**, *309*, 42.

43. Kapoor, R.C.; Mishra, V.N. *J. Ind. Chem. Soc.* **1976**, *53*, 965.

44. Sato, H.; Kawasaki, M.; Kasatani, Y.; Kusumoto, N.; Nakashima, N. Yoshihara, K. *Chem. Lett.* **1980, 12**, 1529.

45. Humphry, R.; Baker.; Gratzel, M.; Steiger, R. *J. Am. Chem. Soc.* **1980**, *102*, 847.

46. Wolff, T.; Bunsenges, B. *J. Phys. Chem.* **1981**, *85*, 145.

47. Diaz Garcia, M.E.; Sanz-Medel, A. *Talanta* **1986**, 33, 255.

48. Rosenthal, K.S.; Koussali, F. *Anal. Chem.* **1983**, *55*, 1115.

49. Garcia Alonso, J.J.; Diaz Garcia, M.E.; Sanz-Medel, A. *Talanta* **1984**, *31*, 361.

50. Diaz Garcia, M.E.; Blanco Gonzalez, E.; Sanz-Medel, A. *Microchem. J.* **1984**, *30*, 211.
51. Tanford, C. *The Hydrophobic Effect: Formation of Micelles and Biological Membranes*, Wiley-Interscience, New York, 1980.
52. Fendler, J.H. *Acc. Chem. Res.* **1976**, *9*, 153.
53. Fendler, J.H.; Fendler, E.J. *Catalysis in Micellar and Macromolecular Systems*, Academic Press, New York, 1975.
54. Muto, S. and Meguro, K. *Bull. Chem. Soc. Japan* **1973**, 46, 1316.
55. O'Connor, C. J.; Lomax, T.D.; Ramage, R.E. *Adv. Colloid Interface Sci.* **1984**, *20*, 21.
56. Mandal, A.K; Pal, M.K. *J. Colloid Interface Sci.* **1997**, *192*, 83.
57. Gokturk, S.; Tuncay, M. *Spectrochemica Acta,, Part A* **2003**, *59*, 1857.
58. Hinze, W.L. *Solution Chemistry of Surfactants*, Mittal, K.L. (Ed.), Vol.-I, pp. 79-127, Plenum Press, New York, 1979.
59. Kapoor, R.C. *J. Ind. Chem. Soc.* **1986**, *63*, 541.
60. Callaham, J.H.; Cook, K.O. *Anal. Chem.* **1984**, *56*, 1632.
61. Rohatgi-Mukherjee, K.K.; Choudhuri, R.; Bhowmik, B.B. *J. Colloid Interface Sci.* **1985**, *106*, 45.
62. Reeves, R.L.; Harkaway, S.A. *Solution-Chemistry of Surfactants*, Mittal, K.L. (Ed.), Plenum Press, New York, p.819, 1979.
63. Dutt, R.K.; Bhat, S.N. *Bull. Chem. Soc. Jpn.* **1992**, *65*, 1089.
64. Gopidas, K.R.; Kamat, P.V. *J. Phys. Chem.* **1990**, *94*, 813.
65. Colichmann, E.L. *J. Am. Chem. Soc.* **1951**, *73*, 1795.
66. Ghosh, A.K.; Mukherjee, P. *J. Am. Chem. Soc.* **1970**, *92*, 6408.
67. Diamond, R.N. *J. Phys. Chem.* **1963**, *67*, 2513.
68. Weir, D.; Scaiano, J.C. *Tetrahedron* **1987**, *43*, 1617.
69. Tanigushi, M.; Yamagichi, A.; Iwamoto, T. *J. Phys. Chem.* **1990**, *94*, 2534.
70. Hiskey, C.P.; Downey, T.A. *J. Phys. Chem.* **1954**, *58*, 835.
71. Cockbain E.G. *Trans Fraday Soc.* **1954**, *49*, 104.
72. Hayashi M. *Bull. Chem. Soc. Japan* **1961**, *34*, 119.

73. Matibinkov, M.A.; Namaka, D. Varkevich, N.M.; Kaskov, B.N.; Monkher, D. Vest Akad Navak Belarus SSR 35R Ser Fiz Mat Naruk, **1973**, *87*, *Chem. Abstr.* 80, 101, 9447, 1974.

74. Rohatgi-Mukherjee, K.K.; Bhattacharya, S.C.; Bhowmik B.B. *Ind. J. Chem.* **1983**, *22A*, 911.

75. Bhowmik, B.B.; Bhattacharya, S.C.; Rohatgi-Mukherjee K.K. *Indian J. Chem.* **1986**, *25A*, 126.

76. Ketelaar, J.A.A.; Vande Stolpe, C.; Gersmann, H.R. *Rec. Trav. Chim.* **1952**, *70*, 499.

77. Scott, R. L. *Rec. Trans. Chim.* **1956**, *75*, 787.

78. Bhowmik, B.B.; Chaudhury, R.; Rohatgi-Mukherjee, K.K. *Ind. J. Chem.* **1987**, *26A*, 95.

79. Benesi, H A.; Hildebrand, J.H. *J. Am. Chem. Soc.* **1949**, *71*, 2703.

80. Scatchard, G.; Aun, N.Y. *Acad. Sci.* **1949**, *51*, 660.

81. Mukhopadhyay, M.; Sen Verma, C.; Bhowmik, B.B. *Colloid Polym. Sci.* **1990**, *268*, 447.

82. Mulliken, R.S. Person, W.B. *Molecular Complexes*, Wiley, New York, 1969.

83. Sarkar, M.; Poddar, S. *Spectrochimica Acta A*, **1999**, *55*, 1737.

84. Gawndi, V.B.; Guha, S.N.; Priyadarshini, K.I.; Mohan, H. *J. Colloid, Inf. Sci.* **2001**, *242*, 220.

85. Kalyanasundaram, K. *Chem. Soc. Rev.* **1978**, *7*, 453.

86. Moroi, Y.; Baraun, A.M.; Gratzel, M. *J. Am. Chem. Soc.* **1979**, *101*, 567.

87. Moroi, Y.; Infelta, P.P.; Gratzel, M. *J. Am. Chem. Soc.* **1979**, *101*, 573.

88. Turro, N. J.; Gratzel, M.; Baraun, A.M. *Angrew Chem. Int. Ed. Engl.* **1980**, *19*, 675.

89. Kawait, T.; Yasuda, Y.; Kon-no, K. *Bull. Chem. Soc. Jpn.* **1995**, *68*, 2175.

90. Mittal, K.L. *Micellization, Solubilization and Microemulsions*, Vols. 1 and 2, Plenum, New York, 1977.

91. Pandit,P.; Basu, S. *Environ. Sci. Technol.* **2004**, *38*, 2435.

92. Moulik, S.P.; Paul, B.K. *Adv. Colloid. Interface. Sci.* **1998**, *78*, 99.

93. Haandrikman, G.; Daane, G.J.R.; Kerkhof, F.J.M.; Van Os, N.M.; Rupert, L.A.M. *J. Phys. Chem.* **1992**, *96*, 9061.

94. Moran, M.; Bowmaker, G.A.; Cooney, R.P. *Langmuir* **1995**, *11*, 738.
95. Fendler, H.J.; *Membrane Mimetic Chemistry*, Wily, New York, 1982.
96. Harada, S.; Schelly, Z.A. *J. Phys. Chem.* **1982**, *86*, 2098.
97. Herrmann, U.; Schelly, Z.A. *J. Am. Chem. Soc.* **1979**, *101*, 2665.
98. Verbeeck, A.; Galade, E.; DeSchryver F.C. *Langmuir* **1982**, *2*, 448.
99. Tatikolov, A.S.; Costa, S.M.B. *Photochem. Photobiol. Sci.* **2002**, *1*, 211.
100. Oldfield, C.; Robinson, B.H.; Freedman, R.B. *J. Chem. Soc. Faraday Trans.* **1990**, *86*, 833.
101. Fletcher, P.D.I. *J. Chem. Soc. Faraday Trans. 1* **1986**, *82*, 2651.
102. Neimeyer, E.D.; Bright, F.V. *J. Phys. Chem. B* **1998**, *102*, 1474.
103. Fujii, H.; Kawai, T.; Nishikawa, H.; Ebert, G. *Colloid Polym. Sci.* **1998**, *260*, 697.
104. Belletete, M.; Durocher, G. *J. Colloid Interface Sci.* **1990**, *134*, 289.
105. Ishchenkoa, A.A.; Shapovalov, S.A. *J. Appl. Spectrosc.* **2004**, *71*, 605.
106. Gohain, B.; Saikia, P.M.; Sarma, S.; Bhat, S.N.; Datta, R.K. *Phys. Chem. Chem. Phys.* **2002**, *4*, 2617.
107. Pramanick, D.; Mukherjee, D. *J. Colloid Interface Sci.* **1993**, *157*, 131.
108. Zhu, D.; Schelly, Z.A. *Langmuir* **1992**, *8*, 48.
109. Foley, M.S.C.; Beeby, A.; Parker, A.W.; Bishop, S.M.; Phillips, D. *J. Photochem. Photobiol. B: Biol.* **1997**, *38*, 18.
110. Mackay, R.A.; Lai, W.-C. *Colloid Surfaces A: Physicochem. Eng. Aspects 254*, **2005**, 115.
111. Biswas, S.; Bhattacharya, S.C.; Bhowmik, B.B.; Moulik, S.P. *J. Colloid Interface Sci.* **2001**, *244*, 145.
112. Hung, H.C.; Chang, G.G. *J. Chem. Soc. Perkin Trans.* **1999**, *2*, 2177.
113. Hazarika, R.; Datta, R.K.; Bhat, S.N. *Indian J. Chem.* **1993**, *32A*, 239.
114. Dakiky, M.; Manassra, A.; Kareem, M.A.; Jhmean, F.; Khamis, M. *Dyes Pigments* **2004**, *63*, 101.
115. Arunkumar, E.; Forbes, C.C.; Smith. B.D. *Eur. J. Org. Chem.* **2005**, *19*, 4051.
116. Jana, N.R.; Pal, T. *J. Surf. Sci. Technol.* **2001**, *17*, 191.
117. Simončič, B.; Kert, M. *Dyes Pigments* **2002**, *54*, 221.
118. Rohatgi-Mukherjee, *Ind. J. Chem.* **1992**, *28*, 721.

119. Antonov , L.; Gergov, G.; Petrov, V.; Kubista, M.; Nygren, J. *Talanta* **1999**, *49*, 99.

120. Pagfeldt, A.; Graetzel, M. *Chem. Rev.* **1995**, *95*, 49.

121. West, W.; Gilman, P.B.Jr. in *The Theory Of The Photography Process*, 4th Ed.; James, T.H. Ed. Macmillan; New York, 1997.

122. Kemnitz, K.; Yoshihara, K.; Ohzeki, K ; *J. Phys. Chem.* **1990**, *94*, 3099.

123. Spitler, M.T. *J. Imaging Sci.* **1991**, *35*, 351.

124. Law, K.Y. *Chem. Rev.* **1993**, *93*, 449.

125. Kamat, P.V. *Chem. Rev.* **1993**, *93*, 267.

126. Parkinson, B.A.; Spitler, M.T., *Electrochim. Acta* **1992**, *37*, 943.

127. Das, S.; Thomas, K.G.; Kamat, P.V.; George M.V. Proc. *Ind. Acad. Sci. (Chem. Sci.)* **1993**, *105*, 513.

128. Chau, L.K.; Arbour, C.; Collins, G.E.; Nebesuy, K.W.; Lee, P.A.; England, C.D. Armstrong, N.R.; Parkinson, B.A. *J. Phys. Chem.* **1993**, *97*, 2690.

129. Taguchi, T.; Hirayama, S.; Okamoto, M. *Chem. Phys. Lett.* **1994**, *231*, 561.

130. Kim, Y.S.; Liang, K; Law, K.Y; Whitten, D.C. *J. Phys. Chem.* **1994**, *98*, 984.

131. Harrison, W.J.; Mateer, D.L.; Tiddy, G.J.T. *J. Phys. Chem. B.* **1996**, *100*, 2310.

132. Lydon, J.E. *Curr. Opin., Colloid Interface Sci.* **1998**, *3*, 458.

133. Lydon, J.E.; in *Hand Book Of Liquid Crystals*, vol. 2B; Demus, D.; Goodby, J.; Gray, G W; Spies, H.W.; Vill, V.; Eds. Willy. VCH, Weinheim, pp. 981-1007, 1998.

134. Kock-Yec Law, H.C.; Peristein, J.; Whitten, D.G. *J. Am. Chem. Soc.* **1995**, *117*, 7257.

135. Von. Berlepsch. H.; Bottcher, C.; Ouart, A.; Burger, C.; Dahne, S.; Kirstein, S. *J. Phys. Chem. B* **2000**, *104*, 5255.

136. Spitz, C.; Dahne, S.; Quart, A.; Abraham, H.W. *J. Phys. Chem. B* **2000**, *104*, 8664.

137. Rubires, R.; Farrera, J.A.; Ribo, J.M. *Chem. Eur. J.* **2001**, *7*, 436.

138. Burdett. B.C. *Aggregation Process in Solution*, Ed. Jones, E.W.; Gormally, J. (Elsevier, Armsterdam, 1983) Chap. 10, p. 241.

139. Aquilera, O.; Neckers, D.C. *Acc. Chem. Res.* **1989**, *171*, 22.

140. Rohatgi-Mukherjee, K.K. and Singhal, G.S. *J. Phys. Chem.* **1960**, *70*, 1695.

141. Mukherjee, P.; Ghosh, A.K. *J. Am. Chem. Soc.* **1970**, *92*, 6419.

142. Rabinson, B.H.; Loffler, A.; Schawarz, G. *J. Chem. Soc. Faraday Trans. 1* **1973**, *69*, 56.

143. Schubert, M.; Levine, A. J. Am. Chem. Soc., **77**, 4197, 1955.

144. Turner, R.; Cowmann, M.K. *Arch. Biochem. Biophys.* **1985**, *237*, 253.

145. Vitagliano, V. in *Aggregation Processes in Solution*, Eds. Jones, E.W.; Gormally, J. (Elsevier, Armsterdam, 1983) Chap. 11, p. 271.

146. Shirai, M.; Dhyabu, M.; Ono, Y.; Tanaka, M.; *J. Polym. Sci. Chem.* **1982**, 19, 555.

147. Newmann, M.G.; Hioka, N. *J. Appl. Polym. Sci.* **1987**, *34*, 2829.

148. Bergmann, K.; O'Konsky, C. T. *J. Phys. Chem.* **1963**, *67*, 2169.

149. West, W.; Pearce, S. *J. Phys. Chem.* **1965**, *69*, 189.

150. Baranova, E.G.; Levshin, V.L. *Optica. Spetrokopia.* **1961**, *10*, 182.

151. Mataga, N. *Bull. Chem. Soc. Japan* **1957**, *30*, 375.

152. Zanker, V. *Z. Physik. Chem.* **1952**, *200*, 250.

153. Hida, M.; Sanuki, T. *Bull. Chem. Soc. Japan*, **1970**, *43*, 2291.

154. Selwyn, J.E.; Steinfeld, J.I. *J. Phys. Chem.* **1972**, *76*, 762.

155. James, A.D.; Rabinson, B.H. *Adv. Mol. Relax. Process B* **1976**, *8*, 287.

156. Kamat, P.V.; Lichtin, N.N. *J. Phys. Chem.* **1981**, *85*, 814.

157. Zadoroznnaya, E.M.; Nabinvanets, B.I.; Maslei, N.N. *Zh. Anal. Khim.* **1974**, *29*, 993.

158. Arbeloa, I.L. *J. Chem. Soc. Faraday Trans. 2*, **1981**, *77*, 1725.

159. Arbeloa, I.L.; Rohatgi-Mukherjee, K.K. *Spectrochemica Acta.* **1988**, *44A*, 423.

160. Newmann, M.G.; Gessner, F.; Olivelra, V.A. *J. Chem. Soc. Faraday Trans.* **1990**, *86*, 3551.

161. McRae, E.B.; Kasha, M. *Physical Processes in Radiation Biology*, Augenstein, L.; Rosenberg, B.; Mason, R. Ed., Acad. Press , N.Y., p. 23, 1964.

162. Davydov, A.S. *Theory of Molecular Excitons* (Translated by Kasha, M and Oppenheimer, M. Jr.) Mc Graw-Hill, N.Y., 1962.

163. Simpson, W.I. *Theory of Electrons in Molecules*, Prentice Hall, Englewood Cliffs, New Jersey, 1962.

164. McClure, D.S. *Solid State Phys.* **1959**, *8*, 1.

165. Kasha, M. *Rev. Mod. Phys.* **1959**, *31*, 162.

166. Kasha, M. *Radiation Res.* **1963**, *20*, 55.

167. Levinson, G.I.; Simpson, W.T.; Curtis, W. *J. Am. Chem. Soc.* **1957**, *79*, 3414.

168. Kasha, M.; EL-Bayoumi, M.A.; Rhodes, W. *J. Chem. Phys.* **1961**, *58*, 916.

169. EL-Bayoumi, M.A., *Exciton Theory: Application to H-Bonded Complexes*, Doctoral Thesis, Florida State University, Tallahssea, Florida, 1961.

170. Hosoya, H.; Janaka, J.; Nagakura, S. *J. Mol. Spectry.* **1962**, *8*, 257.

171. MacRay, E,G,; Kasha, M. *J. Phys. Chem.* **1958**, *28*, 721.

172. Rohatgi-Mukherjee, K.K.; Mukhopadhyay, A.K. *J. Phys. Chem.* **1972**, *76*, 3970.

173. Arbeloa, I.L. *J. Chem. Soc. Faraday Trans. 2*, **1981**, *77*, 1735

174. Jones, G.R.; Duddell, D.A.; Murry, D.; Cundall, R.B. *J. Chem. Soc. Faraday Trans. 2*, **1984**, *80*, 1181.

175. Basu, S.; Rohatgi-Mukherjee, K.K.; Arbeloa, I.L. *Spectrochemica Acta.* **1986**, *42A*, 1355.

176. Horng, M-L.; Quitevis, E.L *J. Chem. Edu.* **2000**, *77*, 637.

177. Berlepsch, H.V.; Bottcher, C.; Dahne, L. *J. Phys. Chem. B.* **2000**, *104*, 8792.

178. Kawasaki, M.; Sato, T. *J. Phys. Chem. B.* **2001**, *105*, 796.

179. Ahmed, S.; Saha, S.K. *Can. J. Chem.* **1996**, *74*, 1896.

180. Kartal, Ç.; Akbaş, H. *Dyes Pigments* **2005**, *65*, 191.

181. Jirsa, M.; Jirsa Jr, M.; Kubát, P. *J. Photochem. Photobiol. B* **1996**, *36*, 99.

182. Armarego, W.L.F.; Perrin, D.D. *Purification of Laboratory Chemicals*, 4th Ed. Butterworth-Heinemann, Oxford, 1996.

183. Benrraou, M.; Bales, B.L.; Zana, R. *J. Phys. Chem. B* **2003**, *107*, 13432.

184. Pal, M.K.; Schubert, M. *J. Am. Chem. Soc.* **1962**, *84*, 4384.

185. Pal, M.K.; Schubert, M. *J. Phys. Chem.* **1963**, *67*, 1821.

186. Pal, M.K.; Mandel, M. *Biopolymers* **1977**, *16*, 33.

187. Datta, R.K.; Bhat, S.N. *Bull. Chem. Soc. Jpn.* **1993**, *66*, 2457.

188. Datta, R.K.; Bhat, S.N. *Colloids Surf. A* **1996**, *106*, 123.

189. Vinogradov, A.M, Tatikolov, A.S.; Costa, M.B. *Phys. Chem. Chem. Phys.* **2001**, *3*, 4325.

190. Nigam, S.; Belletête, M.; Sarpal, R.S.; Durocher, G. *J. Chem. Soc. Faraday Trans.* **1995**, *91*, 2133.

191. (a) Mukherjee, P.; Mysels, K.J. Critical Micelle Concentrations of Aqueous Surfactant Systems, US-NBS, No. 36, US. GPO, Washington DC, 1971. (b) Hait, S.K.; Majhi, P.R.; Blume, A.; Moulik, S.P. *J. Phys. Chem. B* **2003**, *107*, 3650.

192. Datta, R.K.; Chowdhury, R.; Bhat, S.N. *J. Chem. Soc. Faraday Trans. 1* **1995**, *91*, 681.

193. Ahmed, S. *Ph. D. Thesis*, University of North Bengal, 1996.

194. F. Tavčer, *Dyes Pigments* **2004**, *63*, 181.

195. Havelcová, M.; Kubát, P.; Němcová, I. *Dyes Pigments* **2000**, *44*, 49.

196. Gak, V.Y.; Nadtochenko, V.A.; Kiwi, J. *J. Photochem. Photobiol. A* **1998**, *116*, 57.

197. Lang, K.; Luňak, S.; Sedlák, P.; Kubát, P.; Zeit, J. *J. Phys. Chem.* **1995**, *190*, 203.

198. Drummond, C.J.; Grieser, F.; Healy, T.W. *J. Chem. Soc. Faraday Trans.1.* **1989**, *85*, 561.

199. Rao, N.V.; Narayana, R.L. *Indian J. Chem.* **1982**, *21A*, 995.

200. Wormuth, K.R.; Cadwell, L.A.; Kaler, E.W. *Langmuir* **1990**, *6*, 1035.

201. Keh, E.; Valeur, B. *J. Colloid Interface Sci.* **1981**, *79*, 465.

202. Drummond, C.J.; Grieser, F.; Healy, T.W. *Faraday Discuss. Chem. Soc.* **1986**, *81*, 95.

203. Warr, G.G.; Evans, D.F. *Langmuir* **1988**, *4*, 217.

204. Zinsli, P.S. *J. Phys. Chem.* **1979**, *83*, 3223.

205. Sabaté, R.; Gallardo, M.; de la Maza A.; Estelrich, J. *Langmuir*, **2001**, *17*, 6433.

206. Havelcová, M.; Kubát, P.; Němcová, I. *Dyes Pigments* **2000**, *44*, 49.

207. Siu, H.; Duhamel, J. *J. Phys. B* **2008**, DOI: 10.1021/jp801105q.

208. Kurucsev, T. *J. Chem. Edu.* **1978**, *55*, 128.

209. Adhikari, R.; Saha, S.K. *Z. Phys. Chem.* **2005**, *219*, 1373.

210. Dye, J.L.; Nicely, V.A. *J. Chem. Edu.* **1971**, *48*, 443. (The program has been updated in 1992)

211. Fulton, R.L.; Gouterman, M. *J. Chem. Phys.* **1964**, *41*, 2280.

212. Fornasiero, D; Kurucsev, T. *J. Chem. Soc., Faraday Trans, 2*, **1986**, *82*, 15.

213. Gianneschin, L.P.; Kurucsev, T. *J. Chem. Soc. Faraday Trans, 2*, **1976**, *72*, 209.

214. Gianneschin, L.P.; Cant., A; Kurucsev, T. *J. Chem. Soc. Faraday Trans 2*, **1977**, *73*, 664.

215. Valdes-Aguilera, O.; Neckers, D.C. *J. Phys. Chem.* **1988**, *92*, 4286.

216. Rohatgi-Mukherjee, K.K *Ind. J. Chem.* **1992**, *31*, 500.